Elucidation of the Three-Dimensional Structure of an Antimicrobial Peptide, SakP(N24C + 44C), in a Membrane-Mimicking Environment by the use of NMR Spectroscopy

Thesis Submitted for the Degree of *Candidata Scientiarum*

by

Marianne Uteng

Department of Biochemistry

Faculty of Mathematics and Natural Sciences

University of Oslo 2003

Acknowledgments

Nuclear magnetic resonance (NMR) measurements, resonance assignments and structure calculations were carried out at the European Molecular Biology Laboratories (EMBL), Heidelberg, while NMR sample preparation was carried out at the Department of Biochemistry, University in Oslo.

First of all, I wish to thank Doctor Claudia Muhle-Goll for an outstanding supervision in two-dimensional NMR spectroscopy of proteins. I am deeply grateful for your skilful help, your patience and the social times we spent together.

A special thank goes to Professor Jon Nissen-Meyer for an excellent follow-up of this project, always being available to help and for critical reading of this thesis. Your enthusiasm for this project has been highly contagious.

I also want to thank Dr. Håvard Hildeng Hauge, Dimitris Mantzilas, Dr. Gunnar Fimland, Dr. Per Eugen Kristiansen, Fabian Filipp, Åsmund Kjendseth Røhr and the members of my group for all your help, fruitful tips, interesting discussions and fun times on and off work.

Last, but not least, I wish to thank my mother, Hilde Uteng, for her support and encouraging words throughout all my years of study.

Oslo, Norway, January 2003
Marianne Uteng

Publications Resulted from this Study

Uteng M. Hauge HH. Brondz I. Nissen-Meyer J. Fimland G. **Rapid two-step procedure for large-scale purification of pediocin-like bacteriocins and other cationic antimicrobial peptides from complex culture medium.** *Applied & Environmental Microbiology. 68(2):952-6, 2002 Feb.*

Uteng M. H.H. Hauge. P. Markwick. G. Fimland. D. Mantzilas. J.Nissen-Meyer. C. Muhle-Goll. **Three-dimensional structure in lipid micelles of the pediocin-like bacteriocin sakacin P and a sakacin P variant that is structurally stabilized by an inserted C-terminal disulfide bridge.** *To be submitted.*

Table of Contents

1 Abstract

The antimicrobial peptide, sakP(N24C + 44C) is a mutant of a class IIa bacteriocin, sakacin P, produced by lactic acid bacteria. SakP(N24C + 44C) consists of 44 residues and possesses a C-terminal disulphide bond that ties the C-terminal tail to the mid part of the peptide-sequence, in contrast to the wild-type peptide which lacks a C-terminal disulphide bond. The three-dimensional structure of sakP(N24C + 44C) in a membrane-mimicking environment (dodecylphosphocholine (DPC) micelles) was investigated by circular dichroism (CD) and by two-dimensional homo nuclear resonance spectroscopy (NMR). CD spectra indicated that sakP(N24C + 44C) exists as a random coil in water, whereas NMR results indicate that sakP(N24C + 44C) has a well-defined structure in DPC micelles. Simulated annealing calculations based on distance restraints derived from NMR spectra, were used to generate structures of sakP(N24C + 44C). The structures revealed an amphipathic central α-helix (residues 18-33), a less well-defined β-sheet-like structure in the N-terminal half (residues 1-17), and a defined structured C-terminal half (residues 34 -44) without any common secondary structural motif. Comparison of sakP(N24C + 44C) with leucocin A, another pediocin-like (class IIa) bacteriocin, revealed a striking resemblance, which may indicate that these two bacteriocins have the same mode of action on their target cells. The structural features of sakP(N24C + 44C) and their possible role in an antimicrobial mechanism are discussed.

In the lack of a rapid large-scale purification procedure for the purification of sakP(N24C + 44C) that was needed in this study, a new and simple two-step purification procedure for pediocin-like bacteriocins and other cationic peptides was developed. The new procedure yields more than 80% of the activity that is initially in the culture supernatant, and the final bacteriocin preparation is more than 90% pure. With the new purification procedure, it is possible to purify milligram quantities of pediocin-like bacteriocins within a few hours.

2 Introduction

2.1 The Role of Antimicrobial Peptides

Antimicrobial peptides were independently discovered by two research groups in the early 1980ties. One group in Sweden studied how insects kill bacteria [1], while another group in California studied how phagocytes kill bacteria inside the phagolysosome [2]. It has now become clear that antimicrobial peptides are important components of the innate defence systems of all species of life, ranging from bacteria and plants to insects and animals [3-7]. Antimicrobial peptides tend to be found in those parts of animals that are most likely to come into contact with pathogens from the environment. They are therefore often found on the skin, ear, eye and on the epithelial surfaces of various internal organs including tongue, trachea, lungs and gut, as well as in the bone marrow of animals [8].

The peptides are antimicrobials due to their ability kill Gram-negative and Gram-positive bacteria, fungi, parasites, cancer cells and even enveloped viruses like HIV and herpes simplex virus [8,9]. However, no single type of peptide is able to kill all of these organisms. Their initial contact with the target organism is an electrostatic binding to the negatively charged surface of the target organism. The peptides then tend to permeabilize the surface membrane in a manner that is not yet fully understood, and then inactivate the organism [10].

Antimicrobial peptides may vary in structure, size and activity, although most of them are amphipathic and have a net positive charge [5,10]. There are today two definitions of antimicrobial peptides. Hancock and Scott define antimicrobial peptides to be positively charged peptides with antimicrobial activity, ranging from 12 to 50 amino acids in size, where 50% of the residues are hydrophobic [8]. Ganz and Lehrer have a more broad definition that includes positively charged peptides with less than 100 amino acids [11]. However, in practise there is little difference between these two definitions. It is today normal to classify antimicrobial peptides according to their structure, which usually reflects their mode of action [4,8]. It is important not to confuse antimicrobial peptides

with antibiotics. The latter are synthesized by unique enzymatic systems, whereas antimicrobial peptides are gene encoded and ribosomally synthesized [5,12].
The great interest in antimicrobial peptides is mainly a result of the desire to develop new types of antimicrobials due to the increase in antibiotic-resistant bacteria. In the future, antimicrobial peptides may complement or become a substitute for antibiotics that are no longer effective. Antimicrobial peptides are also studied due to their potential as biological food preservatives. Naturally occurring metabolites produced by selected bacteria may replace the use of chemical preservatives such as sulphur dioxide, benzoic acid, sorbic acid, nitrate, nitrite etc. The antimicrobial peptides produced by lactic acid bacteria (LAB) are today among the most promising biological food preservatives, since several of them are active against pathogenic microorganisms that are found in food [5,10,12-14]. Nisin, which belongs to this group (produced by LAB), is already in use as a food preservative [15,16]. The following introduction will focus on antimicrobial peptides (often termed bacteriocins) produced by LAB, and especially on the peptides that belong to class IIa (often termed the pediocin-like bacteriocins), since these are central to this study.

2.2 Bacteriocins Produced by Lactic Acid Bacteria

Lactic acid bacteria (LAB) are Gram-positive, non-sporulating microaerophilic bacteria whose main fermentation product is lactate. LAB comprise both cocci (*Lactococcus, Vagococcus, Leuconostoc, Pediococcus, Aerococcus, Tetragenococcus, Streptococcus, Enterococcus*) and rods (*Lactobacillus, Carnobacterium, Bifidobacterium*).
LAB have been used by man for hundreds of years as starter cultures for the fermentation of foods and beverages, and the use of LAB for conserving food is the oldest known technique for food preservation. It has been known for a long time that the main preservative effect of LAB is due to the acidic environment they create, which is a result of the metabolic production of lactic acid. In recent decades, however, it has become clear that the overall inhibitory action of LAB is also due to a more complex antagonistic system, which the antimicrobial peptides are a part of [12]. Today, antimicrobial peptides produced by LAB are perhaps the most studied and best characterized of all known antimicrobial peptides [3,14]. Since antimicrobial peptides are produced by bacteria, they

may also be called bacteriocins [5,16,17], and these two terms (antimicrobial peptides and bacteriocins) will be used interchangeably throughout this thesis. The bacteriocins produced by LAB form a heterogeneous group with respect to physical and chemical properties, however, they all show a bactericidal mode of action towards various Gram-positive bacteria, and particularly towards species closely related to the bacteriocin-producer.

2.3 Classification of Bacteriocins Produced by Lactic Acid Bacteria

Three defined classes of LAB bacteriocins have been established, class I: the modified peptide-bacteriocins, often called lantibiotics, class II: the unmodified small heat stable peptide-bacteriocins, and class III: the large heat labile protein-bacteriocins. The bacteriocins have been classified according to common characteristics, mainly structural [14]. The data available may not be sufficient to formulate a definite and permanent natural classification scheme, since new knowledge on already existing and novel bacteriocins are continually acquired.

Class I bacteriocins (often termed lantibiotics) contain the modified amino acid residues lanthionine and/or methyl-lanthionine, and often other modified residues such as 2,3 didehydro-threonine, 2,3 didehydroalanine and D-alanine. The modified residue lanthionine may be described as two L-alanine residues linked by one sulphur atom, through a thioether bond. The thioether bond in lanthionine presumably functions to stabilize the three-dimensional structure, and is therefore analogous to the disulphide bond often found in proteins [14,18]. The lantibiotics have been divided into two major subgroups (class Ia and Ib) based on their structure [19,20].

Class Ia bacteriocins are elongated, screw-shaped, and amphipathic and have a molecular mass range of 2 – 5 kDa. The type Ia lantibiotics interact with the membrane of susceptible cells and form transient voltage-dependent pores [19]. A well-characterized bacteriocin that belongs to this group is nisin [15,21]. This peptide is used as a food

preservative and has been considered for use in the treatment of gastric *Helicobacter* infections and ulcers [10].

Class Ib bacteriocins are more globular in shape and have a molecular mass of about 2 kDa. It has been shown that lantibiotics belonging to this group inhibit the functioning of enzymes. For instance, mersacidin and actagardine interfere with the cell-wall synthesis in gram-positive bacteria [19].

Class II bacteriocins are peptide-bacteriocins that do not contain modified residues. They are small peptides about 30 to 70 amino acid residues long. They are cationic at neutral pH, and they often have a hydrophobic and/or an amphipathic region. A large number of different class II bacteriocins have been characterized [14]. From a practical point of view, it has been useful to sub-classify (class IIa and IIb) these bacteriocins according to sequence similarities, mode of secretion, target specificity, and the number of peptides that constitutes the bacteriocins.

Class IIa bacteriocins, often called pediocin-like bacteriocins, is a major and important subgroup. The reason for this is not only the large number of peptides that belong to this group, but also due to the fact that they are the most promising bacteriocin-candidates for various industrial applications, since they are active against many food born pathogenic microorganisms. All class IIa bacteriocins identified so far are highly active against *Listeria* strains, and many of them are also active against spoilage LAB, *Brochotrix spp*, *Clostridium spp*, *Bacilllus spp*, *Staphylococcus spp*, *Streptococcus* and *L. monocytogenes* [3]. The pediocin-like (class IIa) bacteriocins are all between 37 and 48 amino acid residues long, cationic and share amino acid sequence similarities ranging from 40 to 60 percent [5]. The fist bacteriocins of this group to be identified and thoroughly characterized were leucocin A [22], sakacin P [23], curvacin A [24,25], mesentericin Y105 [26], and pediocin PA-1 [18,27] from which the term pediocin-like bacteriocins has been derived. Multiple sequence alignments of pediocin-like bacteriocins are shown in Figure 2.3.1.

Class IIb is another important subgroup. This group contains bacteriocins, often termed two-peptide bacteriocins, whose activity depends on the complementary action of two peptides. These bacteriocins have optimal activity when both peptides are present in approximately equal amounts, and very low activity, if any, when they appear

individually [28,29]. Accordingly, the genes encoding the two complementary peptides are located next to each other on the same transcriptional unit, and presumably transcribed to the same extent [17,30,31]. Several examples of such bacteriocins have been studied. Structural analysis of two-peptides bacteriocins indicate a direct physical interaction between the complementary peptides when they exert their bactericidal effect [32,33]. Lactococcin G was the first two-peptide bacteriocin that was isolated and characterized [28].

Class III is the third class, and this includes heat labile bacteriocins with high molecular mass, above 15 KDa. Due to their relatively large size, one may assume that their mode of action is different from that of the other smaller peptide-bacteriocins. Helveticin J and enterolysin A are the only class III LAB bacteriocins that are thoroughly characterized biochemically and genetically [14,34].

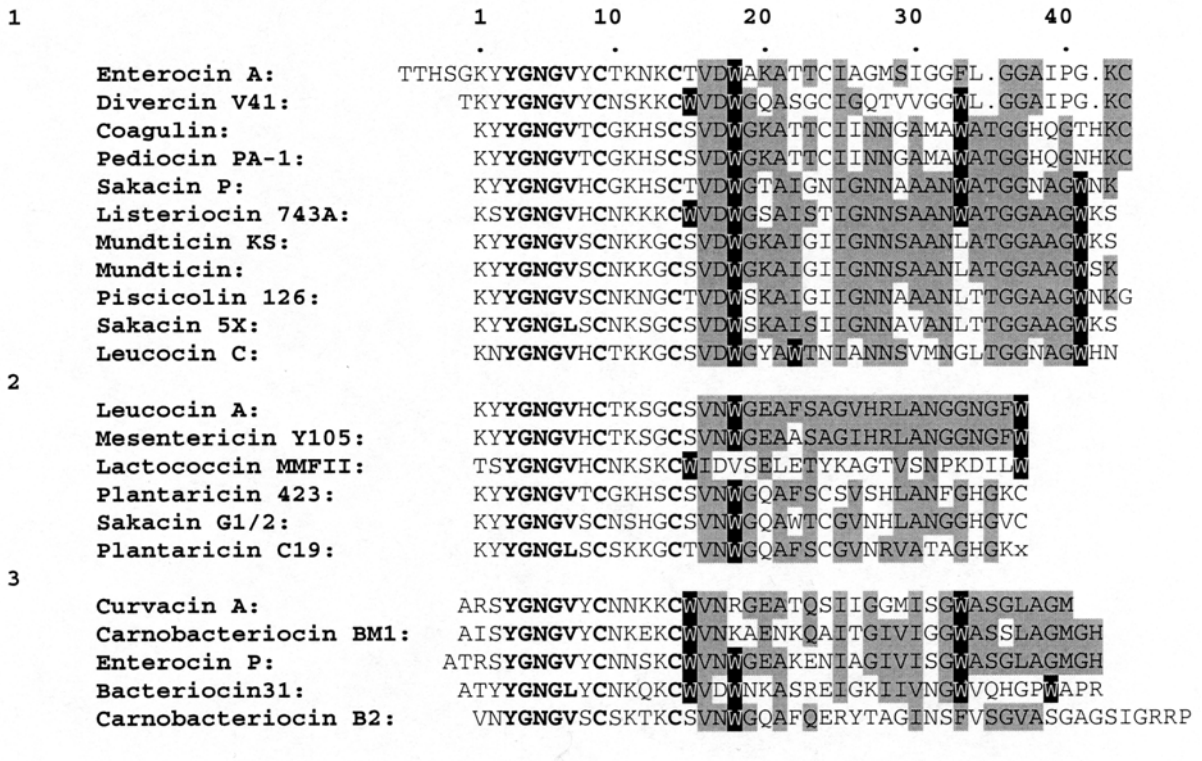

Figure 2.3 1 Multiple sequence alignment of pediocin-like bacteriocins, highlighting the YGNGV/L motif, tryptophan residues (black boxes), and also conserved residues in the C-terminal half of the peptides (Fimland et al. (2002))[35]. Residues in the C-terminal parts are in grey box if they occur in at least 4 (group 1) or 3 (groups 2 and 3) of the sequences. The following residues were considered similar: I = L = V; E = D; K = R; S = T. The pediocin-like bacteriocins contain a disulphide bond between the conserved Cys9 and Cys14 residues. Some group 1 (and putatively group 2) bacteriocins also have a disulphide bond between Cys24 and the cysteine residues at the C-terminal end [35].

2.4 Primary, Secondary, and Tertiary Structural Features of the Pediocin-Like Bacteriocins (Class IIa), and their Possible Role

As mentioned earlier, the amino acid sequences of class IIa show similarities ranging from 40 to 60 percent [5]. The similarities are especially pronounced in the N-terminal halves, where one finds a pediocin-box motif: YGNGVXCXK/NXXC, where X represents a polar residue [5]. It is assumed that the YGNGV consensus motif is involved in the recognition of a docking-site on the target-cell surface [36,37]. The motif has been coined the *Listeria* active part of class IIa bacteriocin, since modifications and/or deletions in YGNGV seem to have serious consequences on the anti-Listeria activity of class IIa bacteriocins [38-40].

An important characteristic of class IIa bacteriocins is their cysteine content. While other (non-lanthionine) class II bacteriocins generally do not contain cysteine residues, class IIa bacteriocins contain at least two cysteines connected by a disulphide bond. The two cysteine residues in the N-terminal half (in the pediocin box motif) are present in conserved positions, and the disulphide bond forms consequently a six-member ring in all class IIa bacteriocins. This N-terminal disulphide bond seems to be crucial for activity. This has been shown by mutational analysis of mesentericin Y105 and pediocin PA-1, where the lack of an N-terminal disulphide bond made the peptides completely inactive [38,39].

The five class IIa bacteriocins pediocin PA-1, enterocin A, coagulin, divercin V41, plantaricin 423, and probably also plantaricin C19 are unique in the sense that they possess an extra disulphide bond involving a second pair of cysteine residues located in the C-terminal region, Figure 2.3.1. The presence of the extra disulphide bond in the C-terminal half seems to be important for the activity of these class IIa bacteriocins. In a comparative study, Eijsink et al. (1998) [41] have recently shown that the "two-disulphide bond" bacteriocins, pediocin PA-1 and enterocin A, are more efficient antimicrobials than the "one-disulphide bond" bacteriocins, sakacin P and curvacin A, especially against *Listeria* strains, and that they display an overall broader spectrum of activity. The significance of the C-terminal disulphide bond was also studied by Fimland et al. (2000) [42] by site-directed mutagenesis of pediocin PA-1 (which has two disulphide bonds) and sakacin P (which has only one disulphide bond). Introduction of the C-terminal disulphide bond into sakacin P

broadened the target cell specificity and increased the potency at elevated temperatures, while removing the C-terminal disulphide bond from pediocin PA-1 by Cys→Ser mutations resulted in reciprocal effects (decreased potency and more narrow target cell specificity).

Although the pediocin-like bacteriocins have very similar sequences, there is enough diversity in their C-terminal halves to enable sub-classification of these peptides into at least 3 groups, Figure 2.3.1. These sequence differences may indicate differences in tertiary structures in the C-terminal half. A striking feature of bacteriocins that belong to subgroup 1 and 2 is that some of these bacteriocins possess a C-terminal disulphide bond and no tryptophan at position 41 (in subgroup 1) or position 37 (in subgroup 2), while those, which lack the disulphide bond, do possess tryptophan at these positions. Mutating Trp 18 and Trp 41 to leucine led to deleterious effects in sakacin P, however, these deleterious effects were overcome by introducing a disulphide bond between residues 24 and 44. One may therefore hypothesize that the Trp 41 is involved in the stabilization of a hairpin like structure, folding the C-terminus back onto the central part of the peptide. Another interesting feature is the conserved glycine residues at position 36 and 37 for all of the bacteriocins in subgroup 1, and the glycine residues at position 32 and 33 in leucocin A and mesentericin Y105 in subgroup 2. These glycine residues may be conserved since they may be required for the peptides to attain the structural flexibility needed to allow the C-terminal tail to fold back. This interesting feature of the C-terminal half folding back onto the central part of the peptide, leads one to speculate that the two tryptophan residues in positions 18 and 41 are important for the anti-microbial peptide. Perhaps tryptophan 18 and 41 are in favourable contact with the membrane-surface interface of the membrane, forcing the C-terminal tail to fold back, even in the absence of a C-terminal disulphide bond [35].

Recently, several studies using nuclear magnetic resonance (NMR), circular dichroism and computer simulation have been done on some class IIa bacteriocins in membrane mimicking environments. Experimental evidence indicates that class IIa bacteriocins are unstructured in watery solutions, but become partly structured in the presence of trifluoroethanol (TFE), dodecylphosphocholine micelles (DPC) or negatively charged liposomes [36,38,43-45]. Two structures of class IIa bacteriocins have been elucidated by NMR, and are shown in Figure 2.4.1 [36,44]. The three-dimensional structure of leucocin A

was analysed in TFE and DPC, and that of carnobacteriocin B2 in DPC. Leucocin A displayed a well structured three-strand β-sheet in the N-terminal region in TFE and a less well-defined three stranded β-sheet in DPC, whereas the N-terminal region of carnobacteriocin B2 was unstructured. Both bacteriocins contain an amphipathic α-helix starting at residue 17/18 and ending at residue 31 in leucocin A and 39 in carnobacteriocin B2. In both bacteriocins, the C-terminal was found to be unstructured. However, there were a few long-range NOESY peaks between residue 26 and 36 in leucocin A in DPC, which suggest that the C-terminus folds back onto the α-helix. This is not shown in Figure 2.4.1 [36]. Recent NMR analysis of sakacin P in DPC and TFE indicated that the structure of this bacteriocin resembles that of leucocin A (Uteng, unpublished).

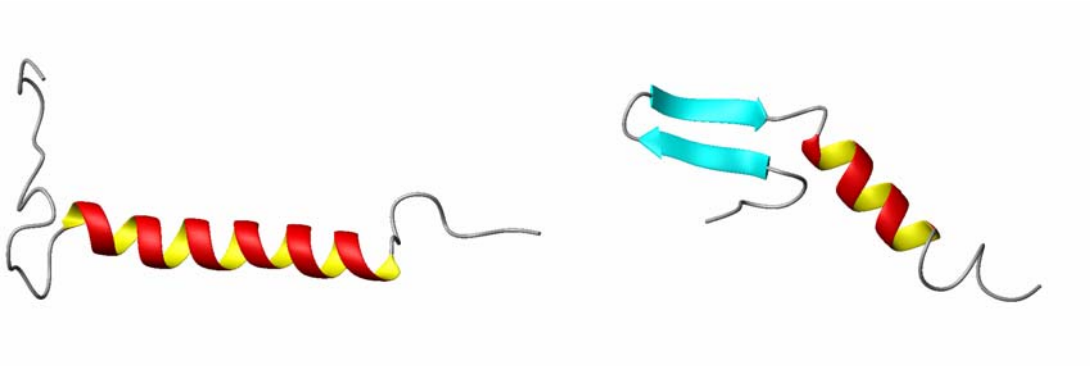

Figure 2.4 1 Carnobacteriocin B2 (to the left) in DPC and leucocin A (to the right), in TFE (Fregeau Gallagher et al. (1997) and Wang et al. (1999)) [36,44]. The structure of Leucocin A in DPC, which is not shown, resembles the structure in TFE. However, the N-terminal β sheet of leucocin A in DPC becomes less defined, and there are also some evidence that the C-terminal half folds back onto the α-helix. The N-terminus is on the left and the C-terminus is on the right for both bacteriocins [36,44]

2.5 Mode of Action of Pediocin-Like (Class IIa) Bacteriocins

The cationic character of the well-conserved N-terminal region of pediocin-like bacteriocins is thought to enable their initial binding to the negatively charged membrane and/or cell wall of the target organism. The bacteriocins then tend to permeabilize the

plasma membrane and this causes cell death [10,14]. Two main models/mechanisms describing how the peptides permeabilize the plasma membrane have been proposed, Figure 2.5.1 [46]. The barrel-stave model proposes that the peptides form amphipathic α-helices that penetrate through the cell membrane and that several peptide helices associate side-by-side, thereby forming a pore through the membrane. In this pore, the hydrophilic sides of the helices face in toward the pore centre while the hydrophobic sides face out toward the membrane. This permits water-soluble particles to pass through the pore. The carpet model proposes that amphipathic helical peptides float on the plasma membrane (the α-helix being parallel with the membrane) with the hydrophobic side of the α-helix facing (and penetrating into) the hydrophobic membrane, and the hydrophilic side of the α-helix facing the watery solution. When a high local concentration of membrane-bound peptides has been reached (forming a localized "carpet"), the phospholipids will be pushed aside, causing the membrane to fold inwards, and eventually to become ruptured by the peptides.

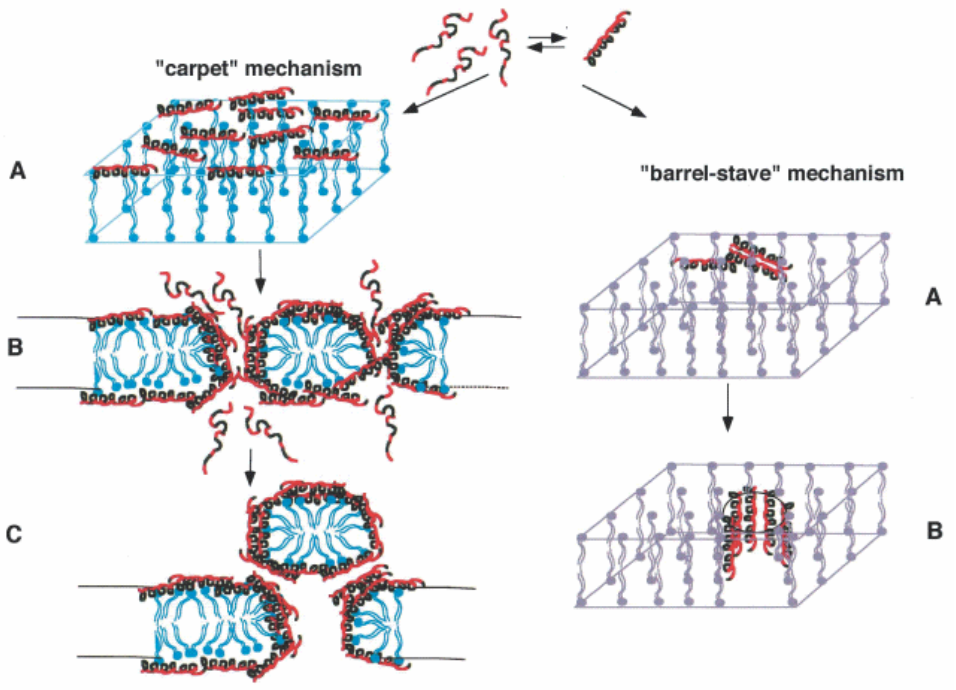

Figure 2.5.1 Illustration of the "barrel-stave" (to the right) and the "carpet" (to the left) models suggested for membrane permeation (Shai et al. (1999))[46]. In the "carpet" model the peptides are bound to the surface of the membrane with their hydrophobic surfaced facing the membrane and their hydrophilic surfaces facing the solvent (step A). When a threshold concentration of peptide monomers is reached, the membrane goes into pieces (step B and C). At this stage a transient pore is formed. In the "barrel-stave" model peptides first assemble in the surface of the membrane, then insert into the lipid core of the membrane following recruitment of additional monomers [46].

In spite of sequence similarities, the pediocin-like bacteriocins have different target-cell specificities. The hydrophobic or amphipathic C-terminal region, which is thought to penetrate into the target cell membrane, appears to play a central role in mediating specificity. This is consistent with hybrid-bacteriocin studies, which reveal that peptides containing N- and C-terminal regions from different pediocin-like bacteriocins have antimicrobial spectra similar to that of the bacteriocin from which the C-terminal region is derived [37]. Moreover, the bacteriocin activity of pediocin PA-1 has been shown to be specifically inhibited by a 15-mer fragment that spans the bacteriocin from the centre towards the C-terminus [47].

The lethal activity of class IIa bacteriocins is mainly due to the dissipation of the proton motive force [19,48,49]. Particularly the intracellular ATP pool is depleted and the uptake of amino acids, which is mediated by active transport, is thereby blocked [50,51]. The observed depletion of intracellular ATP may result from (i) an accelerated consumption of ATP as a result of the cells effort to maintain or restore proton motive force and/or (ii) the inability of the cell to produce ATP due to phosphate efflux [50]. Mode of action studies with purified pediocin PA-1 revealed dissipated transmembrane electric potential and leakage of preaccumulated amino acids and small ions, and with increasing bacteriocin concentration, efflux of molecules of up to 9 kDa [51,52]. It is unclear whether a receptor on the target-cell is necessary for the peptides to permeabilize the cell membrane. Chen et al. (1997) demonstrated that pediocin PA-1 was able to permeabilize synthetic vesicles composed of only phosphatidylcholine, suggesting that the bacteriocin can function in absence of a protein receptor [53].

2.6 Biosynthesis of Pediocin-Like (Class IIa) Bacteriocins

Bacteriocin production is often correlated with the presence of a plasmid, however, genes located on chromosomal fragments have also been reported [3]. Four genes are required to produce class IIa bacteriocins [17]: (i) The structural gene, which encodes the preform of the bacteriocin. (ii) The immunity gene that encodes the immunity protein needed to protect the bacteriocin producer. (iii) A gene that encodes a membrane-associated ATP-binding

cassette (ABC-transporter) that transfers the bacteriocin across the membrane concomitantly with removal of the prepeptide. (iv) A gene that encodes an accessory protein that is also needed for secretion of the bacteriocin, but whose specific role is unknown. These genes are usually found in either one or two operons.

Characteristically, like other low-molecular-weight bacteriocins, class IIa bacteriocins are first formed as ribosomally synthesized precursors or pre-forms of bacteriocins, which are not biologically active. These pre-forms contain an N-terminal extension leader sequence of about 18 to 27 residues. The function of this extension may be to stabilize the peptide during translation, keep it biologically inactive and facilitate its translocation across the membrane. Cleavage of the pre-form at a specific processing site removes the leader sequence from the antimicrobial peptide, concomitantly with its export to the outside of the cell [54]. One important feature of the majority of these leader-sequences is the presence of two glycine residues in the C-terminus, at position -2 and -1 relative to the processing site. The two glycine residues may serve as a recognition signal for a dedicated sec-independent transport system which involves two distinct proteins: an ABC-type translocator and an accessory protein [17,55,56].

The accessory protein is required for successful externalisation of class IIa bacteriocins, however, the specific role of the accessory protein in the translocation process is still not fully understood. The accessory proteins contain about 460 amino acid residues and often share significant sequence homology. The proteins consist of a large hydrophilic C-terminal region and a hydrophobic N-terminal section that may span the membrane [14].

The ABC-transporters are proteins that contain from 715 to 724 amino acid residues [3]. There are no distinctive structural characteristics of class IIa bacteriocin ABC-transporters, since most of their features are shared by a wide range of ABC-transporters. The C-terminal part of ABC-transporters contains a highly conserved ATP-binding domain, while the N-terminal region is a hydrophobic integral membrane domain that contains an extension of 150 amino acid residues. This extension has been shown to be able to cleave off the leader-sequence, at the C-terminal side of the double glycine motif [17,54,57].

Five different class II bacteriocins (acidocin B, divergicin A, enterocin P, bacteriocin 31 and lactococcin 972) that lack the double glycine motif on their leader-sequences are

known. These bacteriocins all have a typical sec-type signal peptide, and are thus secreted by general secretion pathway (GSP) [14]. It has been suggested that these bacteriocins should be classified in a special sub-class consisting of the sec-dependent bacteriocins. However, except for their sec-dependent leaders, these five bacteriocins share the general characteristics of other class II bacteriocins. Judged from their primary structures, enterocin P and bacteriocin 31 are in fact pediocin-like bacteriocins. It has been shown that among class II bacteriocins one may replace a sec dependent leader with a double glycine leader and vice versa, without grossly effecting bacteriocin secretion [14]. The N-terminal bacteriocin leader-sequences apparently specifies which secretion system is to be used for externalisation of bacteriocins. This phenomenon is of great interest since this would allow development of LAB producing multiple bacteriocins, each one having its specific range of target bacteria. This will enhance the antimicrobial efficiency of bacteriocin producers in food.

The production of many class IIa bacteriocins is transcriptionally regulated through a three-component signal transduction system that consists of a peptide-pheromone, a histidine protein kinase and a response regulator [3,14,17]. The pheromone is a bacteriocin-like peptide with a double-glycine leader-sequence. The bacteriocin production is activated when the concentration of the pheromone reaches a threshold value as a result of high cell density and/or changes in environmental conditions. The histidine kinase is presumed to function as a receptor for the pheromone. Signal transduction starts when the peptide pheromone binds to the histidine kinase and triggers autophosphorylation of the kinase. The histidine kinase then transfers a phosphate group to the response regulator, which then activates transcription by binding to regulated promoters in front of the bacteriocin genes. In addition to activating bacteriocin production, the accumulated pheromone induces its own production, thus starting an autoinduction loop. This three-component regulation of bacteriocin production is illustrated in Figure 2.6.1.

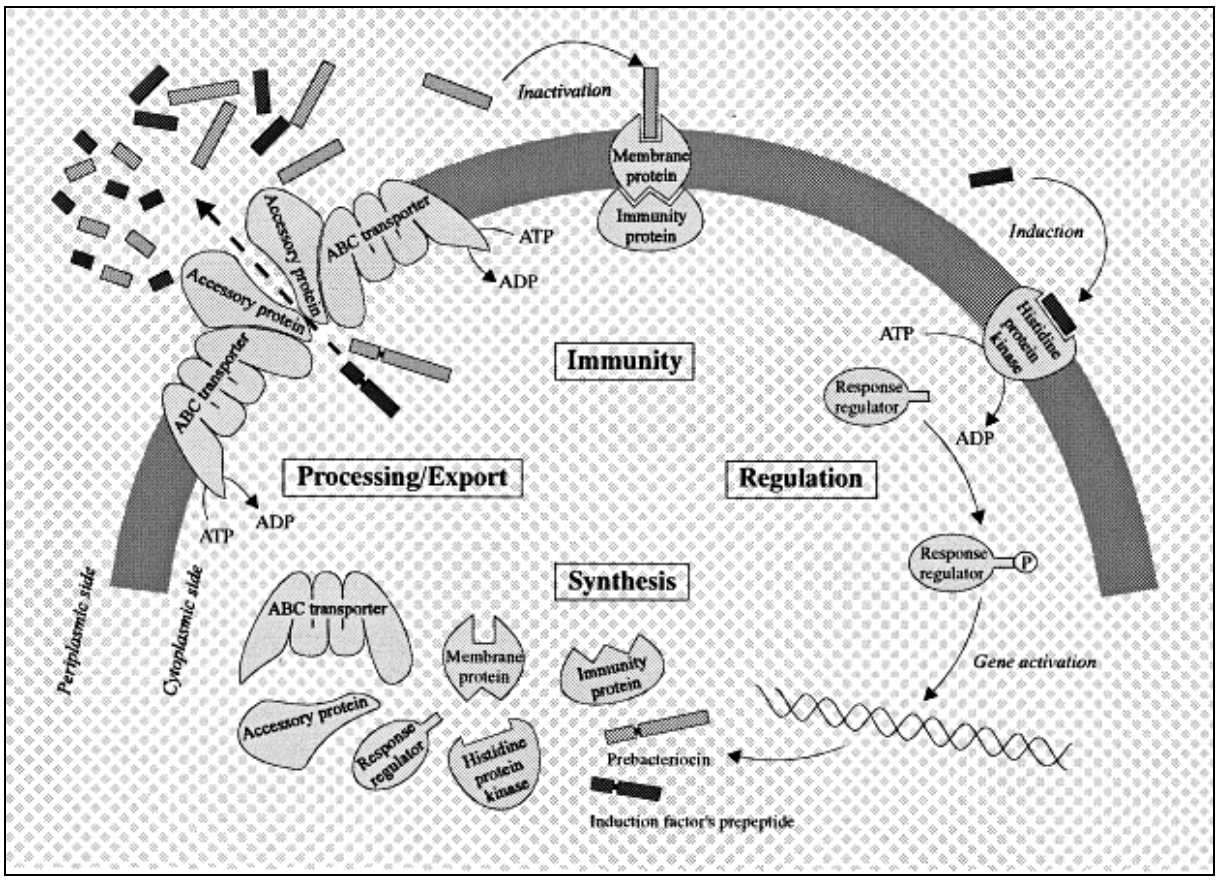

Figure 2.6.1 Schematic overview of the suggested machinery for production of class IIa bacteriocins: three-component regulatory system, synthesis, processing, excretion and immunity (Ennahar et al. (2000))[13]. For explanation of the immunity, see text below.

2.7 Immunity of Class IIa Bacteriocins

All bacteria that produce class IIa bacteriocins also produce an immunity protein that protects the bacteria from being killed by its own bacteriocin [17]. These immunity proteins contain between 80-120 amino acid residues and they show surprisingly low sequence similarities, considering the high content of similarities among the corresponding bacteriocins [41]. In spite of this, there is reported some cross-immunity between class IIa bacteriocins [58]. It is not known how the immunity proteins function, however, it has been shown that a major part of the immunity protein CbiB2 of carnobacteriocin B2 is found in the cytoplasmic compartment, with only a small proportion detected in the membrane. While the expression of CbiB2 within the cells provided immunity against carnobacteriocin B2, externally applied CbiB2 failed to protect the host. Experiments also

demonstrated that CbiB2 has poor affinity for carnobacteriocin B2 and that no direct interaction occurs in aqueous solution between the two proteins [3].

2.8 The Aim of this Study

Optimal use of peptides as antimicrobial agents requires insight into their mode of action and structural features that are important for antimicrobial activity and specificity. This in turn requires insight into the tertiary structure of these peptides.

The main goal of this study was to elucidate the tertiary structure of an antimicrobial peptide, sakP(N24C + 44C) [42], which is a mutant of a pediocin-like bacteriocin (class IIa), sakacin P [23], produced by lactic acid bacteria. SakP(N24C + 44C) possesses a C-terminal disulphide bond that ties the C-terminal tail to the mid part of the peptide-sequence in contrast to the wild-type peptide, sakacin P. It has previously been proposed by Fimland et al. (2002) that this peptide has the same spatial three-dimensional structure as the wild-type peptide, sakacin P, and perhaps also other pediocin-like bacteriocins [35].

Elucidation of their tertiary structure requires homogeneity as well as an adequate yield of the peptides to be studied. Investigators involved in this field have utilised a wide variety of different purification procedures, all with varying success. The procedures that have been used are quite time consuming due to the many purification steps that are involved and the relatively low yields that are obtained. Another aim of this study was therefore to establish a rapid procedure suitable for large-scale purification of pediocin-like bacteriocins (and other cationic peptide bacteriocins) to homogeneity.

3 Brief Description of Important Methods used in this Study

3.1 Chromatographic Methods

Modern separation methods rely heavily on chromatographic procedures. The sample mixture, which is the mobile phase, is percolated through a column consisting of a porous solid matrix known as the stationary phase. The interactions of the individual solutes with the stationary phase act to retard their progress through the matrix in a manner that varies with the properties of each solute. The different retarding forces on each component cause them to migrate at different rates and this will eventually cause the mixture to separate into bands of "pure" substances. Chromatographic methods may be classified according to the nature of the dominant interaction between the stationary phase and the substances being separated [59]. In this study, ion exchange, hydrophobic interaction and reverse phase chromatography were used. For more detailed description of these techniques, the reader is referred to "Principles and Techniques of Practical Biochemistry" by Wilson, K and Walker, J [60].

3.2 Capillary Zone Electrophoresis

Capillary zone electrophoresis (CZE) is the simplest form of capillary electrophoresis, and is a very useful tool for separation of proteins and peptides, since complete resolution can often be obtained from analytes differing by only one amino acid substituent. The separation mechanism is based on differences in charge. After sample injection and application of voltage, the components of a sample mixture separate into discrete zones [61]. The electrophoretic mobility, μ_{ep}, can be approximated from Debye-Hückel-Henry theory:

$$\mu_{ep} = \frac{\nu_{ep}}{E} = \frac{q}{6\pi\eta R} \qquad \textbf{Equation 3.2.1}$$

in which ν_{ep} is the electrophoretic velocity (cm/s), E is the electric field strength, q is the net charge, R is the Stokes radius, and η is the viscosity [61]. One of the fundamental

processes that drive capillary electrophoresis is the electroosmotic flow (EOF). This phenomenon is a consequence of the surface charge on the wall of the capillary. The negatively charged wall, which usually consists of silica, attracts positively charged ions from the buffer, creating an electrical double layer. When a voltage is applied across the capillary, cations in the diffuse portion of the double layer migrate in the direction of the negative electrode, carrying water with them. The result is a net flow of buffer solution in the direction of the negative electrode, a phenomenon called electroosmosis [61].

During electrophoresis, the interplay between electroosmotic flow and the electrophoretic mobility will determine the direction and speed of the peptides. At basic conditions, the silica wall is negatively charged, and a thick double layer of positively charged ions will exist. The electroosmotic flow is then stronger than the electrophoretic migration, such that all species are swept towards the negative electrode. The order of migration is then cation, neutral and anions last. Under acidic conditions, there will only be a small double layer of positive ions due to the almost neutral silica, and only a weak electroosmotic flow will exist [61]. The electrophoretic forces will then dominate over the electroosmotic forces, and consequently, only cations and most zwitterions will migrate toward the negative electrode [61].

3.3 Matrix-Assisted Laser Desorption Ionization Time of Flight (MALDI TOF) Mass-Spectrometry

MALDI-MS is a reliable and effective technique for analysis of peptides and proteins with masses from 300 – 600,000 Da, with accuracies as high as 1 part in 10,000. The total amount of protein required is usually in the range of 1 –10 pmol [62].

The protein sample is solubilized in a matrix of small organic molecules that strongly absorb ultraviolet wavelength laser light. The sample is hit by intense, short-duration pulses of laser light, and the energy absorbed by the matrix will consequently produce protein ions in gas phase. The pulse of ions is then accelerated by a strong electric field (25 –30 KeV), and moves towards a detector. Light ions move more quickly down the

flight tube than heavy ions and therefore strike the detector first. The time the ions use to hit the detector is therefore a function of their mass. The mass-to-charge ratio (m/z) corresponding to a particular signal is then calculated from the equation:

$$m = \frac{2qV\Delta t^2}{l^2} \qquad \textbf{Equation 3.3.1}$$

in which m is the mass of the ion, q is the charge of the ion, V is the potential through which the ion is accelerated, Δt is the interval between the pulse of laser light and the ion impact on the detector and l is the length of the flight tube [62-64].

3.4 Circular Dichroism (CD)

Circular dichroism is an absorptive phenomenon represented as the difference in the absorption of left-handed and right-handed circularly polarized light. In order to obtain a CD spectrum, the sample of interest has to contain an asymmetric chromophore or a symmetric chromophore in an asymmetric environment, which are properties nearly all bio-molecules possess.

The most utilized form of CD spectroscopy is determination of the secondary structure content of proteins in the "far-UV" band, ranging from 170 to 240 nm, which is the region where the contribution from the peptide bonds dominates. The CD band position and intensity depend on the peptide bonds dihedral angles, although some side chains may also contribute. This means that individual bonds with dihedral angles close to those occurring in a certain type of secondary structure will show the spectrum of that particular structure. For instance, a single residue with Φ and Ψ angles of -57^{o} and -47^{o}, respectively, will show an α-helical CD spectrum, whereas a single residue with Φ and Ψ angles of -139^{o} and $+135^{o}$, respectively, will give an antiparallel β-sheet CD spectrum [65]. Spectra of secondary structure that are typically obtained are shown in Figure 3.4.1.

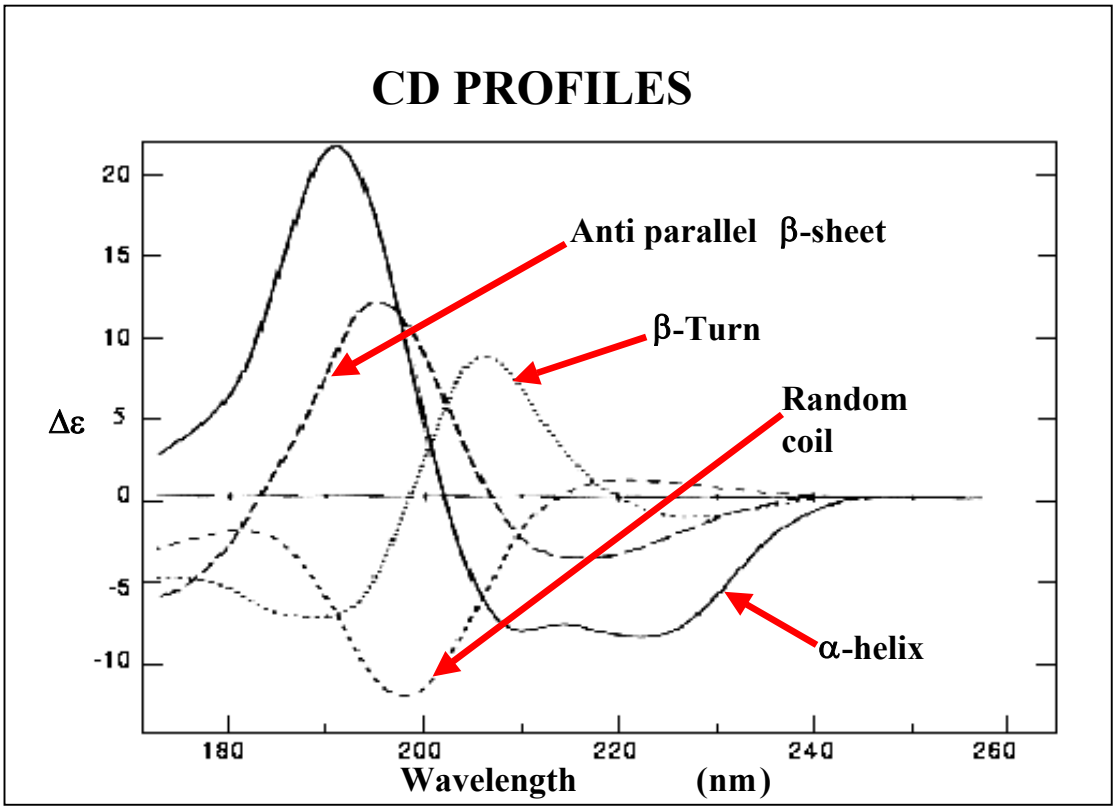

Figure 3.4.1 Characteristic circular dichroism spectra for α-helix, antiparallel β-sheet, β-turn and random coil [65,66]. The Figure is taken from Physical Biochemistry [67].

The strongest and most characteristic spectrum is obtained from the α-helical structure. This spectrum has a negative peak at about 208 and 222 nm, and a positive peak at 192 nm. By contrast, a randomly arranged polypeptide chain has a negative CD band centred at 199 nm. While estimation of α-helices agree well with values obtained from x-ray crystallographic studies, estimation of β-sheet structures is much more uncertain since β-sheets are less regular than the α-helices and contribute less to the CD spectrum [66,68].

Several methods have been developed to quantify the secondary structure of proteins from their "far-UV" CD spectra. One of the oldest uses model polypeptides with assumed pure secondary structure, and the spectrum of the unknown structure is then linearly fitted in terms of these model compounds. In more advanced methods, the pure secondary structure spectra are derived from a large reference set of proteins with structure known from X-ray diffraction [65,66,69].

The parameter measured in CD is Δε, and is directly related to normal absorption which follows from the Lamber-Beer law as:

$$\Delta\varepsilon = \frac{\Delta A}{cL} = \frac{(AL \div AR)}{cL} \qquad \textbf{Equation 3.4.1}$$

in which AL and AR are the absorption of left and right handed polarized light, c is the concentration of the chromophore in mole/dm^3, L is the path length in centimetres, and Δε is the molar absorption difference in litre mole^{-1} cm^{-1} [65].

An alternative parameter is the molar ellipticity, $[\theta]_\lambda$, which originates from the fact that CD causes a circularly polarised light beam to become elliptically polarized after passing through an optically active sample. The molar ellipticity is given as:

$$[\theta]\lambda = 3300\Delta\varepsilon \qquad \textbf{Equation 3.4.2}$$

in which $[\theta]\lambda$ is given in degrees dl mole^{-1} dm^{-1} [66,69].

3.5 Nuclear Magnetic Resonance (NMR)

A more thorough description will be devoted to NMR than to the other methods, since NMR experiments were especially central to this study.

NMR is dealing with the interaction experienced by nuclear spins exposed to magnetic fields. A nuclear spin has a magnetic moment, μ, associated with it, which is according to the classical picture, precessing randomly distributed on the surface of a cone with a certain frequency, called the Larmor frequency, ν_L, Figure 3.5.1 [70].

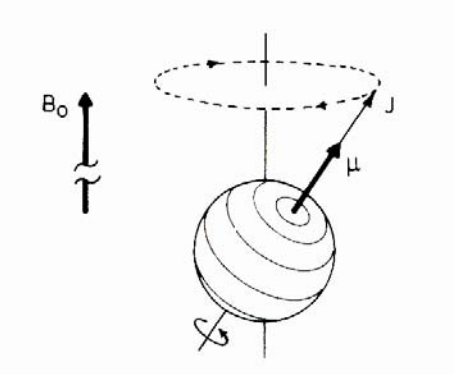

Figure 3.5.1 Nucleus with spin > 0 placed in a magnetic field, B_0. The spin-associated, magnetic moment (μ), is precessing on a surface of a cone, J.

When nuclei are placed in an external applied magnetic field, the precessing magnetic moments of the nuclei will take up preferential orientations relative to the direction of the applied field. The spin angular momentum of the nuclei are quantized, and is 2I + 1, where I is the angular momentum quantum number. Thus for nuclei with spin I = ½, as for example ^{1}H, ^{13}C, ^{15}N, ^{19}F or ^{31}P, there are two preferential orientations of the net spin angular momentum (either parallel or anti-parallel to the applied magnetic field) and hence two energy levels corresponding to the magnetic spin quantum numbers +½ and -½. By contrast, ^{16}O and ^{12}C, the main building block of organic compounds, have zero spin, and can consequently not be observed by NMR [70].

The preferred energetic orientation of nuclei in a magnetic field is the situation where the net intrinsic magnetic moment, μ, is parallel to the external field direction (as apposed to being anti-parallel to the external field)[70]. The energy difference between adjacent levels is given as:

$$\Delta E = \gamma \hbar B_0(1- \sigma) \qquad \textbf{Equation 3.5.1}$$

in which γ is a constant for each nuclide and is called the gyromagnetic ratio, ħ is the Planck constant, and B_0 is the strength of the external magnetic field and σ is a shielding constant which is determined by the electronic and magnetic environment of the nuclei being observed [70]. As can be seen from the equation 3.5.1, detection sensitivity (which involves increasing ΔE) depends on the identity of the nuclide (γ). ^{1}H and ^{19}F have large gyromagnetic ratios (γ), and are consequently easy to observe by NMR. The detection sensitivity also depends on the strength of the applied magnetic field. Development of

high field spectrometers in recent years has therefore increased the power of the NMR technique. The highest commercial field NMR instrument today is operating at 900 MHz (for proton transitions), which corresponds to 21.14 T [70].

NMR spectra are generated by applying complex sequences of radio-frequency pulses, which perturb the equilibrium nuclear magnetization [70]. (For an explanation of pulse sequences and how they effect the intrinsic magnetic moments of the nuclei, the reader is referred to "Spin dynamics" [71]). The nuclei in the sample are excited to flip between the energy levels when the applied frequency matches the energy difference between two adjacent energy levels, or put in another way, is equal to the Larmor frequency of the precessing magnetic moments of the nuclei [70]. Based upon equation 3.5.1, and the well known formula, $\Delta E = h\nu \leftrightarrow \Delta E = \nu\hbar 2\pi$, the generator frequency is easily deduced to:

$$\nu = \frac{\gamma B_0}{2\pi}(1 \div \sigma) \qquad \textbf{Equation 3.5.2}$$

Due to the population excess in the lower level, the absorption of energy from the irradiating field is the dominant process. This is observed as a signal, whose intensity is proportional to the population difference, and thus also the concentration of the sample. As the system relaxes back to equilibrium, the motion of the net magnetization vector (often called free induction decay (FID)) is detected as transient time domain signals in a receiver coil. A mathematical technique called Fourier transformation, converts the transient time domain signals into frequencies, which yields a one-dimensional NMR spectrum, a series of resonances from the various nuclei at different frequencies, Figure 3.5.2 [70].

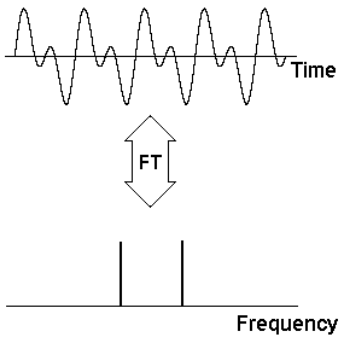

Figure 3.5.2 A time domain spectrum converted to frequency domain spectrum by a Fourier transfomation.

At present, almost all NMR studies of biological macromolecules depend heavily upon two- or higher-dimensional methods, which improve the resolution by spreading out the resonances in, respectively, two or more dimensions. A two-dimensional (2D) experiment consists of a preparation period, an evolution period (t_1) during which the spins are labelled according to their resonance frequencies, a mixing period during which the spins are correlated with each other, and finally a detection period (t_2). A number of experiments are recorded with successively incremented values of the evolution period t_1. With each t_1 value, a FID is recorded in the usual way. However, the pulse sequences are designed so that the signals detected in t_2 are modulated in amplitude as a function of the delay t_1. Subsequent Fourier transformation of the already recorded FIDs (which are sinusoidally modulated by intensities) then gives the desired 2D spectrum. The diagonal in the 2D spectrum corresponds to the one-dimensional spectrum, while the off-diagonal peaks contain information about connections between resonances on the diagonal. The nature of these connections depends on the kind of experiment being carried out [70,72,73].

Two-dimensional methods have proved to be a powerful technique for structure determination of small proteins; however, several problems arise when investigating large proteins (more than 100 residues) due to overlap of the resonances. The overlap of the resonances is caused by the many protons that the large protein constitute and that the resonance line width increase with size of the protein. The problems associated with spectral overlap can be solved by increasing the dimensionality of the spectrum, which requires isotopic labelling with ^{13}C or ^{15}N. Overlapping resonances can then readily be characterized with the additional frequency of an associated nucleus. Three- and four-dimensional NMR methods are today standard methods for investigation of large proteins comprising a molecular mass larger than ~12 kDa [72].

3.5.1 Resonance Assignment of Proteins by ^1H NMR Spectroscopy

In general, three physical phenomena are exploited in structure determination by liquid-state NMR: Chemical shift, scalar coupling, and cross-relaxation, which gives rise to the nuclear overhauser effect (NOE) [72,73]. These three parameters will be briefly introduced.

Chemical shift:

Virtually every nucleus within a biological molecule is influenced by a slightly different magnetic field, which is less than the applied magnetic field. This effect can be attributed to several factors, the most important being the electron density surrounding the nucleus and nearby magnetic dipoles (from nuclei as well as electron spin). The effect can be expressed as $B_{effective} = B_0 - \sigma$, where B_0 is the applied magnetic field and sigma, σ, is a shielding constant that is determined by the electronic and magnetic environment of the nuclei being observed. As can be seen in equations 3.5.1 and 3.5.2, both ΔE and the generator frequency are dependent on the shielding constant, σ [70].

The resonance frequencies are detected relative to a standard, and given the name, chemical shifts, values given as ppm or hertz. All protons in a molecule are characterized by its unique chemical shift property, unless the molecule consists of protons that are surrounded by identical environments. Under investigation of interaction of various groups of spin in a protein sample, chemical shifts are used to correlate the identity of one nucleus to another. Chemical shift assignments are therefore a first step in structure elucidation by NMR spectroscopy[70].

Exact theoretical predictions of chemical shifts are practically impossible, and the spectroscopist must therefore proceed with interpretation in an empirical way. A number of investigators have experimentally determined the random-coil chemical shifts for the 20 natural amino acids, while others have adopted a statistical approach by using information from assigned protein resonances [74].

The fact that chemical shifts are dependent on local geometries and electronic properties, and therefore also on secondary structure, has led to the development of an "assignment-independent" NMR technique to determine the secondary structure content of proteins. The method is applicable to proteins as large as 30 kDa and is generally more accurate than CD or Fourier transform infrared (FT-IR) spectroscopy in estimating secondary structure content of proteins[74].

Scalar coupling:

Nuclei that are connected by chemical bonds can exhibit scalar coupling (also known as spin-spin couplings) that are mediated by electrons forming the chemical bonds between

the nuclei. For instance, a coupled two-spin system, consisting of two nuclei, A and B, will display four energy levels corresponding to possible combinations of spin states. The orientations of the nuclear spin A, will affect the local magnetic environment of nucleus B, acting via the electrons of the bonds between them. Since nucleus, A has two possible orientations (with or against the applied magnetic field), nucleus B will have two possible and slightly different energies. In the same way, nuclei A, will also have two slightly different energy levels. Consequently, both nuclei A and B, have two different resonance frequencies each [70].

The first stage in the elucidation of the structure of proteins by NMR involves the identification of the spin-spin coupled resonances, generally by the use of a two-dimensional experiment, called Total Correlation SpectroscopY, TOCSY. A spin system is defined as a group of spins that are connected by scalar spin-spin couplings. For practical purposes, in biological macromolecules such couplings can usually be observed between hydrogen atoms that are separated by three or less covalent bonds. Since the spin-spin coupling across the peptide bond is to weak to be seen, each spin system corresponds to the resonances of an individual amino acid residue [72,73,75,76]. Many of the amino acids have unique spin system topologies and will consequently give rise to unique patterns of cross-peaks in a TOCSY experiment, Figure 3.5.1.1.

Spin systems are often described by using different letters, with the letter representing the highest field resonance preceding the others in the alphabet. When the chemical difference between the coupled nuclei is much greater than the coupling constant, the coupled nuclei are represented by letters that are well separated in the alphabet. When several chemically equivalent nuclei are present, they will all have the same letter, and the number of nuclei is added as a number [70,73]. Spin system notations will be used in the result and discussion chapter, 5.3

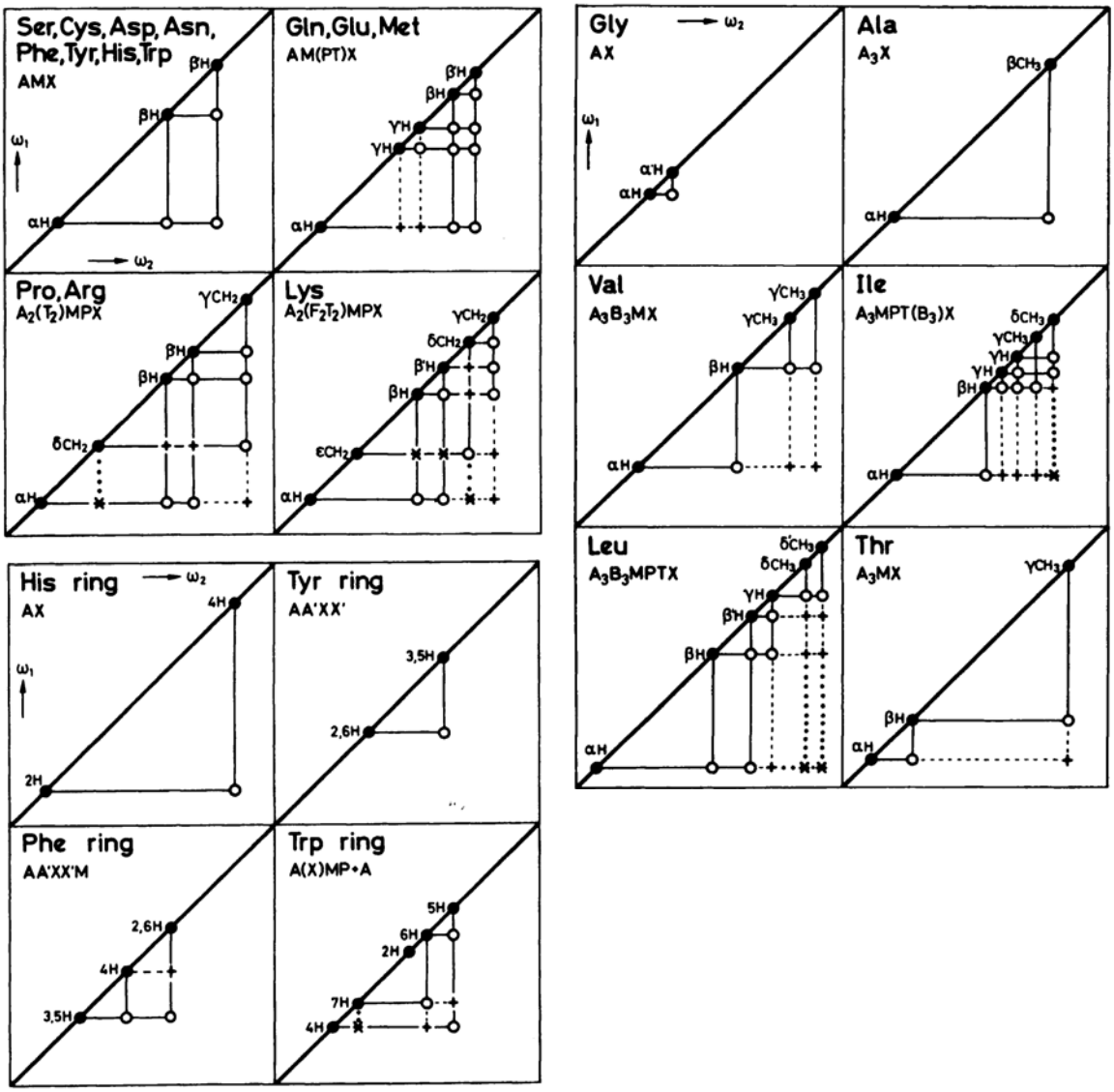

Figure 3.5.1.1 Spin systems of amino acids. All peaks may be shown in a TOCSY experiment. Figure is taken from "NMR of proteins and nucleic acids" [73].

NOE:

In short, the effect is based upon a magnetisation transfer that occurs through space, and is detected as changes in intensities of the resonance frequencies. The magnetisation transfer takes place after a perturbation of the spin states, when the system relaxes back to equilibrium by dipole-dipole relaxation. The dipole-dipole relaxation process involves an interaction between fluctuating magnetic fields of nearby nuclei, close in space. When a nucleus has a fluctuating magnetic field with components of the appropriate frequency, it can induce relaxation of the neighbouring nuclei. However, depending on which relaxation pathway that is taken (single, double or zero quantum transitions), a new equilibrium with a new population distribution is established, and consequently the intensity of the signal will change. The nuclear overhauser effect is strongly distance dependent, falling off as the sixth power of the inter-nuclear separation, and can only be detected if the distance between the dipolar-coupled nuclei is less than 5 Å. Since NOE is a phenomenon that only depends on interactions through space, the technique can be used to derive information on which nuclei that are close to each other, and hence, the three-dimensional structure [70,72,73].

The two-dimensional technique, Nuclear Overhauser Effect SpectroscopY (NOESY), is used for determination of distances between protons. Having identified the spin systems of the amino acids as much as possible from TOCSY experiments, the next stage in the structure elucidation of proteins, is to obtain sequential assignments by detailed analysis of NOESY spectra. These sequence-specific assignments are achieved by correlating one amino acid spin system with the spin systems of its neighbouring residue in the sequence by observing NOE interactions as $d_{\alpha N}(i, i + 1)$ and $d_{\beta N}(i, i +1)$, Figure 3.5.1.2 [72,73,75,76].

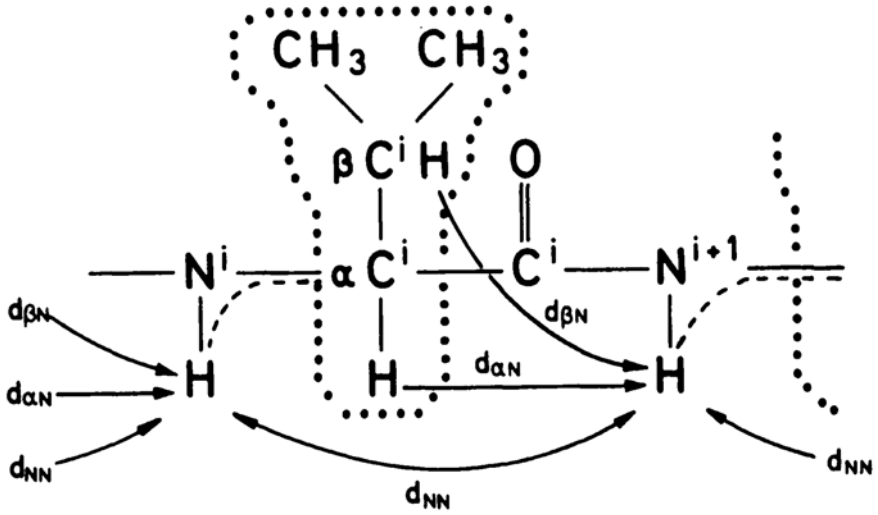

Figure 3.5.1.2 Polypeptide segment with indication of spin system to Val (inside dotted lines), and sequential connectivities shown with arrows. Figure is taken from "NMR of Proteins and Nucleic Acids" [73].

Once the sequence-specific resonance assignment is done, the common secondary structures can be obtained by looking at medium-range and long-rang H-H distances. For instance, typical medium range distances in α-helices are: $d_{\alpha N}(i, i + 3)$, $d_{\alpha N}(i, i + 4)$, $d_{NN}(i, i + 2)$ and $d_{\alpha\beta}(i, i + 3)$. Finally, long-range NMR constraints are used to determine the relative spatial locations of the secondary structure elements [72,73,75,76].

Integration of the volume or intensity of the assigned NOE-cross-peaks, yields distance-restraints, which are subsequently put into a structure calculation program to obtain the three-dimensional structure of the protein [72,73].

3.5.2 Structure Calculation from NMR Data

The inter-proton distances, r_{ij}, derived from calculated NOE intensities, is the main source of information for structural determination of three-dimensional structures. The distances are calculated according to equation 3.5.2.1, with an appropriate reference for distance calibration [72].

$$r_{ij} = r_{ref}\left(\frac{I_{ref}}{I_{ij}}\right)^{1/6}$$ **Equation 3.5.2.1**

Since experimental distances are imprecise due to peak integration errors, spin diffusion and internal dynamics, they are always specified between lower and upper boundaries. As an example, a NOE peak with either strong, medium or weak intensity can for instance correspond to the distance ranges of 1.8-2.5 Å, 1.8-3.3 Å and 1.8-5.0 Å, respectively [72].

The available NOE distances alone, cannot determine the three-dimensional structure, and the experimental information must therefore be extended by knowledge about the chemistry such as bond lengths, bond angles and van der Waal radii of the macromolecular system. This knowledge is introduced into the calculation via a hybrid energy function, E_{hybrid}, which is a weighted sum of the experimental data and theoretical internal geometric data. The structure calculation is then a search of a global minimum of E_{hybrid}, which corresponds to a family of three-dimensional structures with the lowest values of E_{hybrid} [72,73,75,76].

One of the major bottlenecks in structure determination of biological macromolecules by NMR, is the assignments of ambiguous NOEs. In NMR spectra, several protons will have the same chemical shift by coincidence or due to limited spectral resolution, which means that the NOESY peaks are ambiguous. A solution to this problem is a computational method involving ambiguous distance restraints (ADRs), which does not make any explicit assignments of the ambiguous peaks. Instead, ambiguous NOE peaks are defined as the summed distance (D) of all the k contributions that are possible on the basis of the chemical shifts values [77]:

$$NOE \propto \sum_k D_k^{-6}$$ **Equation 3.5.3.2**

Prior to the introduction of ADRs, ambiguous data were generally not used in NMR structure calculations for the simple reason that there was no easy way to specify their direct use in calculations [77].

The structure calculation program, Ambiguous Restraints for Iterative Assignments (ARIA), is based upon the computational method involving ADRs, and was used for structure calculation of sakP(N24C + 44C) in this study. The user provides ARIA a list of assigned chemical shifts and uninterpreted or partly assigned multi-dimensional homonuclear or heteronuclear resolved NOE cross-peak lists. Additionally, torsion angles, J couplings, residual dipolar couplings, H-bonds, disulphide bonds, and planarity restraints can be specified. The user can specify whether ARIA is allowed to assign unassigned peaks or only use fully assigned peaks, and whether peaks should be "thrown away" if they exceed a certain violation boundary [77].

When ARIA starts, it converts the NOE peak lists to calibrated ambiguous distance restraints. The calibration method includes a spin diffusion correction in order to improve the accuracy. The calculation is performed in an iterative way, starting with iteration 0 which is a preliminary structure that may for instance be based on a few unambiguous NOEs or a model of a different protein with sequence homology. The reason for this iterative calculation is that ambiguous NOEs can only be interpreted on the basis of an initial three-dimensional structure. In every iteration, ARIA calculates a specified number of structures that is typically 20. All iterations (except for it.0) will be based on the merged peak-lists of the lowest energy structures from the previous iteration. The iteration number is also specified by the user and is typically set to 7. The energy, root mean square (RMS) differences, and violation for different experimental restraints will be given for each calculated structure [77].

ARIA leads to a substantial speed-up of structure calculation by automation of one of the most time-consuming steps. Compared with a manual approach where initial structures are calculated based on a small fraction of the NOEs, the automated approach uses much more data to direct the calculation from the start. However, full automation has not been reached at the present state of the art, and in order to obtain high-resolution NMR structures, the spectroscopist still has to check the assignments [77]. ARIA has been successfully applied in several NMR structure determinations in laboratories all over the world. This can easily be verified with a quick search for ARIA-references in a Protein Data Bank.

4 Materials and Methods

4.1 Bacterial Strains and Bacteriocin Assay

Pediocin PA-1 [18,27,78,79] was produced by *Pediococcus acidilactici* LMG 2351 that was isolated from commercial starter cultures obtained from Christian Hansen Laboratories, Copenhagen, Denmark. Sakacin P and sakP(N24C + 44C) were produced by a bacteriocin expression system developed recently [42,80,81].

Bacteriocin activity was measured by using a microtiter plate assay system as described previously [42,82]. Each well of the microtiter plate contained 200 µl MRS broth, bacteriocin fractions at twofold dilutions, and the indicator strain *Lactobacillus sake* NCDO 2714. The microtiter plate cultures were incubated for 15 hours at 30 ^{o}C. The growth inhibition of the indicator organism was measured spectrophotometrically at 600 nm by use of a Dynatech microplate reader. One bacteriocin unit (BU) was defined as the amount of bacteriocin that inhibited the growth of the indicator strain by 50%.

4.2 Isolation of Bacteriocins by Ion Exchange Chromatography

Two different procedures were applied prior to the use of the cation exchange column. Procedure 1 is in accordance with a standard purification protocol [18], while procedure 2 is a new purification procedure established in this study.

1) Standard purification protocol: The over-night culture was centrifuged at ~3,000 x g for 15 min in order to remove the bacterial cells. The bacteriocins were then isolated by ammonium sulphate precipitation (40% wt/v). The precipitate was collected by centrifugation at ~9,000 x g for 20 min, and solubilized in 150 ml 20 mM sodium phosphate buffer (pH = 5.2) per 1 L starting-culture.

2) New established procedure: The over-night culture was applied directly on the cationic exchange column.

In both procedures (newly established purification procedure and standard purification protocol), a 3 ml SP Sepharose Fast Flow cation exchange column (equilibrated with 100 ml of 20 mM sodium phosphate buffer (pH = 5.2)) per 0.5 L starter-culture was used. After applying the sample, the column was washed with 100 ml of the sodium phosphate buffer (pH = 5.2). In the newly established purification procedure, an extra wash of 30 ml 0.15 M – 0.2 M NaCl + 20 mM sodium phosphate buffer (pH = 5.2) was applied prior to elution with 40 ml 1 M NaCl + 20 mM sodium phosphate buffer (pH = 5.2). (The two latter volumes also correspond to 0.5 L starter-culture).

4.3 Isolation of Bacteriocins by Hydrophobic Interaction Chromatography (HIC)

Ten % (wt/v) ammonium sulphate was added to the eluent obtained from the cation exchange column in the standard purification procedure before it was applied to a 1 ml Octyl Sepharose CL-4B column (equilibrated with 10 ml of 20 mM sodium phosphate buffer (pH = 5.2)). After applying the sample, the column was washed with 10 ml of the sodium phosphate buffer, pH = 5.2, and the bacteriocin was eluted with 10 ml 70% ethanol. The eluent from the cation exchange column in the newly established purification procedure was not applied to the HIC column.

4.4 Isolation of Bacteriocins on a Reverse Phase Column using the FPLC-System (Fast Protein Liquid Chromatography)

Before application to the reverse phase column (3 ml RESOURCE RPC) on the FPLC-system, 2-propanol and trifluoroacetic acid (TFA) were added to final concentrations of 5% and 0.1% (v/v), respectively, to the eluent obtained from the ionic exchange column in the new purification procedure, whereas the eluent obtained from the hydrophobic interaction column in the standard purification procedure was diluted 5 times. The column was equilibrated with 50 ml 5% (v/v) 2-propanol containing 0.1% (v/v) TFA before the

eluent from the ion-exchange column was applied (new purification procedure), and equilibrated with 50 ml 0.1% TFA when the eluent from the HIC column was applied (standard purification procedure). A linear elution gradient that started at 12% (v/v) 2-propanol, 0.1% (v/v) TFA and ended at 40% (v/v) 2-propanol, 0.1% (v/v) TFA was applied. The elution volume was 20 ml, and the flow speed was 1 ml/min. The absorbance at 280 nm as a function of ml eluent was recorded.

4.5 Isolation of Bacteriocins on a Reverse Phase Column using the SMART-System (Micro-Preparative/Analytic Chromatographic System)

The SMART system with a reverse phase column (μRPC C_2/C_{18} SC.2.1/110) was used to analyse the degree of purification of the isolated peptides. After equilibrating the column with 10 ml of 5% (v/v) 2-propanol and 0.1% (v/v) TFA, a linear elution gradient was applied that started at 5% (v/v) 2-propanol, 0.1% (v/v) TFA and ended at 40% (v/v) 2-propanol, 0.1 % (v/v) TFA. The elution volume was 2 ml and the flow rate was 100 μl/ml. The absorbance at 214, 254 and 280 nm as a function of ml eluent, was recorded.

4.6 Analysis of SakP(N24C + 44C) by Capillary Zone Electrophoresis

The capillary electrophoresis system with untreated fused silica capillary, diameter = 75 μm, length = 20 cm (P/ACE System 2050, Beckman), was used to verify the purity of the isolated peptides. The cationic peptides were solubilized in 20 mM sodium phosphate buffer pH = 2.5. A voltage of 10 kV and a current of 65.7 μAMP were applied.

4.7 Analysis of SakP(N24C + 44C) by MALDI-TOF MS

MALDI-TOF MS with a reflector mode was used to verify the identity and purity of the isolated bacteriocins. 1:1 ratio of 3% TFA and acetonitril, saturated with α-cyano-4-hydroxycinnamic acid was used as matrix.

4.8 CD Measurement of Sakacin P and SakP(N24C + 44C)

Circular dichroism spectra were recorded by using a Jasco J-810 spectrometer, calibrated with ammonium D-camphor-10-sulfonate. Both peptides were solubilized in water with 0.1% (v/v) TFA. The measurements were performed in the presence TFE (0-90% (v/v)) and DPC (2 –14 mM) with a peptide concentration of 0.1 mg/ml at various temperatures (12 – 52 ^{o}C). A quartz cuvette with a path length of 1 mm was used. Samples were scanned 3-6 times at 20 nm/min with a time constant of 2 s and a slit width of 2 nm, over the wavelength range 260 – 190 nm. The data were averaged, and the spectrum of a protein-free control sample was subtracted, thus giving the mean residual ellipticity of the peptide.

The α-helical content of the peptides under the various solvent conditions was calculated from the mean residual ellipticity at 222 nm, ($[\theta]_{222}$), by using the following equation:

$$f_H = [\theta]_{222} / (-40000(1 - 2{,}5/n)) \qquad \textbf{Equation 4.8.1}$$

in which f_H represents the α-helical content and n represents the number of peptide bonds [83]. All measurements were conducted at least twice, and crucial measurements were repeated several times, until the standard deviations in the percentage of α-helical structure were below 2 %.

4.9 NMR Sample Preparation of SakP(N24C + 44C)

SakP(N24C + 44C) (isolated from approximately 10 L culture), was dissolved in 700 µl 250 mM deuterated DPC (micelles) and 10% deuterated water to a final concentration of 1 mM. The sample was acidified by TFA to a final concentration of 0.1% to obtain a pH = 2.8.

4.10 NMR Spectroscopy of SakP(N24C + 44C)

The spectra for sakP(N24C + 44C) were recorded on a Bruker DRX500 equipped with pulsed field gradients. Two-dimensional homonuclear total correlation spectroscopy (TOCSY) and nuclear overhauser effect spectroscopy (NOESY) were employed to obtain sequential resonance assignments and NOE patterns. In order to solve ambiguities caused by overlapping resonances, various spectra were obtained at temperatures 22 ^{o}C, 32 ^{o}C, 42 ^{o}C and 52 ^{o}C. TOCSY spectra were measured using the DIPSI-2rc sequence [84]. Water suppression was obtained by applying the WATERGATE pulse sequence [85]. A series of mixing times between 40 and 65 ms was used for the TOCSY. NOESY spectra were acquired with 150 ms mixing time for structure calculation and 200 ms mixing time to facilitate sequential assignment.

All spectral data were collected with 512 - 800 increments in the t_1 dimension, 2048 complex data points in t_2 dimension and 16 - 32 scans. Prior to Fourier transformation, the data matrix was multiplied by a Gaussian (F2) and sine bell (F1) window function and zero-filled to 2K x 1K complex points. Data were processed using the Bruker XWIN-NMR software (version 2.6), and further analysed by XEASY software (version 1.3). Integration of NOE correlations observed in NOESY spectra with 150 ms mixing time was obtained in XEASY using the maximum integration mode of XEASY. Thirteen hydrogen bond restraints (range 1.8-2.8 Å) were included in the structure calculations at a later stage. These restraints were determined on the basis of structural NOE patterns in the α-helical region and comprised the range of residues 18 – 33.

The structure calculation was performed with a simulated annealing protocol using CNS v1.1 [86] and ARIA 1.2 [77,87]. A total of 449 NOEs (including 303 intra-residue, 97 medium and 49 long range NOEs) were employed for distance constraints for calculating the structure of sakP(N24C + 44C). A total of 50 structures were generated in the final calculation, of which the 10 best low-energy structures were selected. The molecular models were generated with MOLMOL [88].

5 Results and Discussion

5.1 Purification of Pediocin-Like Bacteriocins and Other Cationic Antimicrobial Peptides from Complex Culture Media

The standard purification protocol for purification of pediocin-like bacteriocins and other cationic antimicrobial peptides was compared with a new purification procedure established in this study.

The standard purification protocol generally includes a centrifugation step for the removal of cells from the bacterial culture medium, followed by ammonium sulphate precipitation in order to concentrate the peptides. The precipitation is then collected by centrifugation and subsequently purified to homogeneity by sequential chromatography on cation exchange, hydrophobic interaction and reverse-phase columns.

The new purification procedure is in contrast to the standard purification protocol, a rapid two-step procedure, which avoids centrifugation and ammonium sulphate precipitation, simply by adding the starting culture directly on the cation exchange column. The eluent from the cation exchange column was then purified to homogeneity by applying it to a reverse-phase column. The hydrophobic interaction column that was used in the standard purification procedure was therefore also avoided in the newly established procedure.

5.1.1 Purification by the Standard Purification Protocol

The standard purification procedure is illustrated by purification of pediocin PA-1 in Table 5.1.1.1.

Table 5.1.1.1 Purification of pediocin PA-1 by standard purification protocol.

Fractionation step/fraction	Volume (ml)	Total A_{280}[a]	Total activity (BU) (10^6)	Specific activity[b]	Increase in specific activity[b]	Yield (%)
Bacterial culture	400	1.35×10^4	8	600	1	100
Step 1[c] (centrifugation)	400	1.35×10^4	8	600	1	100
Step 2[d] (amm. sulph. ppt)	75	250	1	4×10^3	7	15
Step 3[e] (cation exchange)	40	2.4	0.85	3.5×10^5	600	10
Step 4[f] (HIC)	10	1.0	1.5	1.5×10^6	2.5×10^3	20
Step 5[g] (reverse phase) 1st run	1.3	0.20	0.9	4.5×10^6	7.5×10^3	10
Step 5[g] (reverse phase) 2nd run	1.3	0.15[h]	0.7	4.7×10^6	8×10^3	10

[a] Total A_{280} is the A_{280} multiplied by the volume in millilitres.

[b] Specific activity is total activity (in BU) divided by total A_{280}.

[c] Bacteria were removed from culture by centrifugation at ~3,000 x g for 15 min.

[d] Peptides were precipitated (ppt) by adding ammonium sulphate (amm. sulph) (400 g per litre) and pelleting the precipitate by centrifugation at ~9,000 x g for 20 min.

[e] The fraction from step 2 was applied on a 3 ml SP Sepharose Fast Flow cation exchange column equilibrated with 20 mM sodium phosphate, pH = 5.2. The column was subsequently washed with 40 ml of the sodium phosphate buffer, and pediocin PA-1 was then eluted with 40 ml of 1 M NaCl.

[f] The fraction from step 3 was applied on a 1ml Octyl-Sepharose hydrophobic interaction column (HIC), and pediocin PA-1 was then eluted with 70% (v/v) ethanol.

[g] The fraction from step 4 was chromatographed on a reverse-phase column.

[h] The amount of pediocin PA-1 purified from a 400 ml bacterial culture was determined to be 45 μg.

The standard purification protocol functioned reasonably well when purifying smaller quantities of peptides. However, the procedure became very time-consuming and tedious when it was applied for large-scale purification. This was due to the many centrifugation steps that were involved and the relatively low yield that was obtained. As can be seen in Table 5.1.1, only 15% of the activity that was initially in the culture supernatant was recovered after ammonium sulphate precipitation. The large loss of bacteriocin after the ammonium sulphate precipitation was in part due to the fact that the precipitate tended to float, even after centrifugation, and was therefore difficult to collect. Since the standard purification procedure became cumbersome when purifying large quantities of peptide, the procedure was not used for purification of sakP(N24C + 44C) that was needed for this study.

5.1.2 Purification by a Newly Established Purification Procedure

The new purification procedure is also illustrated with the purification of pediocin PA-l, and the results are given in Table 5.1.2.1. It should be noted that the same culture and the same amount was used in this procedure as in the standard procedure described in chapter 5.1.1, making the results comparable.

Table 5.1.2.1 Purification of pediocin PA-1 by newly established procedure.

Fractionation step/fraction	Volume (ml)	Total A_{280}[a]	Total activity (BU) (10^6)	Specific activity[b]	Increase in specific activity[b]	Yield (%)
Bacterial culture	400	1.35×10^4	8	600	1	100
Step 1[c] (cation exchange)	40	40	7	1.7×10^5	300	85
Step 2[d] (reverse phase) 1st run	1.4	1.25	7.5	6×10^6	1×10^4	95
Step 2[d] (reverse phase) 2nd run	1.6	1.0[e]	9	9×10^6	1.5×10^4	110

[a] Total A_{280} is the A_{280} multiplied by the volume in millilitres.

[b] Specific activity is total activity (in BU) divided by total A_{280}.

[c] The bacterial culture was applied on a 3 ml SP Sepharose Fast Flow cation exchange column equilibrated with 20 mM sodium phosphate, pH = 5.2. The column was subsequently washed with 15 column volumes of the sodium phosphate buffer and 5 column volumes of the sodium phosphate buffer containing 0.2 M NaCl, and pediocin PA-1 was then eluted with 40 ml of the sodium phosphate buffer containing 1 M NaCl.

[d] The fraction from step 1 was applied on reverse phase column, using a FPLC system.

[e] The amount of pediocin PA-1 purified from a 400-ml bacterial culture was determined to be 300 µg from the UV absorption at 280 nm and the molecular extinction coefficient calculated from the contribution of individual amino acid residues.

The capacity of the SP Sepharose Fast Flow cation exchange column in the new purification procedure was determined by applying an overnight stationary bacterial culture producing pediocin PA-1. Flow-through fractions were collected and assayed for bacteriocin activity, as can be seen in Figure 5.1.2.1.

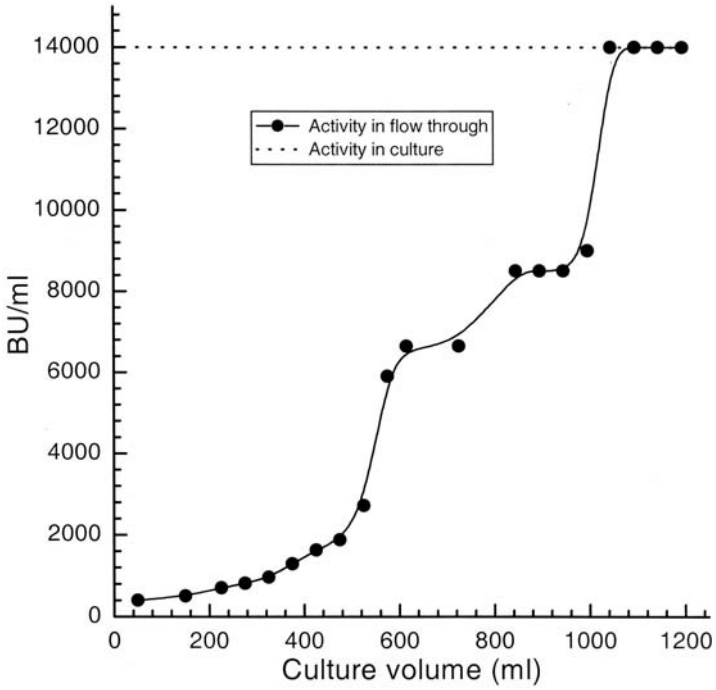

Figure 5.1.2.1 An overnight culture of P. acidilactici LMG 2351, producing pediocin PA-1 was applied on a 3 ml SP Sepharose Fast Flow cation exchange column. The graph represents the amount of bacteriocin activity in the flow-through fraction as a function of the amount of bacterial culture that has percolated the column. The horizontal, stippled line indicates the activity in the bacterial culture before it was applied to the column.

Only about 4 and 7% of the bacteriocin activity were lost in the flow-through fraction when, respectively, 300 and 500 ml of the culture were applied to the 3 ml cation exchange column. Binding of the bacteriocin was, however, significantly reduced when more than 600 ml of culture was applied to the column. After 600 ml of culture had percolated the column, less than 50% were bound, and essentially no further binding was obtained after 1 litre had passed through the column.

The SP Sepharose Fast Flow cation-exchange column could be regenerated after use. The cation-exchange column was then washed with several column volumes of 2 M NaOH without affecting the material's binding capacity for subsequent applications (data not shown).

Since the newly established procedure was chosen for purification of sakP(N24C + 44C) that was needed for this study, the following verification of purity is shown for this peptide. The bacteriocin sakP(N24C + 44C) appeared as a major optical density peak upon reverse-phase chromatography in run 1 and run 2, which are shown in Figure 5.1.2.2.

A) Run 1 on reverse phase column **B) Run 2 on reverse phase column**

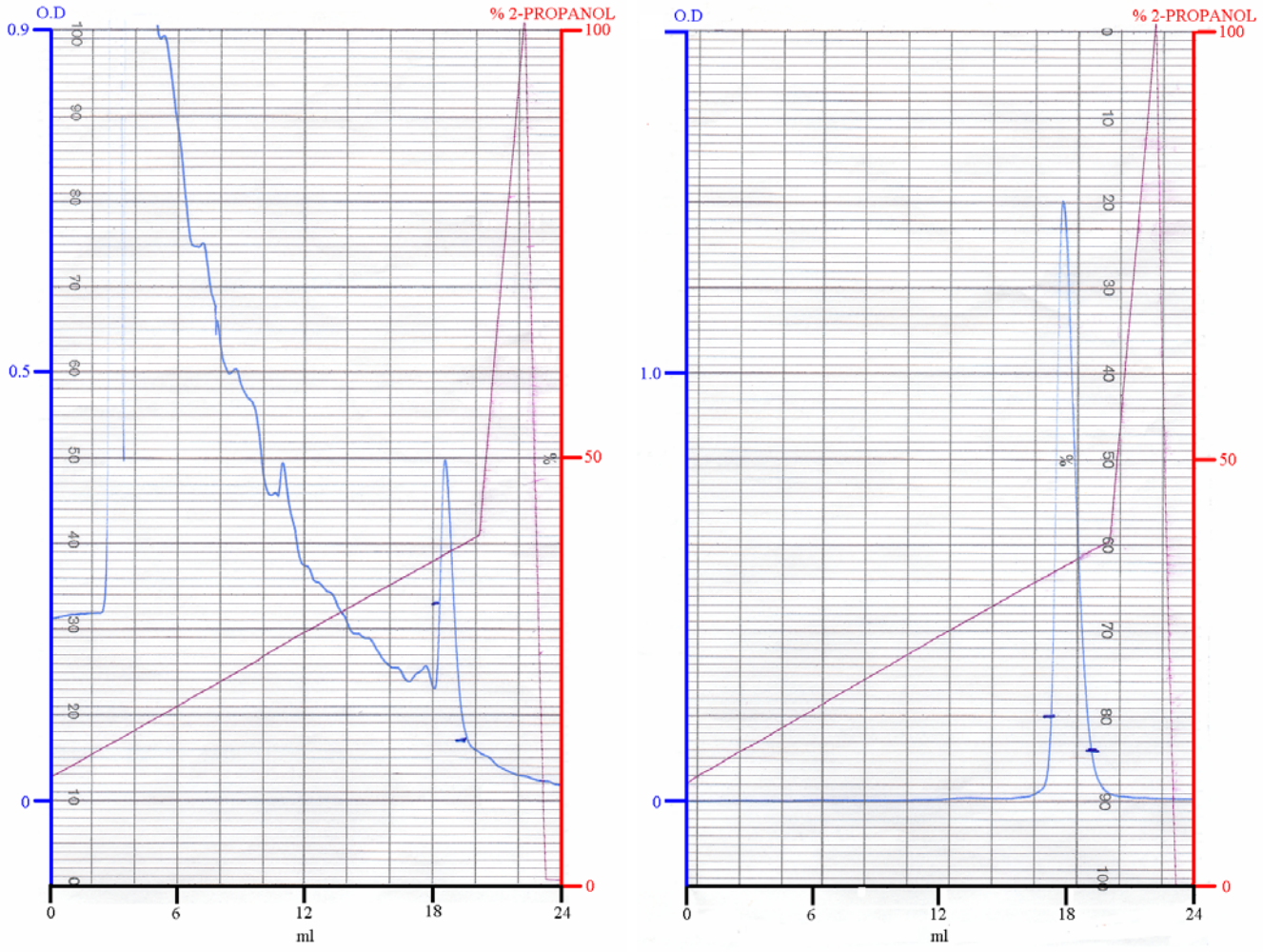

Figure 5.1.2.2 A) Reverse-phase chromatography of sakP(N24C + 44C) obtained from 500 ml starting culture eluted from a cation exchange column. The peptide was eluted from the reverse-phase column with a flow rate of 1 ml/min and a linear propanol gradient, detected as a major optical density (OD) peak at 280 nm, and fractionated as shown by blue horizontal lines. B) Eluent from reverse phase column of sakP(N24C + 44C), isolated from 1.5 L starting-culture, applied for the second time on a reverse phase column.

The identity of the purified sakP(N24C +44C) peptide obtained after reverse-phase chromatography in the new purification procedure, was verified by MALDI TOF mass spectrometry. The result gave a molecular mass of 4523 Da, which is consistent with the true molecular mass, 4524.5 Da, calculated from the amino acid sequence. Mass spectrum of sakP(N24C +44C) after two runs on the reverse phase column is shown in Figure 5.1.2.3.

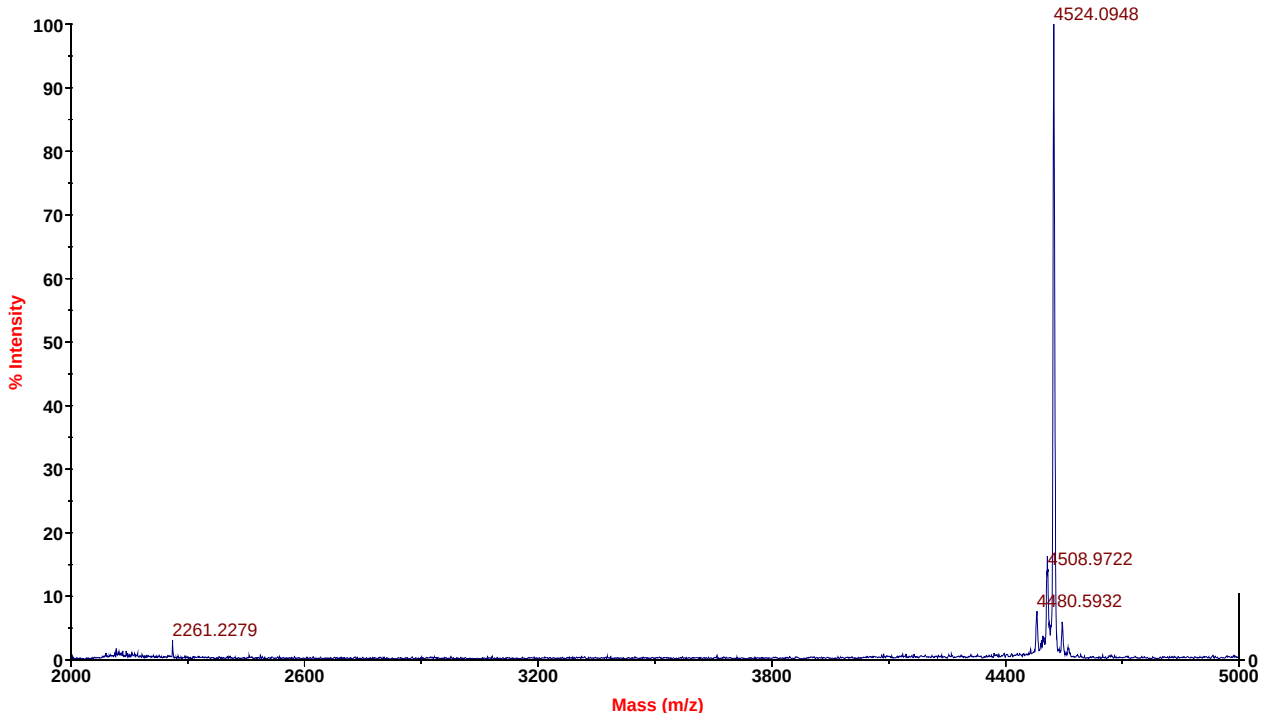

Figure 5.1.2.3 MALDI TOF mass spectrum of sakP(N24C + 44C) after second run on reverse phase column. Intensity is shown as a function of mass/charge.

The isolated peptide was determined to be more than 90% pure after two runs on the reverse phase column as judged by analytical reverse-phase chromatography (data not shown) and capillary electrophoresis. The result of capillary electrophoresis of sakP(N24C +44C) is shown in Figure 5.1.2.4.

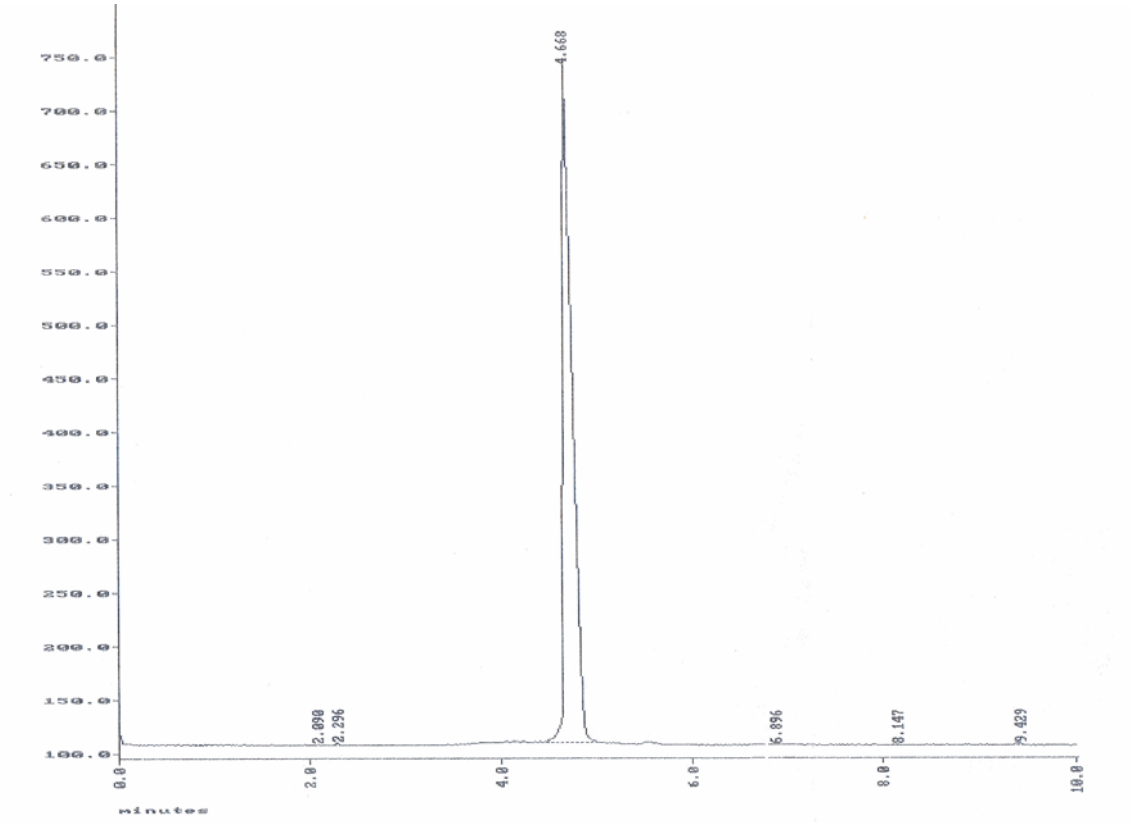

Figure 5.1.2.4 Capillary electrophoretic analysis of sakP(N24C + 44C) after isolation by the new purification procedure. mV is displayed as a function of minutes.

The new purification procedure was also tested for other cationic peptides in addition to pediocin PA-1 and sakP(N24C + 44C). These bacteriocins were the pediocin-like bacteriocins curvacin A, leucocin A and sakacin P and the non-pediocin-like bacteriocins lactococcin G, enterocin B, nisin Z and lactococcin A. The pediocin-like bacteriocins bound to the cation exchanger column, and were recovered with yields of 90% or more after bacterial cultures were passed through the column (data not shown). After passage of a culture producing the two-peptide bacteriocin lactococcin G, 33% of the recovered activity was found in the flow-through fraction, whereas only 67% was found in the 1 M NaCl fraction. A recovery similar to that obtained for lactococcin G was also obtained when a culture of *E. faecium CTC492* that produces two bacteriocins, enterocin B and the pediocin-like bacteriocin enterocin A, was passed through the cation-exchange column. Nisin Z and lactococcin A gave only 30 and 15% recovery, respectively.
The newly established purification procedure worked reasonably well for other cationic peptides, although not as good as for the pediocin-like bacteriocins. Lactococcin G did not bind to the cation exchange column as effectively as pediocin-like bacteriocins. The reason for this low affinity for the cation exchange column may be due to interactions between the two complementary peptides that lactococcin G constitutes. In spite of this, the obtained recovery for lactococcin G was higher than what has been obtained earlier using the standard purification protocol [28].

Optimization of the ion exchange chromatography conditions for purification of non-pediocin-like bacteriocins was not tried in this study, and the conditions could probably be improved to yield a higher recovery. One strategy for improvement of the new purification procedure, could be reducing the pH of the culture medium before application on the cation exchanger in order to increase the peptides affinity for the column. Another strategy could be to optimise the washing conditions before elution of the bacteriocins with 1 M NaCl. The effect of the NaCl concentration during washing strongly depended on the peptide's net positive charge. This was observed for pediocin PA-1 and sakacin P. A lower salt concentration had to be applied for the isolation of sakacin P compared to pediocin PA-1. Pediocin PA-1, which has a net positive charge of 5 to 6, could be washed with a concentration of 0.2 M NaCl without loss of bacteriocin (less than 1%). However, the same salt concentration (0.2 M NaCl) caused a loss of up to 20% during isolation of sakacin P, which has a net positive charge of 3 to 4. Consequently, the concentration of NaCl had to be reduced to 0.15 M NaCl during isolation of sakacin P in order to avoid

bacteriocin-loss of more than 1%. These results suggest that the lower net positive charge of the bacteriocin, the milder washing conditions should be applied.

The new purification procedure proved to be beneficial, especially for the large-scale purification of the pediocin-like bacteriocin sakP(N24C + 44C) that was needed for structural investigation by NMR in this study. The new purification procedure was easily scaled up with relatively little increase in purification time in contrast to the standard purification protocol. This was partly due to the many centrifugation steps that were avoided, but also the high yields obtained. The higher yield obtained by the new purification procedure is illustrated in Tables 5.1.1.1 and 5.1.2.1. More than 80% of the activity that was initially in the pediocin PA-1 culture supernatant was recovered with a purity of more than 90% in the new procedure, whereas the standard purification protocol gave only a 10% recovery. It should be noted that the same amount and the same starting culture were used in both procedures (the newly established procedure and the standard purification procedure), making the procedures comparable. The rapid new procedure made it possible to purify milligram quantities of the pediocin-like bacteriocins within a few hours, in contrast to the standard purification protocol that could take up to a week or more. For these reasons, the new purification procedure was chosen for the purification of sakP(N24C + 44C) that was needed for this study.

5.2 Analysis of Sakacin P and SakP(N24C + 44C) by Circular Dichroism (CD)

5.2.1 CD Studies of Sakacin P and SakP(N24C + 44C) in TFE and DPC Micelles

Both bacteriocins, sakacin P and sakP(N24C + 44C), were analysed by circular dichroism spectrometry in various concentrations of trifluoroethanol (TFE) and dodecylphosphocholine (DPC) micelles at 22 ^{o}C. Both solvents, TFE and DPC micelles, are frequently used in structural investigations of proteins by NMR-spectroscopy. TFE solvent is known to induce and stabilize α-helical structure in peptides that have an intrinsic tendency to adopt this type of secondary structure [89-91], whereas DPC micelles

create a membrane-mimicking environment which structures peptides such as for instance antimicrobial peptides that act upon membranes [32,92]. The CD studies of sakacin P and sakP(N24C + 44C) were done in order to examine whether these two peptides possess structural differences, compare the effect of the two different solvents, and also to find an acceptable concentration of DPC micelles for the NMR sample of sakP(N24C + 44C) that was needed in this study.

The CD spectra of both peptides, sakacin P and sakP(N24C + 44C), in aqueous solution acidified by TFA to a pH of 2.8, were all characteristic of non-structured conformations (random coil, with α-helical contents of less than about 8%). This is illustrated in Figures 5.2.1.1 and 5.2.1.2, and Table 5.2.1.1.

In the presence of TFE (50, 70, 90% (v/v)) at 22 ^{o}C, sakacin P and sakP(N24C + 44C) yielded CD spectra typical for partly α-helical peptides, Figures 5.2.1.1 and 5.2.1.2. However, sakP(N24C + 44C) had a higher degree α-helical content than the wild-type peptide, sakacin P, at all concentrations of TFE, Table 5.2.1.1. The α-helical content increased for sakP(N24C + 44C) when increasing the TFE concentration from 50 to 75% (v/v) (38% α-helix compared to 48% α-helix in, respectively, 50 and 75% (v/v) TFE). On the contrary, no increase in α-helical content was observed for sakacin P upon increasing the TFE concentration from 50 to 90%. The percentages of α-helix in sakacin P and sakP(N24C + 44C), at various TFE concentrations (v/v) are given in Table 5.2.1.1.

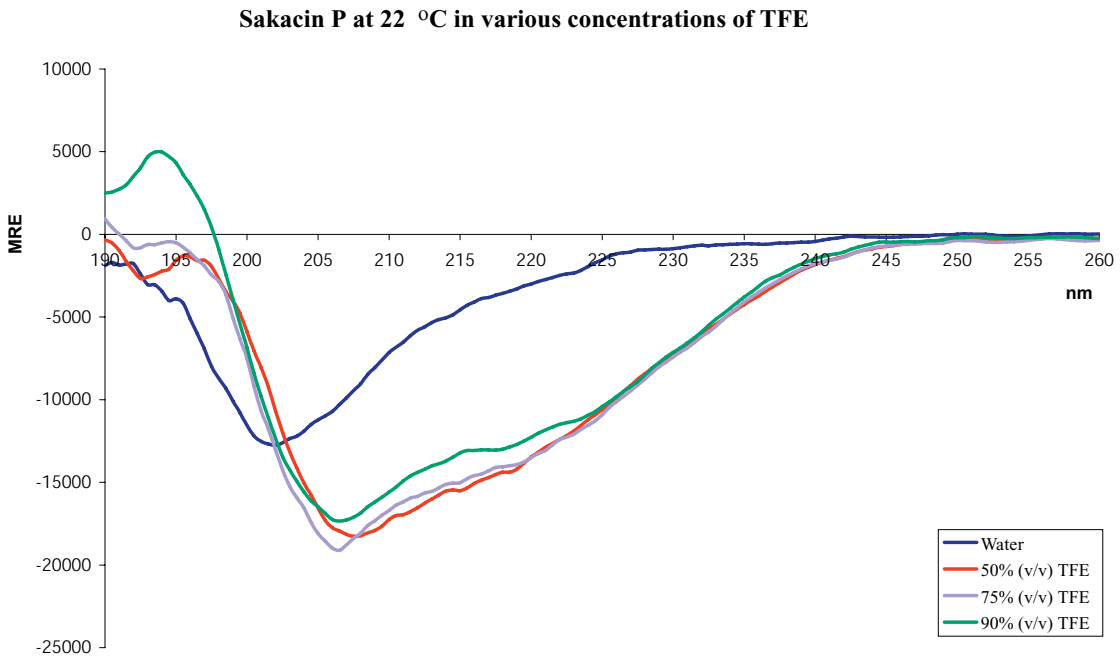

Figure 5.2.1.1 CD spectra of sakacin P at 22 °C in various concentrations (v/v) of TFE. Mean residual ellipticity (MRE) is plotted as a function of the wavelength (nm).

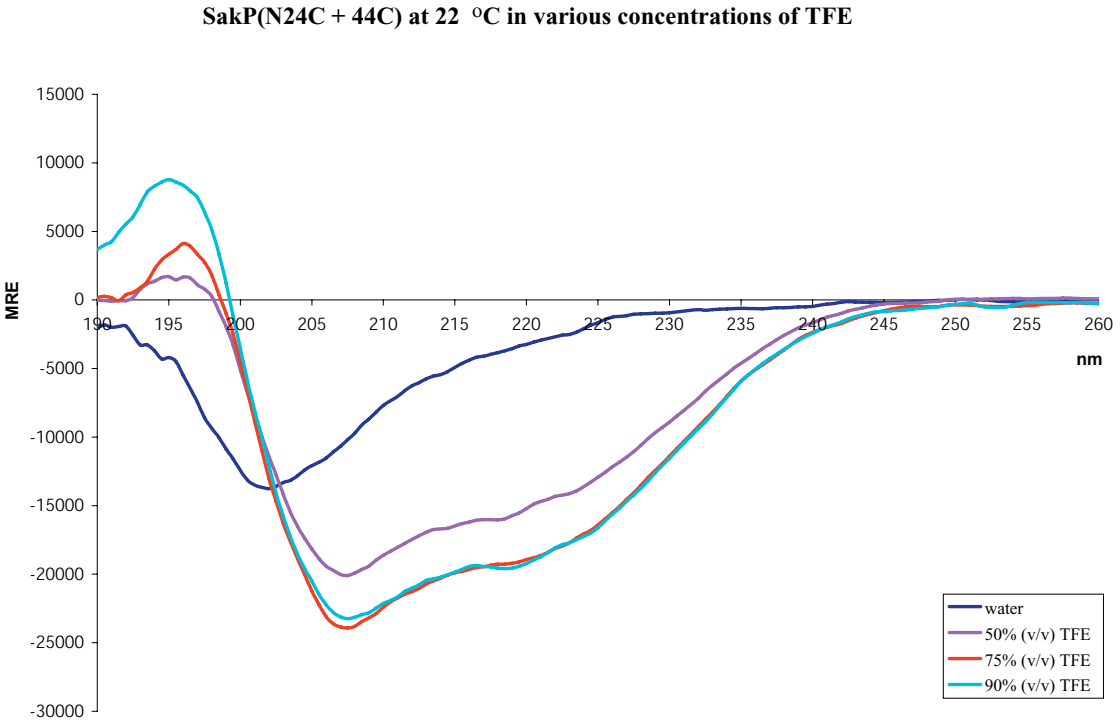

Figure 5.2.1.2 CD spectra of sakP(N24C + 44C) at 22 °C in various concentrations (v/v) of TFE. Mean residual ellipticity (MRE) is given as a function of wavelength (nm).

Table 5.2.1.1 Percentage of α-helical content in sakacin P and sakP(N24C + 44C) at various concentrations (v/v) of TFE.

	Water	**50% TFE**	**75% TFE**	**90% TFE**
Sakacin P	7%	33%	33%	31%
SakP(N24C + 44 C)	7%	38%	48%	48%

DPC at concentrations above the critical micelle concentration (1 mM), at 22 ^{o}C, also induced α-helical structure in sakacin P and sakP(N24C + 44C), Figures 5.2.1.3 and 5.2.1.4. Again, a higher degree of α-helical structure was observed for the mutated peptide than the wild-type peptide, Table 5.2.1.2. Augmentation of α-helical structure was observed for sakacin P with increasing concentrations of DPC, ranging from 2 to 14 mM. However, no additional structuring was observed for sakP(N24C + 44C) above 8 mM DPC. Maximum percentages of α-helical structure in DPC were found to be 24% and 34%, respectively, for sakacin P and sakP(N24C + 44C). Both peptides displayed a lower degree of α-helical structure in 14 mM DPC than in 50% (v/v) TFE, Tables 5.2.1.1 and 5.2.1.2.

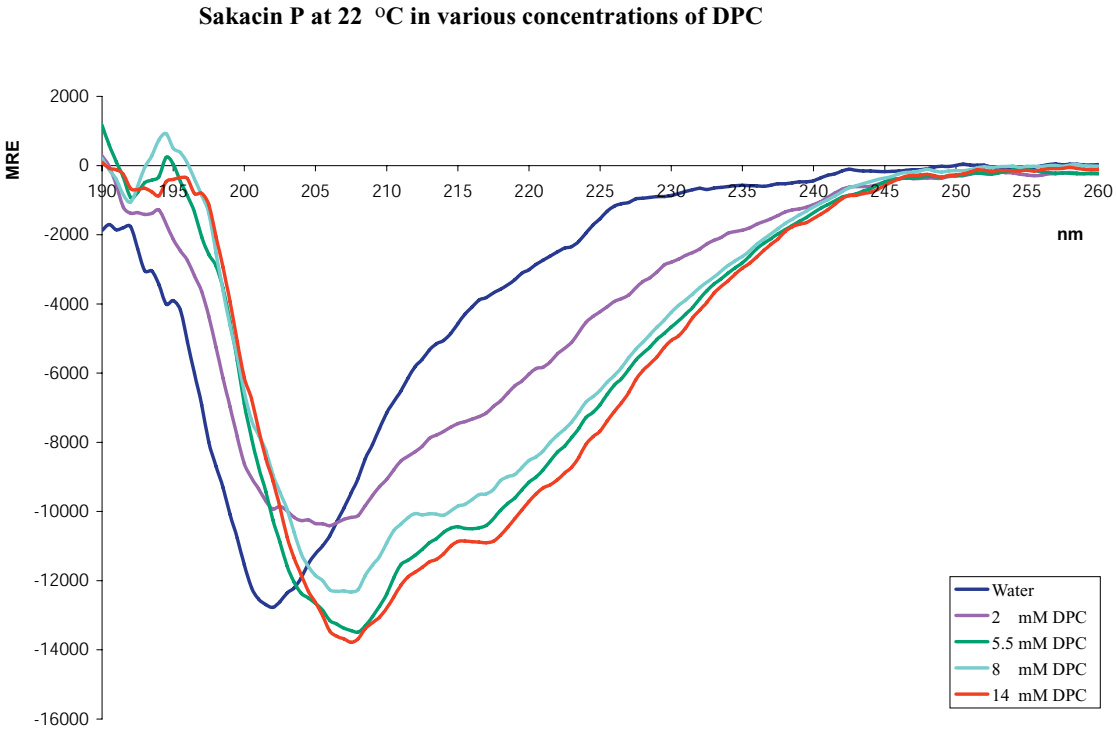

Figure 5.2.1.3 CD spectra of sakacin P at 22 °C in various concentrations of DPC. Mean residual ellipticity (MRE) is given as a function of the wavelength (nm).

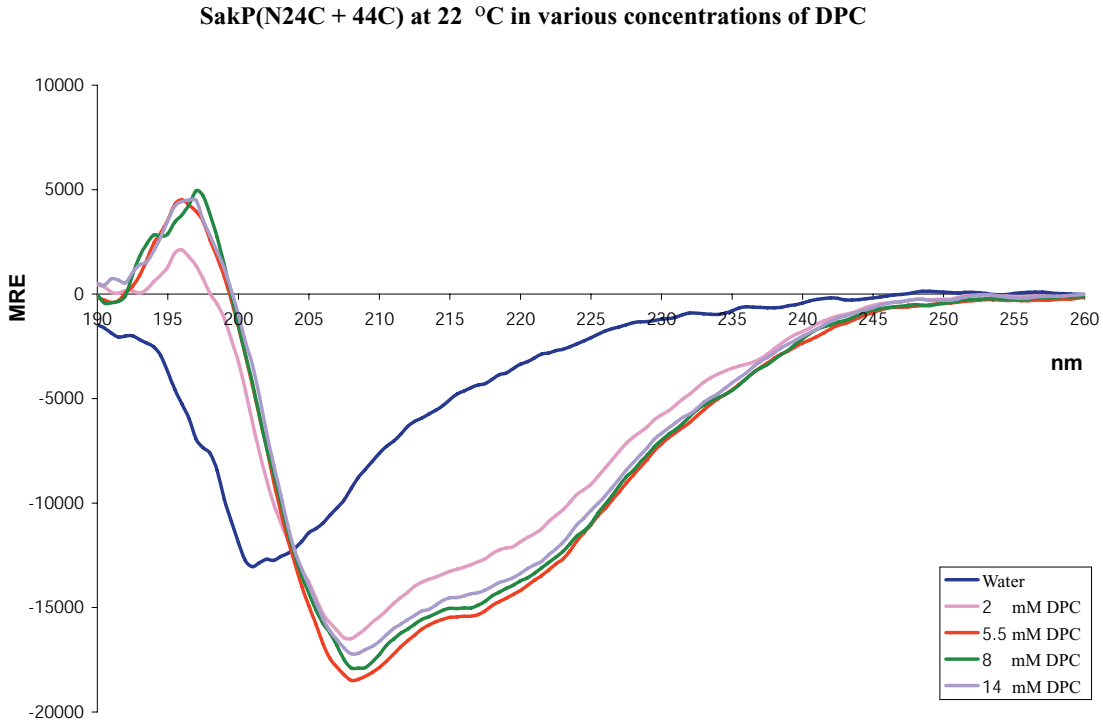

Figure 5.2.1.4 CD spectra of sakP(N24C + 44C) at 22 °C in various concentrations of DPC. Mean residual ellipticity (MRE) is given as a function of the wavelength (nm).

Table 5.2.1.2 Percentage of α-helical content in sakacin P and sakP(N24C + 44C) in various concentrations of DPC.

	Water	2 mM DPC	5.5 mM DPC	8 mM DPC	14 mM DPC
Sakacin P	7%	14%	22%	22%	24%
SakP(N24C + 44 C)	7%	29%	29%	34%	34%

The results of the CD-analysis of sakacin P and sakP(N24C + 44C) in TFE showed that parts of the peptides have an intrinsic tendency to form a right-handed α-helix. The membrane-like entities, DPC micelles, also induced α-helical structure in both sakacin P and sakP(N24C + 44C). A slightly higher percentage of α-helical content was detected for sakP(N24C + 44C) in both solvents, compared to the wild-type peptide. This is due to the extra disulphide bond that is introduced in the C-terminal half, between Cys 24 and Cys 44. This extra disulphide bond ties the C-terminal end up to the centre of the α-helix, thereby making the mutated peptide less flexible compared to the wild-type peptide. This increase in the stability of the mutated peptide accounts for the higher potency at elevated temperatures and broadening of target specifity compared to the wild-type peptide [42].

All studies performed in TFE solvent gave higher percentage of α-helical content than the corresponding studies performed in DPC micelles. This may suggest that TFE is a better solvent than DPC micelles to use in NMR structural studies. However, the use of TFE as a solvent for biological molecules is controversial. It has been claimed that TFE has a tendency to force a secondary structure on a polypeptide even though the polypeptide lacks this structure in its native state. DPC micelles also create an artificial environment, however, it is more similar to the natural environment (biological membranes), which these bacteriocins act upon. The use of DPC micelles was therefore chosen for the structuring of sakP(N24C + 44C) for the NMR-studies.

5.2.2 CD Studies of Sakacin P and SakP(N24C + 44C) in DPC Micelles at Various Temperatures

A DPC concentration of 5.5 mM was selected, since this concentration corresponds to the concentration of DPC, relative to the peptide concentration, that was in the NMR sample of sakP(N24C + 44C) used in this study.

The temperature's influence on sakacin P and sakP(N24C + 44C) in 5.5 mM DPC (at 12, 22, 32, 42 and 52 ^{o}C) is shown in Figure 5.2.2.1 and 5.2.2.2, respectively. The highest degree of α-helical content was observed at 12 ^{o}C, while a reduction in the α-helical content was observed with increasing temperatures for both peptides. Going from 12 to 52 ^{o}C in the presence of DPC micelles, decreased the α-helical content from 26 to 12% for sakacin P and from 37 to 21% for sakP(N24C + 44C). Similarly, in the presence of 90% TFE, the α-helical content decreased from 33 to 23% for sakacin P and from 51 to 38% for sakP(N24C + 44C). The percentages of α-helical content in sakacin P and sakP(N24C + 44C), at the various temperatures for both solvents, TFE and DPC, are given in Table 5.2.2.1.

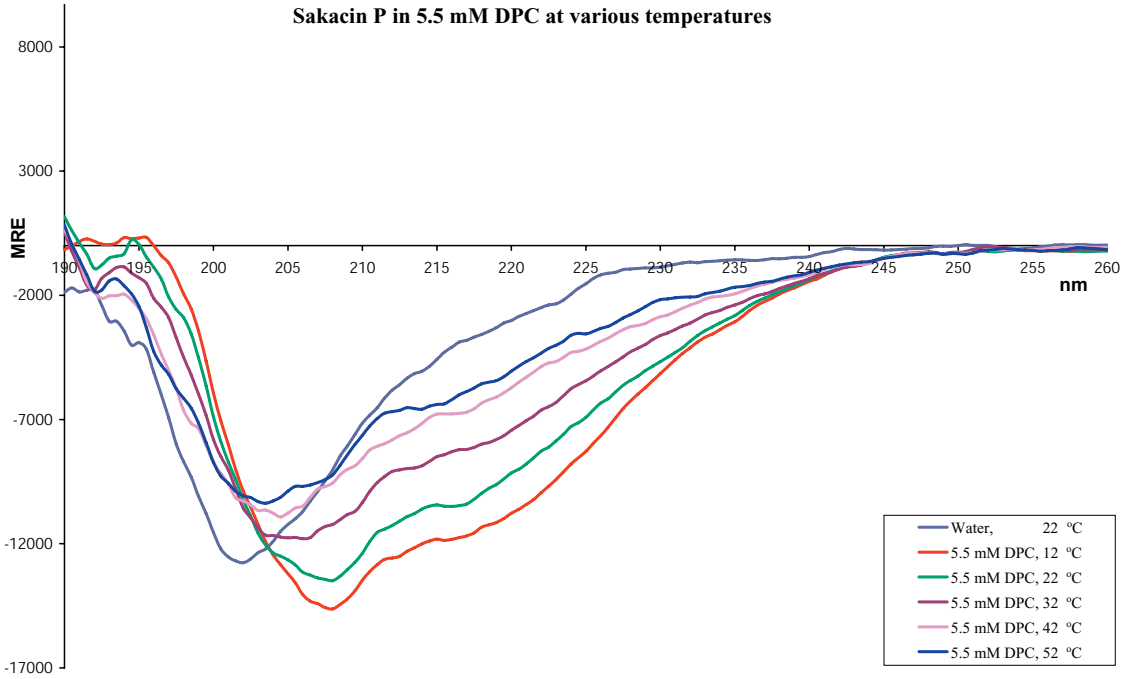

Figure 5.2.2.1 CD spectra of sakacin P in 5.5 mM DPC at various temperatures and in water at 22 °C. Mean residual ellipticity (MRE) is displayed as a function of wavelength (nm).

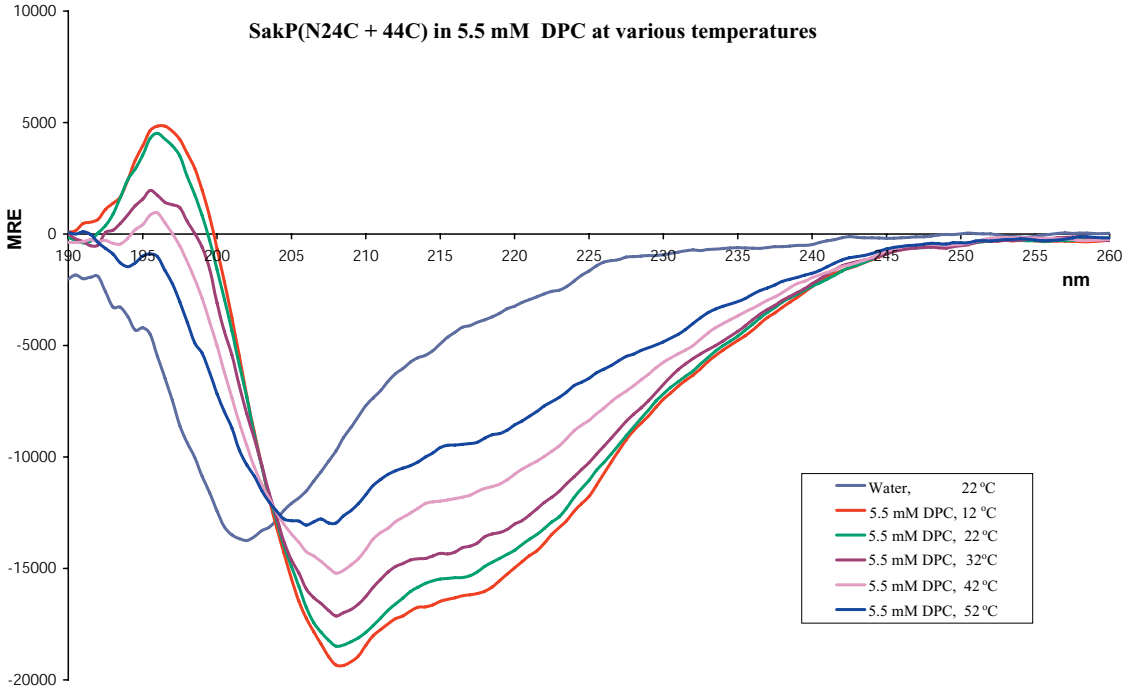

Figure 5.2.2.2 CD spectra of sakP(N24C + 44C) in 5.5 mM DPC at various temperatures and in water at 22 °C. Mean residual ellipticity (MRE) is displayed as a function of wavelength (nm).

Table 5.2.2.1 Percentage of α-helical content in various solvents and temperatures. No experiments were done for the peptides in water at 12, 22, 32, 42 and 52 °C.

	12 °C	22 °C	32 °C	42 °C	52 °C
Sakacin P in water		7%			
Sakacin P (N24C + 44 C) in water		7%			
Sakacin P in 5.5 mM DPC	26%	22%	18%	13%	12%
Sakacin P (N24C + 44 C) in 5.5 mM DPC	37%	35%	32%	27%	21%
Sakacin P in 90% TFE	33%	31%	28%	26%	23%
Sakacin P (N24C + 44 C) in 90% TFE	51%	48%	45%	42%	38%

The fact that the α-helical content decreased with increasing temperatures for both peptides may at first sight seem to be of no interest, since this is a natural result of the increase in vibrational motion. However, these results were quite valuable for the NMR analysis of sakP(N24C + 44C) that was done in this study, since several NMR spectra had to be taken at different temperatures in order to solve ambiguities due to overlapping peaks. CD spectrometry was a quick and easy way to investigate whether the peptide had preserved its secondary structure at the elevated temperatures that were used in the NMR experiments. CD spectrometry at one wavelength with continuous increase in temperature has not been performed, however, this could be an interesting experiment to do in order to determine whether there exists a transition temperature where the tertiary structure of the peptides collapses.

5.3 Structure Elucidation of SakP(N24C + 44C) by NMR Spectroscopy

5.3.1 Resonance Assignments of SakP(N24C + 44C)

The resonance assignments of sakP(N24C + 44C) will for simplicity only be illustrated for 7 amino acids. A complete list of all NMR assignments at 22 °C is given in appendix 6.2.

The spin systems were established through analysis of TOCSY spectra. As an example, four different spin systems, AX, AMX, A3MX and A3B3MX are displayed in the TOCSY spectrum at 42 ^{o}C in Figure 5.3.1.1. At this point, the amino acids valine, threonine and glycine could already be assigned, since these are the only amino acids that have the corresponding spin systems A3B3MX, A3MX and AX. However, there are two valines, three threonines and nine glycines in sakP(N24C + 44C), and it was not possible to assign individual sequence positions from this information alone. The AMX spin systems could correspond to either histidine, tyrosine, tryptophan, aspartate, asparagine, phenylalanine, serine or cysteine. The AMX spin system positioned at ~8.825 ppm could, however, temporarily be assigned to cysteine, due to the relatively high ppm value of the HN, which is caused by the sulphur atom.

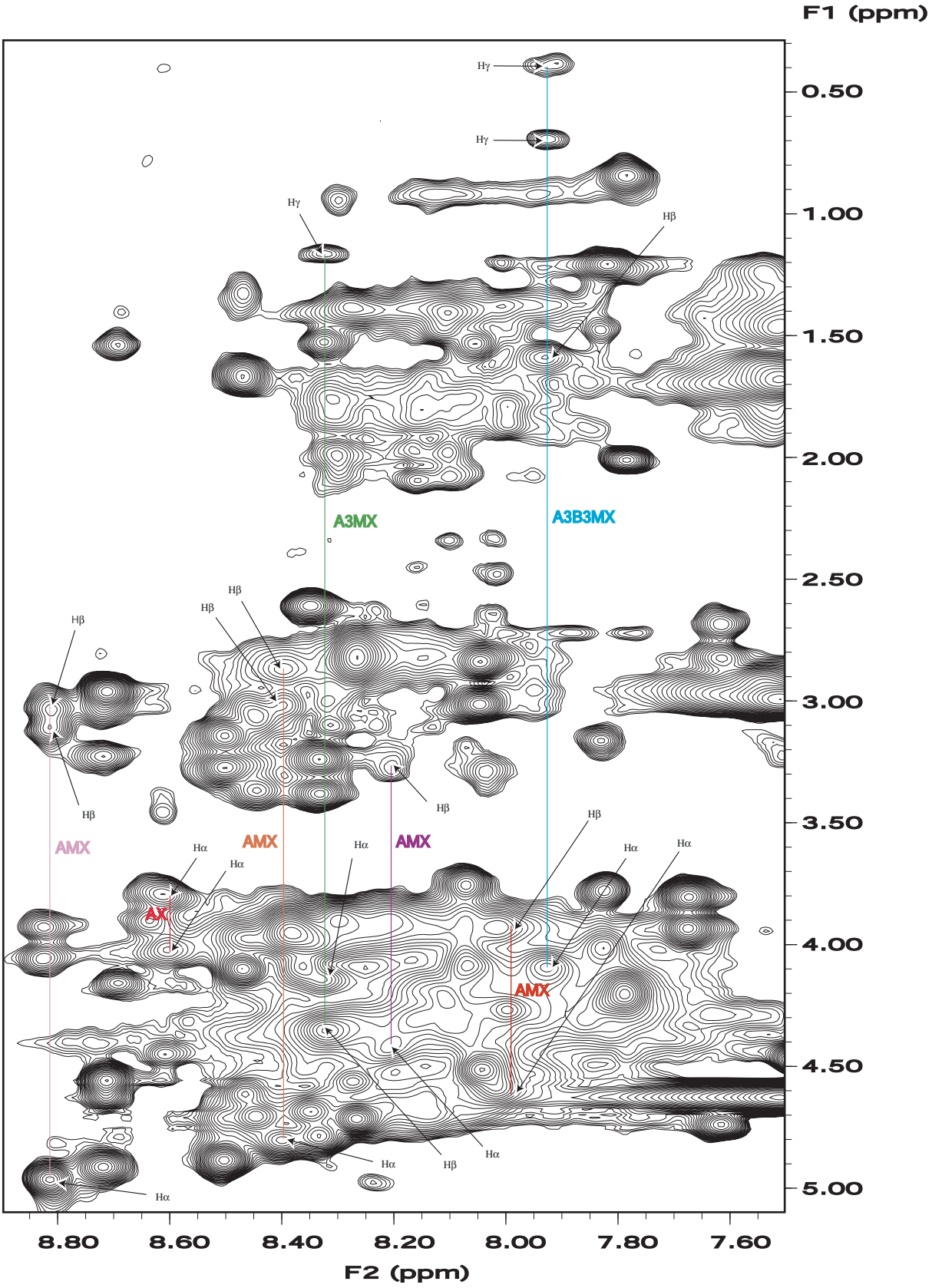

Figure 5.3.1.1 TOCSY spectrum (Fingerprint region) of sakP(N24C + 44C) at 42 °C. Seven spin systems are highlighted in color. The α, β and γ protons to the amino acids are also pointed out.

Sequential assignment was established by observing sequential NOE connectivity between $\alpha CH_i \rightarrow NH_{i+1}$, $_{\beta}CH_i \rightarrow NH_{i+1}$, and $NH_i \rightarrow NH_{i+1}$ in NOESY spectra. Unique segments of two or several sequentially adjoining amino acid residues were identified and attributed to discrete positions in the polypeptide chain. For instance, the A3MX and A3B3MX spin systems which were already assigned (see explanation above) to threonine and valine, respectively, were connected by NOESY peaks Hγ / HN, Hβ / HN and Hα / HN. This di-peptide sequence was only found once in sakP(N24C + 44C), and could therefore be sequentially assigned to threonine number 15 and valine number 16. Valine 16 was furthermore connected by a Noesy peak to an AMX spin system, which could then readily be assigned to asparagine number 17. An example of sequential assignments manifested upon NOE connectivity peaks, is given in a NOESY spectrum at 42 ^{o}C, displayed in Figure 5.3.1.2. The same spin systems that were previously shown in the TOCSY spectrum in Figure 5.3.1.1 are shown again, however, this time with the assigned residue number and the one letter code identifying the amino acid.

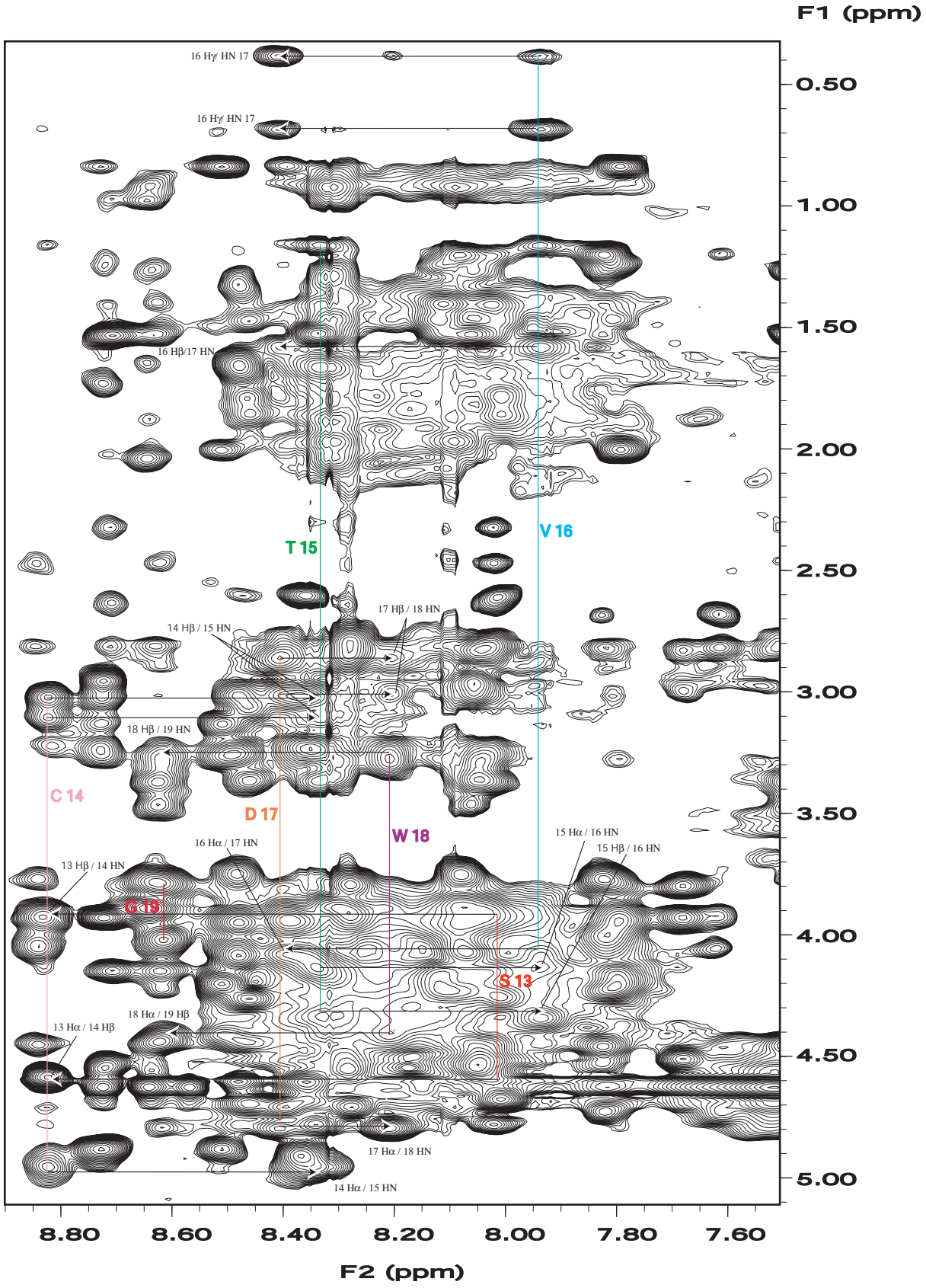

Figure 5.3.1.2 NOESY spectrum (Fingerprint region) of sakP(N24C + 44C) at 42 °C. Amino acid spin systems are highlighted in color. An arrow points from each TOCSY peak in each spin system to the corresponding NOESY peak which connects amino acid (i) to amino acid (i + 1), read from the N-terminus of the peptide.

As can be seen in Figure 5.3.1.1 and 5.3.1.2, both TOCSY and NOESY spectra contained extensive overlap, especially in the α-proton region where the many glycines (8 in total) are positioned. Consequently, the assignment of the spin systems and the NOE peaks had to be done with prudence. All assignments were of course checked and confirmed at the other side of the diagonal.

The heavy overlap in the spectra is mainly due to line broadening of the resonances. An explanation for the line broadening lies in the nature of the solvent, which consists of DPC micelles. DPC molecules are relatively large in size (54-65 molecules/micelle corresponding to a mass of roughly 20 kD) [93], and consequently they have a relatively slow correlation time. Correlation time corresponds roughly to the interval between two successive reorientations or positional changes of the molecule. This relatively slow tumbling rate of the DPC micelles causes a short T2 relaxation rate due to the increased contact with magnetic dipoles of neighbouring nuclei (explained in a simple way). Line broadening caused by a short T2 relaxation rate can be accounted for by "The Principle of Uncertainty" by Heisenberg: The shorter lifetime of a particle, the larger is the uncertainty of the particles energy state. An uncertain ΔE, means an uncertain frequency for transition, which then consequently gives a broad signal [70,94].

Another explanation for line broadening could also be the properties of the peptide itself. Flexibility may lead to multiple conformations, and accordingly multiple resonances. However, increasing the temperature (and thereby increasing the exchange process between the conformations), will merge the resonances into one resonance since only an average structure is detected [70]. The temperatures that were chosen for the NMR spectra in this study had to be a compromise between two opposing effects caused by increase in temperature. A high temperature as possible would be favourable in order to increase the tumbling rate and also possibly just give one conformation. However, the temperature could not be too high, as vibrational motions would cause the peptide to loose its conformation. NMR spectra at 22, 32 and 42 ^{o}C were especially useful in this study to clear out ambiguities caused by overlap, since the resonances appeared at slightly different ppm in each spectrum.

In all NMR spectra that were taken, there were additional peaks that could not be accounted for, which may be due to the presence of several conformations in the sample.

An "ideal" temperature where no additional peaks were present was not found. Three histidine TOCSY peaks were found in the NMR spectra of sakP(N24C + 44C), whereas there are only two histidines in this peptide. Several resonances (three to four), all blurred together, were found for isoleucine 22. Other additional peaks that could not be accounted for were also found (data not shown). However, some of the additional peaks in the NMR spectra of sakP(N24C + 44C) were unfortunately due to impurities and low deuteration grade of DPC that was used as solvent. The impurities in DPC were verified by comparison of NMR spectra of DPC ordered elsewhere (data not shown).

The possible multiple conformations do not necessarily need to be too different. For instance, reorientation of the ring in tryptophan 18 relative to isoleucine 22 may cause quite large changes in the chemical shifts of isoleucine 22. This is due to an effect called anisotropi, and is caused by a current in the tryptophan ring, which may shield or deshield the magnetic field felt by nearby atoms [70]. However, one cannot rule out the possibility that the conformations are quite different due to more than one favourable conformation in the DPC micelles. For instance, some peptides may have partly penetrated into the micelles, while others may just be laying on top of the micelles. Another possibility may also be that the peptides are rapidly exchanging between a random coil and defined structure. This could be the case if the peptides also spend some time in the watery solution instead of always being associated with micelles, (CD measurement indicate that the peptide exists as random coil in water, chapter 5.2.1). The latter hypothesis, that the peptide is exchanging between random coil and defined structure was supported by amide hydrogen exchange experiments, using D_2O (data not shown). The hydrogen atoms involved in hydrogen bonds in the α-helical part were expected to exchange slowly with deuterium atoms, however, unfortunately they all exchanged too rapidly to detect the presence of an α-helix.

Essentially all sequential connectivities for adjacent residues, which include $d_{NN}(i, i + 1)$, $d_{\alpha N}(i, i+1)$ and $d_{\beta N}(i, i+1)$ were identified, which is seen in Figure 5.3.1.3. The HN to HN connectivity is also shown in Figure 5.3.1.4. Medium range inter residue NOEs like $d_{\alpha N}(i, i+3)$, $d_{\alpha N}(i, i+4)$ and $d_{\beta N}(i, i+3)$, which are typical for α-helical structure were observed from amino acid 18 through 33, and is depicted in Figure 5.3.1.3 and Figure 5.3.1.5.

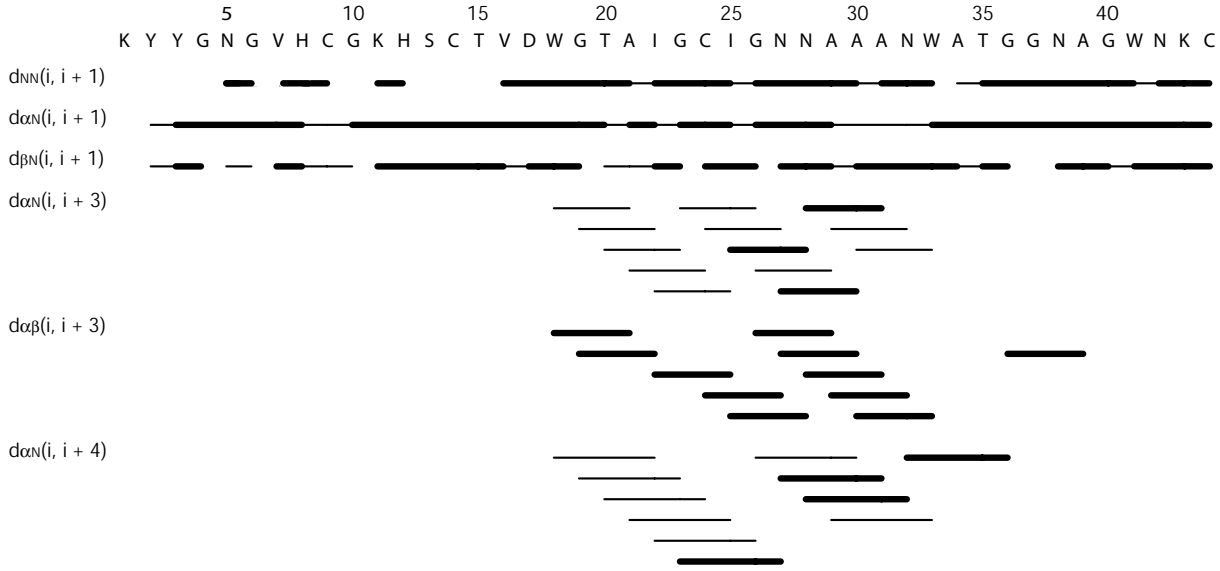

Figure 5.3.1.3 Pattern of interresidue NOEs observed for sakP(N24C + 44C) in DPC. Thick bars represents unambiguous peaks, while thin bars represents ambiguous peaks due to overlap.

Sequential connectivities as $d_{NN}(i, i + 1)$ were found in the C-terminal half, from residue 34 through residue 44. This could indicate α-helical structure, although this could not be confirmed since no medium range NOEs like $d_{\alpha N}(i, i+3)$, $d_{\alpha N}(i, i+4)$ and $d_{\beta N}(i, i+3)$ were observed for this region of the peptide.

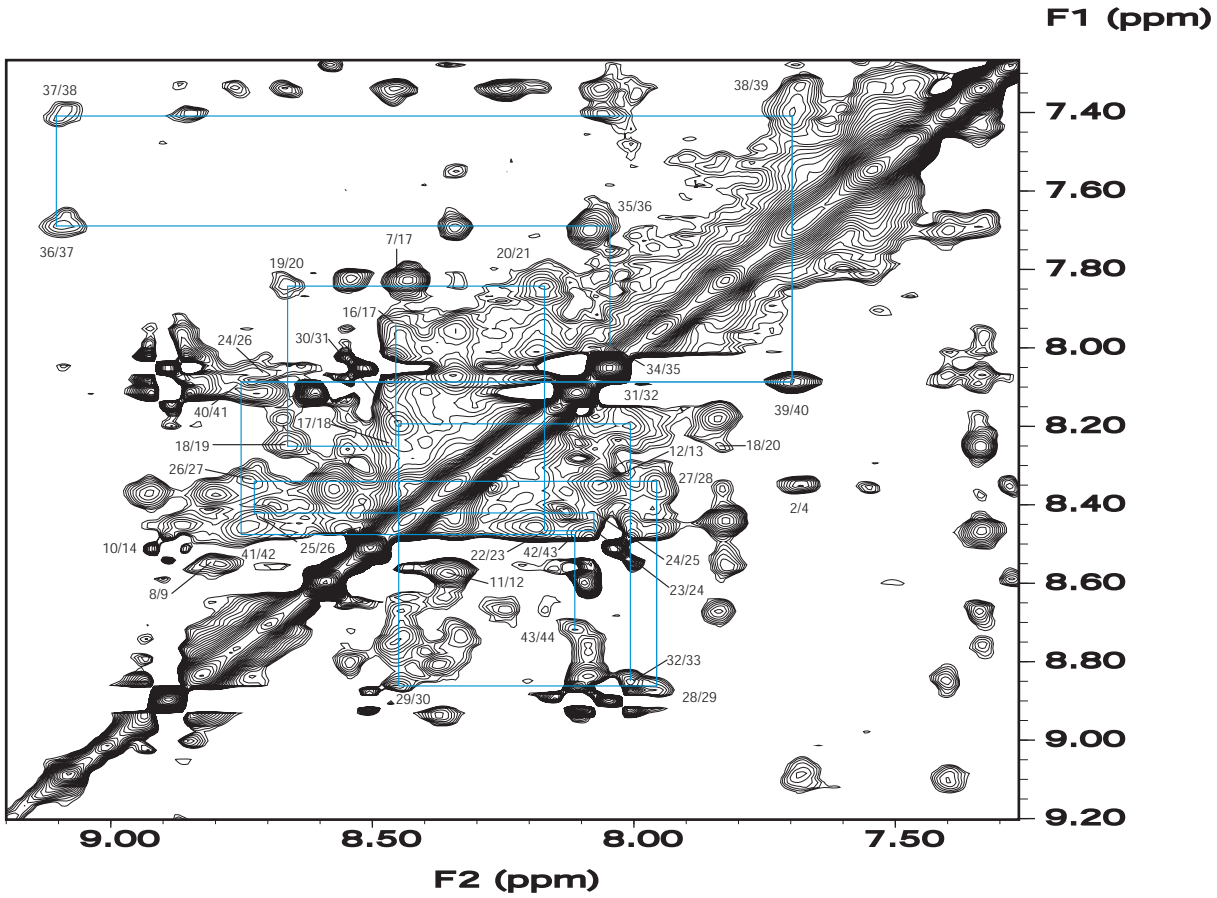

Figure 5.3.1.4 Sequential, $d_{NN}(i, i + 1)$ connectivity, indicated by the solid lines in NOESY spectrum at 22 ^{o}C of sakP(N24C + 44C).

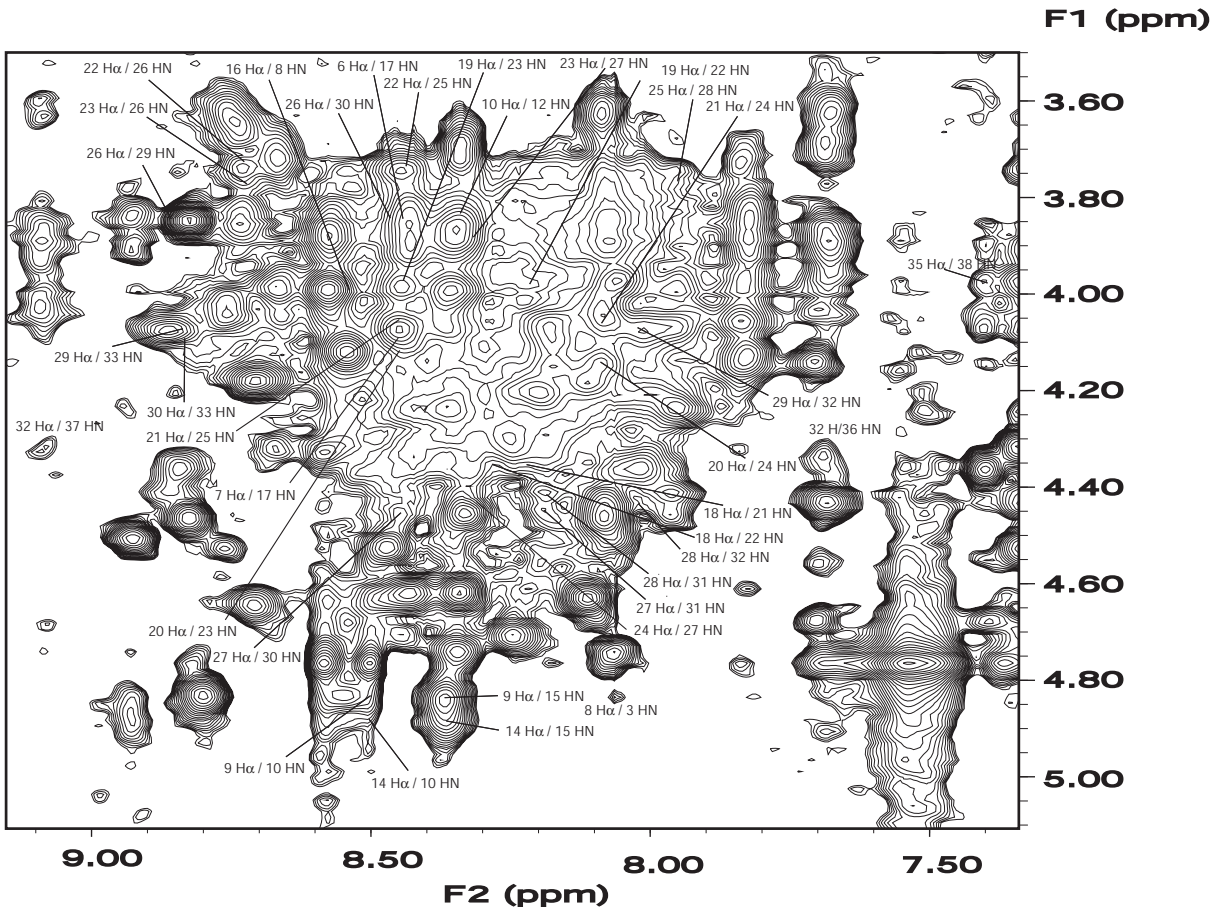

Figure 5.3.1.5 Medium range inter-residue NOEs in NOESY spectrum at 22 ^{o}C of sakP(N24C + 44C). $d_{\alpha N}(i, i+3)$ and $d_{\alpha N}(i, i+4)$ NOEs, which are typical for α-helix structure, were observed from amino acid residue 18 through 33. A few Hα / HN NOEs in the N-terminal half were also observed.

There were also found medium- and long–range NOEs in the N-terminal half that gave an indication of a three stranded antiparallel β-sheet extending from the N-terminus to Val 16. These NOEs include Lys 1 H_β to Cys 9 HN, Tyr 3 HN to His 8 H_α, Val 7 H_α to Asn 17 HN, His 8 HN to Val 16 H_α, Cys 9 H_β to Cys 14 H_β, Thr 10 HN to Cys 14 H_α, Thr 10 H_α to Ser 12 HN. However, some of these NOEs were found in overlapped regions, and could therefore not be unambiguously assigned. The β-turns were found to be around the disulphide bond (Cys 9 to Cys 14), between Thr 10 and Ser 13, and between Gly 4 and Val 7. In contrast to all the NOEs that indicated a β-sheet, there were also found NOEs which rather disrupted the suggested β-sheet structure, as can be seen in the calculated structures in Figures 5.3.2.1 and 5.3.2.3. These "non β-sheet-like" NOEs were especially pronounced among the side chains of the residues, see appendix 6.2.

NOE between the side chains of valine 7 and 16, which are the only hydrophobic side chains of the N-terminal half (residues1-16), indicated that these two amino acids point in the same direction, making the N-terminus slightly amphipathic.

A few long range NOEs were observed for the C-terminal half, confirming that the tail is tied up to the α-helix via a disulphide bond between Cys 24 and Cys 44. These connections include Ile 25 H_γ to Trp 41 ring, Ala 29 H_β to Trp 41 ring and Asn 28 H_β to Trp 41 ring. These NOEs are shown in Figure 5.3.1.6. The turn at the C-terminal end of the α-helix was found to be between Trp 33 and Gly 36, confirmed by NOE between Asn 32 H_α to Gly 37 HN.

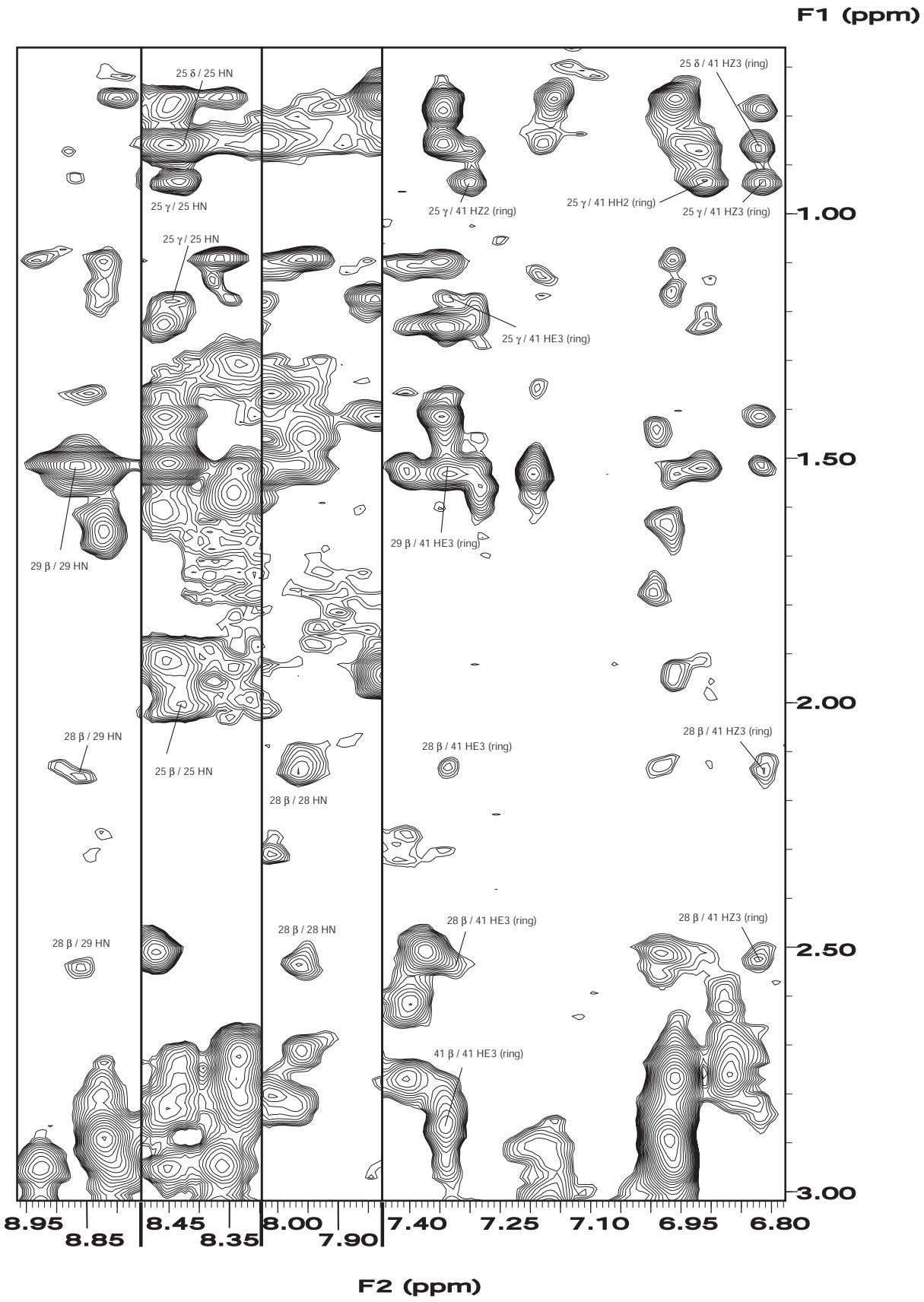

Figure 5.3.1.6 Long range NOEs observed in the C-terminal half of sakP(N24C + 44C) in NOESY spectrum at 22 ^{o}C, confirming that the C-terminal tail is tied up to the α-helix (cysteine bond between Cys 24 and Cys 44). The notations HZ2, HZ3, HH2, corresponds to 7H, 6H, and 5H of the tryptophan ring.

The presence of secondary structure elements in sakP(N24C + 44C) can be illustrated by the use of the chemical shift index developed by Wishart and Sykes [74] in Figure 5.3.1.7. This technique employs a comparison of the chemical shifts of H_α to a set of empirically determined ranges. A value of +1 is assigned to those residues that are downfield of the index, -1 for upfield chemical shifts, and 0 for those within the range. A "dense" grouping of five or more "-1's" not interrupted by a "1" is an α-helix, while a "dense" grouping of three or more "1" not interrupted by a "-1" is a β strand. All other regions are designated as coil.

The chemical shifts of the residues ranging from 18 to 44 are shifted upfield from random coil values (with an exception of residues Cys 24, Gly 37 and Asn 38, and Cys 44, which have a value of "0"), and are therefore likely to be located in an α-helix. This gives an α-helical content of 61% in sakP(N24C + 44C). A small indication of β-sheet was observed for residues 7-10. However, a β-sheet structure in the N-terminal half could not be verified based upon the chemical shifts alone. The upfield shifts ranging from residues 3-6 and at residue 11 are in the region of the observed turns in the N-terminal half.

In contrast to the relatively high percentage of α-helical content (61%) that was observed by NMR, CD experiments revealed only 29% α-helical content in sakP(N24C + 44C). The much lower degree of α-helical content observed by CD may be due to the fact that CD only measures the average of the several different structures that may exist in the sample. As explained previously, the peptides may exchange between a random coil and defined structure if the peptides also spend some time in the watery solution instead of always being associated with the micelles, (peptides not associated with micelles exist as random coil, chapter 5.2.1). Although NMR is considered as a more accurate method than CD for estimation of secondary structure content in proteins [74], the true value of α-helical content in sakP(N24C + 44C) may in this case be closer to the value obtained from the CD experiments. This assumption is supported by the observed medium range NOEs that were found in the NOESY spectra of sakP(N24C + 44C). The medium range inter residue NOEs like $d_{\alpha N}(i, i+3)$, $d_{\alpha N}(i, i+4)$ and $d_{\beta N}(i, i+3)$, which are typical for α-helical structure, were only found located between residues 18-33. This gives a percentage of 36% α-helix in sakP(N24C + 44C), a value closer to that obtained from the CD experiments (29%).

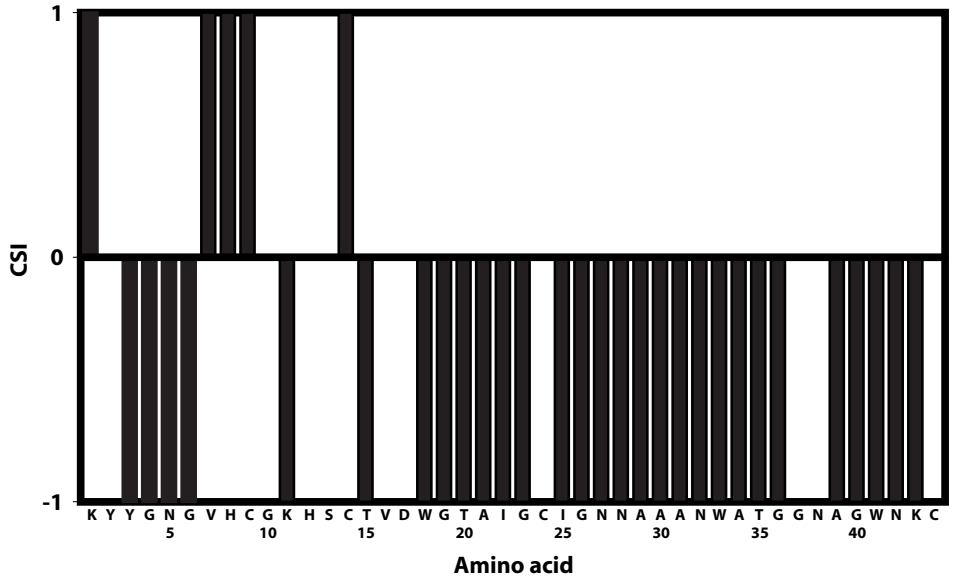

Figure 5.3.1.7 Hα chemical shifts of sakP(N24C + 44C) minus Hα chemical shifts of random coil (chemical shift index developed by Wishart and Sykes [74]). Hα of residues 18 to 43 are shifted upfield (with an exception of residue 24) from random coil values which give indication of α-helical structure. No regular secondary structure could be dedicated to the N-terminal half.

5.3.2 Three-Dimensional Structure of SakP(N24C + 44C)

A total of 449 NOEs (including 303 intra-residue, 97 medium and 49 long range NOEs) were employed for distance constraints for calculating the structure of sakP(N24C + 44C) in DPC micelles (given in an appendix, 6.2).

Ten "low energy structures" out of fifty calculated structures were chosen. A set of structures with superimposition over different sequential parts of the backbone of sakP(N24C + 44C) in DPC is shown in Figure 5.3.2.1. The root mean square deviations for the various superimpositions are given in Table 5.3.2.1.

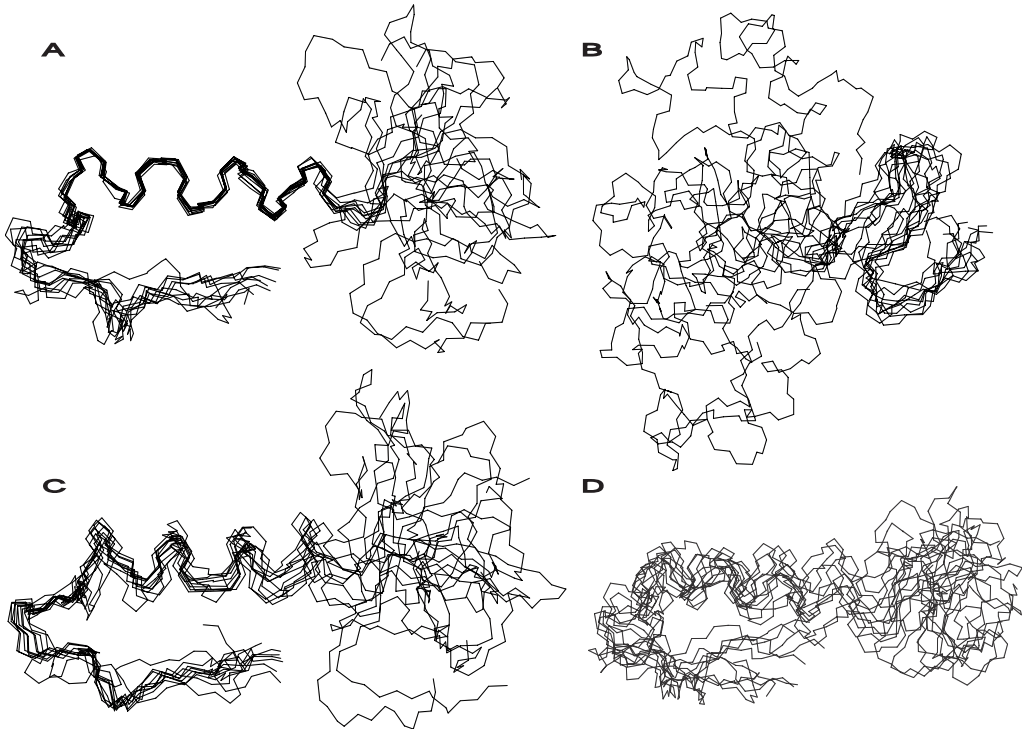

Figure 5.3.2.1 Various superimpostition of 10 calculated peptide backbone (N, Cα, CO) structures for sakP(N24C + 44C) in DPC micelles. The superimpostitions are performed over residues: A) 18-33, B) 1-17, C) 34-44 and D) 1-44 (entire peptide). The N-terminus is on the right and the C-terminus is on the left in all figures.

Table 5.3.2.1 Root mean square deviations (Å) for superimposition over various parts of the backbone atoms of sakP (N24C + 44C). The backbone atoms are defined as nitrogens, and α and carbonyl carbons.

Residues (backbone)	Root mean square deviation (RMSD)
18-33	0.361
1-17	2.367
34-44	1.951
1-44 (entire peptide)	3.375
1-33	3.104
18-44	0.914
17-33	0.459
18-34	0.411

Superimposition over residues 18-33, gives a relatively low RMSD value of 0.361, while a superimposition over residues 17- 33 and 18-34, increased the RMSD values to respectively, 0.459 and 0.411. These results clearly indicate that the α-helical part of sakP(N24C + 44C) is located between residues 18-33. Interestingly, a comparison of sakP(N24C + 44C) and the pediocin-like bacteriocin leucocin A [36], revealed that the α-helices are approximately the same size and also located on nearly the same positions. These results may indicate that these two peptides probably have the same mode of action. A superimposition of the helices (residues 18-30) to the 10 calculated structures of sakP(N24C + 44C) and 19 calculated structures of the pediocin-like bacteriocin leucocin A (imported from a protein data bank) in DPC micelles, is shown in Figure 5.3.2.2. The root mean square deviation of the superimposition was 0.409.

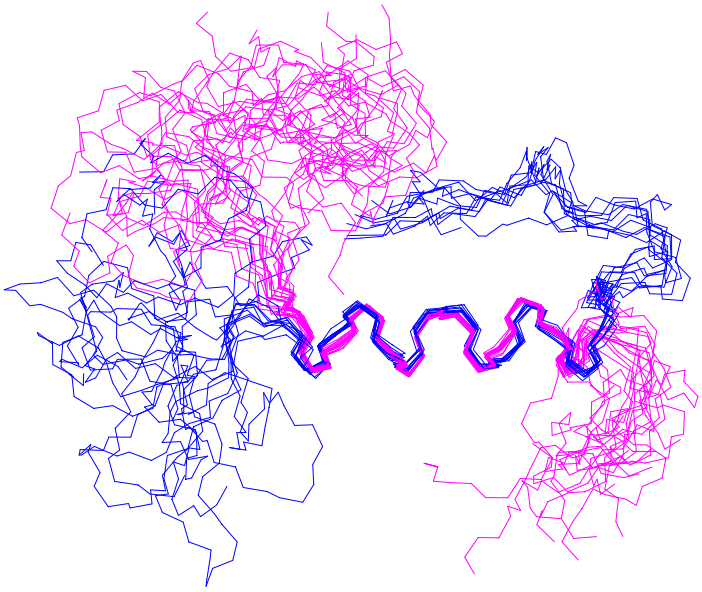

Figure 5.3.2.2 Superimposition over residues 18 to 30 of, respectively, 10 and 19 calculated structures of sakacinP(N24C + 44 C) and leucocin A in DPC micelles. N-terminus is at the left and C-terminus is at the right side. The structure of leucocin A [36] is imported from a protein data bank.

A closer examination of the α-helix to sakP(N24C + 44C) also revealed that the α-helix is amphipathic, displaying hydrophobic residues on one side and hydrophilic residues on the other side. This is shown in Figure 5.3.2.3, where all side chains of the peptide are shown. The side chains are colored green if hydrophilic and pink if hydrophobic. The hydrophobic residues in the α-helix are Trp 18, Ala 21, Ile 22, Ile 25, Ala 29, Ala 30, Ala 31, Trp 33, while the hydrophilic residues are Thr 20, Cys 24, Asn 27, Asn 28, Asn 32. Glycines are considered as neutral.

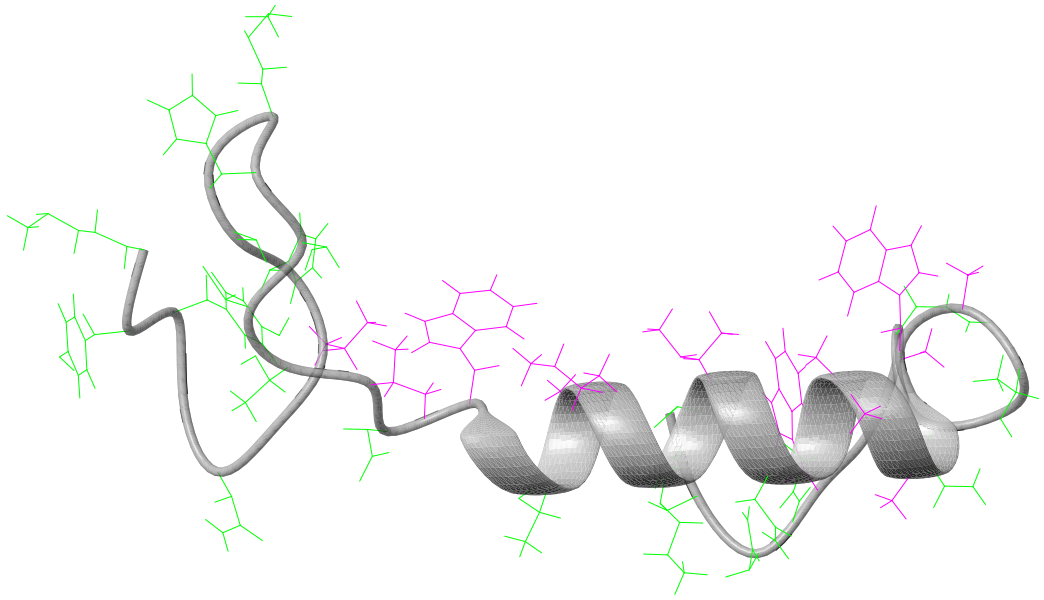

Figure 5.3.2.3 Structure of sakP(N24C + 44C). Hydrophobic side chains are shown in pink and hydrophilic side chains in green.

This amphipathic α-helix motif is found in several different types of membrane-permeabilizing eukaryotic antimicrobial peptides, as well as in class II bacteriocins (including leucocin A) excreted from lactic acid bacteria [2,11,33,36,44]. For these reasons, it is clear that the physical property of their helices must be important for how the peptide functions. Perhaps these amphipathic α-helices are able to permeabilize cell membranes by either of the two models (pore or carpet model) that are described in the introduction 2.5.

The large RMSD (2.367) for the N-terminal half (residues 1-17) indicated that the structure of this part of the peptide is relatively poorly defined, as also can be seen in Figure 5.3.2.1 B. As described previously in chapter 5.3.1, there were found NOE peaks that distorted the assumed β-sheet structure, which was only based upon some few NOEs. A comparison of sakP(N24C + 44C) in DPC micelles with leucocin A in TFE solvent [36], reveals a much more defined β-sheet in leucocin A. (The structure of leucocin A is shown in the introduction, Figure 2.4.1). However, a comparison of the structures, both found in DPC micelles, reveals that the N-terminal half of leucocin A is as poorly defined as for sakP(N24C + 44C). Since the difference in sequence identity in the N-terminal half of

these two peptides is less than 30%, it is not surprising that sakP(N24C + 44C) has a similar N-terminal structure to that of leucocin A in DPC. By contrast, carnobacteriocin B2 in DPC revealed no evidence for either β-sheet or β-sheet-like structure in the N-terminal half, Figure 2.4.1 [44]. However, it should be noted that the N-terminal half of carnobacteriocin B2 is more different from leucocin A and sakP(N24C + 44C) [36,44].

The lack of long range NOEs between the N-terminus and the α-helix makes the N-terminus fluctuate in many directions with respect to the α-helix. This is shown previously in Figure 5.3.2.1 A, when a superimposition over the α-helical part is performed. Superimposition over residues 1-33, a region that spans the N-terminus and the α-helical part, gives a high RMSD value of 3.104, while a separate superimposition over these parts gives RMSDs of, respectively, 2.367 and 0.361. A hinge region may be positioned around aspartate 17, which is the residue before the start of the α-helix.

The C-terminal half located between residues 34-44, had an RMSD of 1.951, which also makes this part of the peptide less defined. However, this is solely due to the lack of observed NOEs. As described previously in chapter 5.2.1, there were only found a few NOEs that could tie up the tail to the α-helix. Interestingly, a superimposition of sakP(N24C + 44C) and leucocin A over residues 19-30, makes the C-terminal half of both peptides point in different directions. It should be noted that the C-terminal end of sakP(N24C + 44C) is tied up to the α-helix by a disulphide bond between two cysteine residues, positioned at 24 and 44, while leucocin A lacks this disulphide bond. Due to the disulphide bond in sakP(N24C + 44C), its C-terminal tail cannot be positioned on the same side as the C-terminal tail of leucocin A. The superimposition of sakP(N24C + 44C) and leucocin A over the α-helix is shown previously in Figure 5.3.2.2, although the disulphide bonds are not shown, since only backbone atoms are displayed.

5.3.3 Possible Orientation of the Pediocin-Like Bacteriocins (Class IIa) in the Cell Membrane

The N-terminal structure of sakP(N24C + 44C) and leucocin A in DPC, and carnobacteriocin B2 in TFE, did not reveal a perfect β-sheet. However, one may speculate that these peptides actually do possess a perfect β-sheet when they are in contact with a real cell membrane and that this secondary structural motif could be vital for making these peptides active as antimicrobials. As mentioned previously in the introduction 2.4, bacteriocins that lack the N-terminal disulphide bond are almost completely inactive [38,39]. Perhaps the disulphide bond (positioned between Cys 9 and Cys 14) is necessary for stabilizing the β-sheet, thereby explaining why this disulphide bond is conserved in all pediocin-like bacteriocins. One may also speculate that the importance of the cationic β-sheet may not only be to enable the initial contact with the negative surface of the membrane through electrostatic interactions, but also to associate with a docking site, which consists of unique parts of the cell membrane. Perhaps the quite flexible β-sheet-like N-terminus allows different favourable conformations, and only in contact with a specified docking site, will it adopt a complete β-sheet structure. (This hypothesis would be analogous to an induced fit model for enzymes [59]). The lack of this docking site in the DPC micelles would then explain why a perfect β-sheet structure in the N-terminal half was not observed.

One may also speculate that the hinge region, which is located at Asp 17, also is important for the function of the peptides, and that this is the reason why Asp 17 is conserved in all pediocin-like bacteriocins that belong to subgroup 1, Figure 2.3.1. Interestingly, it was shown that the exact position in space of the carboxylate group on the aspartate 17 is of great importance, since the D17E mutation in sakacin P resulted in a 10-fold reduction in activity [95]. The importance of the hinge region may be to allow the peptide to have the right conformation relative to the membrane and/or perhaps relative to other peptides, enabling them to form a pore. In light of the carpet model, the hinge region could be important for rendering flexible motion of the α-helix in the membrane, which then may cause ions to leak out through the membrane.

Recently, there has been some discussion about the importance of the location of the tryptophans that the pediocin-like bacteriocins contain. As described previously in the introduction 2.4, one has hypothesized, based upon mutational studies, that tryptophan 18 and 41 may be key residues involved in stabilizing a hairpin-like structure for those bacteriocins that lack the C-terminal disulphide bond [35]. This stabilization could involve a hydrophobic ring stacking by tryptophan 41 and 18 [35]. No long range NOEs could confirm the assumption of ring stacking, however, although this may be due to the disulphide bond in the C-terminal half of sakP(N24C + 44C), making it impossible to position these two tryptophans close to each other. The hairpin structure could also be stabilized just by positioning the tryptophans 18 and 41 in the membrane-surface interface [35]. (It is well known that tryptophans and other aromatic residues in membrane-proteins are likely to be found in the membrane-surface interface [96]). This idea, that the tryptophans 18 and 41 are positioned in the membrane-surface interface, is consistent with several mutational analyses [35]. Tryptophan 18 and 41 in the bacteriocins that lack the C-terminal disulphide bond could not be substituted with other residues without a drastic decrease in activity. However, some activity was still present if the tryptophans were substituted with the aromatic residues phenylalanine or tyrosine, emphasizing the importance of aromaticity in these positions [35]. Interestingly, the mutations of Trp 18 and 41 could be overcome by introducing a disulphide bond in the C-terminal half, while mutating the tryptophans 18 and 41 in the bacteriocins that already have the hairpin structure stabilized by the C-terminal disulphide bond did not cause any drastic affect of the activity of these peptides [35].

Positioning tryptophan 18 and 41 of the pediocin-like bacteriocins next to each other in the membrane-surface interface would allow the central α-helical part of the peptide to have an oblique orientation, penetrating into the hydrophobic core of the membrane, as previously proposed by Fimland et al. (2002) [35]. Such an orientation of the peptide would position the tryptophan 33 into the hydrophobic core of the membrane. Mutational analyses of Trp 33 has shown that this residue can be replaced with a hydrophobic residue [35]. A Trp 33 to Leu mutation had only a marginal effect on the activity, whereas replacement of Trp 33 with the more polar Tyr or Arg residues reduced the activity drastically [35]. That Trp 18 and 41 are in a different environment than Trp 33 was also supported by the chemical shift analysis performed in this study. Many of the chemical shifts of the ring-protons of Trp 18 and 41 were overlaid, while the chemical shift of the ring protons to Trp 33 were distinct.

Interestingly, by turning sakP(N24C + 44C) in such a way that Trp 18 and 41 are located at the same level, (for instance the membrane-surface interface), while Trp 33 is located below (deeper into the hydrophobic core of the membrane), the α-helix does in fact have an oblique orientation. An oblique orientation of the α-helix in the membrane is shown in Figure 5.3.3.1, next page. Whether this orientation of the peptide is involved in a carpet model or a pore model remains to be elucidated.

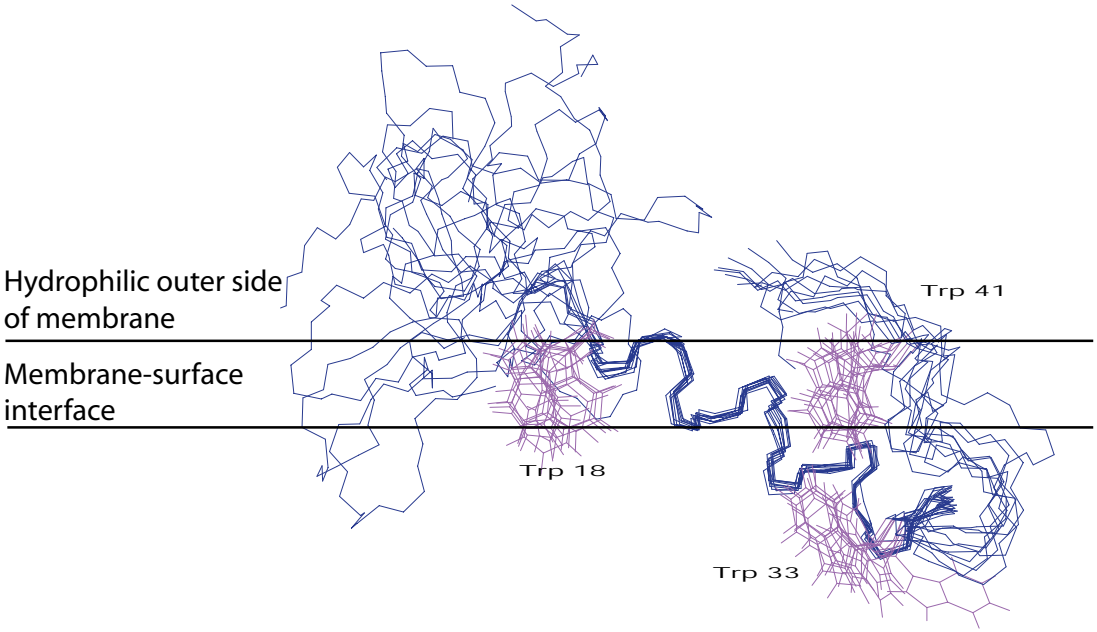

Figure 5.3.3.1 10 calculated structures of sakP(N24C + 44C) positioned in an oblique orientation in a cell membrane. Only backbone atoms and side chain of the the tryptophans are shown.

6 Concluding Remarks

The structure of sakP(N24C + 44C) in DPC micelles has been determined by NMR spectroscopy. The results showed that this peptide adopts a well-defined α-helix in the central part of the peptide. A closer examination of this α-helix reveals an amphipathic structure, where hydrophobic and hydrophilic residues are located on each side of the α-helix. A less well-defined β-sheet-like structure was observed in the N-terminal half, while a defined structure without any common secondary structure was observed in the C-terminal tail. The hypothesis that the peptide has an oblique orientation relative to the membrane, by positioning tryptophan 18 and 41 in the membrane-water interface, and tryptophan 33 deeper into the hydrophobic core, is compatible with the structure of sakP(N24C + 44C). Interestingly, the structure of sakP(N24C + 44C) clearly resembles the structure of leucocin A in DPC. For these reasons, it is reasonable to believe that other pediocin-like bacteriocins adopt similar structures, and that these structures are crucial for their mode of action. Knowing the structure of these peptides is definitely a further step in understanding how they permeabilize their target cell membranes. However, to understand whether these peptides aggregate to form a pore or follow a carpet model remains to be elucidated.

It should be stressed that the structure elucidation of sakP(N24C + 44C) was performed in DPC micelles, which constitute an artificial environment. Although there is today a substantial record of NMR studies of membrane proteins in micelles, where excellent concordance is found with results in lipid bilayers [72], one cannot rule out the possibility that the structure of sakP(N24C + 44C) may be somewhat different in a real cell-membrane. This hypothesis is supported by CD studies of two-peptide bacteriocins that have given contradicting results in respectively DPC-micelles and liposome-environments created by dioleoyl-L-α-phosphatidyl-DL-glycerol (DOPC). An additional structuring was observed when the two complementary peptides were combined in liposomes, while no additional structuring was observed in TFE or DPC. This may indicate that DPC micelles do not have the appropriate shape and/or size, and thus do not permit formation of a functional multimer complex of peptides [32]. It would be interesting to elucidate the structure of sakP(N24C + 44C) in liposomes and compare whether it has the same tertiary conformation. This kind of study has to be done using solid-state NMR, since liquid-state

NMR would not be feasible due to the large size of the liposomes. Since the peptides are immobilized or motionally restricted in solid-state, the orientation of the peptide relative to the membrane and other peptides can also be elucidated. Solid-state analysis would require isotopic labelling of the peptide with ^{13}C and ^{15}N. In order to label sakP(N24C + 44C), the bacteriocin-producing bacteria has to be grown in a minimal medium containing only a ^{13}C and ^{15}N enriched nitrogen and carbon source. This is however not feasible for lactic acid bacteria, but introducing an expression system for sakP(N24C + 44C) into *Escherichia coli* would probably be ideal for this purpose. An efficient over-expression system for sakP(N24C + 44C) in *Escherichia coli* has, however, not yet been developed.

7 Appendix

7.1 Equipment and Chemicals

Equipment:	**Manufacturer:**
Avanti centrifuge J-25	Beckman
Biofuge pico	Heraeus instruments
DRX 500 NMR spectrometer	Bruker
FPLC system	Amersham Biosciences
JA-10 Beckman rotor	Beckman
J-810 Spectropolarimeter	Jasco
Microtiter plate (96 wells)	Costar
mm quartz cuvette	Starna
MR 700 Microplate Reader	Dynatech
P/ACE System 2050 Capillary Electrophoresis	Beckman
Resource RPC column (3ml)	Amersham Biosciences
SMART- system	Amersham Biosciences
TXI Pobehead (5 mm)	Bruker
Untreated fused silica capillary	Beckman
UV-visible recording spectrophotometer	Shimadzu
μRPC C_2/C_{18} column	Amersham Biosciences
Voyager-DE RP mass spectrometer	Perseptive biosystems

Chemicals:	
Acetonitril	Merck
α-cyano-4-hydroxycinnamic acid (CHCA)	Sigma
Deuterated dodecylphosphocholine (DPC) (99.9 % D)	CDN isotopes
Deuterium oxide	Cambridge Isotope Lab.
Dodecylphospholcholine (DPC)	Sigma
Ethanol	Arcus
MRS Broth	Oxoid
NaCl	Merck
NaH_2PO_4	Merck
Na_2HPO_4	Merck
Octyl Sepharose CL – 4B	Amersham Biosciences
Propanol	Merck
SP Sepharose Fast Flow	Amersham Biosciences
Trifluoroacetic acid (TFA)	Sigma
Trifluoroethanol (TFE)	Sigma

7.2 Resonance Assignment of SakP(N24C + 44C)

Long-range peaks:

Residue number (w1)	Proton identity (w1)	Residue number (w2)	Proton identity (w2)	ppm (w1)	ppm (w2)	Comment
9	HA	14	HB3	4.84	2.95	
15	HN	8	HN	8.37	8.54	
16	HA	8	HN	3.98	8.54	
7	HA	17	HN	4.11	8.45	
32	HB3	37	HN	2.28	9.09	
28	HB2	41	HE3	2.54	7.34	
28	HB3	41	HE3	2.14	7.34	
28	HD21	42	HN	6.82	8.47	
25	HA	41	HZ3	3.75	6.83	
25	HA	41	HH2	3.75	6.91	
29	HA	41	HH2	4.08	6.91	
9	HN	3	HD	8.82	6.97	
6	HA1	17	HN	3.85	8.45	
17	HB2	6	HN	2.94	8.09	
16	HA	7	HN	3.98	7.82	
29	HB	41	HE3	1.51	7.34	
1	HB2	9	HN	1.64	8.81	
9	HB2	2	HN	3.2	8.35	
7	HN	17	HN	7.82	8.45	
7	HG2	17	HN	0.77	8.45	ambiguous
7	HG1	17	HN	0.77	8.45	ambiguous
9	HA	15	HN	4.83	8.37	
16	HA	7	HA	3.99	4.11	
15	HN	9	HN	8.38	8.81	
32	HA	37	HN	4.34	9.09	
29	HA	41	HE3	4.08	7.34	
28	HA	41	HE3	4.42	7.34	
25	HG2	41	HH2	0.94	6.91	
25	HG2	41	HZ2	0.94	7.29	
25	HG2	41	HZ3	0.94	6.83	
25	HD1	41	HZ3	0.86	6.83	
25	HG13	41	HE3	1.2	7.34	
35	HG2	30	HN	1.24	8.46	
7	HG2	16	HG2	0.77	0.25	ambiguous
7	HG1	16	HG2	0.77	0.25	ambiguous
7	HG2	16	HG1	0.77	0.61	ambiguous
7	HG1	16	HG1	0.77	0.61	ambiguous
7	HG2	14	HB2	0.77	3.04	ambiguous
7	HG1	14	HB2	0.77	3.04	ambiguous
7	HG1	17	HB2	0.77	2.94	ambiguous
7	HG2	17	HB2	0.77	2.94	ambiguous
25	HN	42	HD22	8.44	6.7	
28	HB3	41	HZ3	2.14	6.82	
9	HB2	14	HB3	3.2	2.94	
8	HA	3	HN	4.83	8.06	

Residue number (w1)	Proton identity (w1)	Residue number (w2)	Proton identity (w2)	ppm (w1)	ppm (w2)	Comment
17	HB3	6	HN	2.82	8.09	
37	HA2	32	HB2	3.87	2.81	
21	HB	16	HG2	1.4	0.25	
21	HB	16	HG1	1.4	0.62	

Medium-range peaks:

Residue number (w1)	Proton identity (w1)	Residue number (w2)	Proton identity (w2)	ppm (w1)	ppm (w2)	Comment
16	HG2	18	HD1	0.25	7.34	
16	HG1	18	HD1	0.61	7.34	
7	HG1	3	HD	0.77	6.97	ambiguous
7	HG2	3	HD	0.77	6.97	ambiguous
7	HG1	3	HE	0.77	6.7	ambiguous
7	HG2	3	HE	0.77	6.7	ambiguous
18	HN	20	HN	8.25	7.84	
7	HG2	9	HN	0.77	8.81	ambiguous
7	HG1	9	HN	0.77	8.81	ambiguous
20	HG2	23	HN	1.18	8.44	
7	HB	3	HD	1.95	6.97	
7	HB	3	HE	1.95	6.7	
18	HA	21	HB	4.32	1.4	
28	HA	31	HB	4.42	1.37	
29	HA	32	HB3	4.08	2.28	
29	HA	32	HB2	4.08	2.8	
43	HA	41	HD1	4.18	6.99	
40	HN	38	HN	8.08	7.4	
39	HA	41	HE1	4.14	10.56	
6	HN	3	HD	8.08	6.96	
18	HA	21	HN	4.32	8.17	
18	HA	22	HN	4.32	8.2	
19	HA1	22	HN	3.96	8.2	
20	HA	23	HN	4.13	8.44	
20	HA	24	HN	4.13	8.09	
21	HA	24	HN	4.07	8.09	
28	HA	31	HN	4.42	8.19	
29	HA	32	HN	4.08	8.01	
29	HA	33	HN	4.08	8.85	
30	HA	33	HN	4.08	8.85	
29	HA	33	HD1	4.08	7.19	
22	HG2	18	HZ3	0.87	6.95	
38	HA	40	HN	4.67	8.1	
24	HN	26	HN	8.09	8.73	
12	HA	10	HN	4.73	8.51	
32	HA	36	HN	4.34	7.69	
2	HN	4	HN	8.35	7.68	
35	HA	33	HD1	3.97	7.19	
44	HN	41	HD1	8.73	6.99	
15	HB	18	HD1	4.24	7.34	
44	HA	41	HD1	4.63	6.99	

Residue number (w1)	Proton identity (w1)	Residue number (w2)	Proton identity (w2)	ppm (w1)	ppm (w2)	Comment
22	HG2	18	HE3	0.87	7.34	
22	HD1	18	HE3	0.79	7.34	
22	HD1	18	HH2	0.79	6.82	
43	HB3	41	HD1	1.45	6.99	ambiguous
43	HB2	41	HD1	1.45	6.99	ambiguous
43	HB2	41	HD1	1.76	6.99	
43	HD3	41	HE3	1.46	7.34	ambiguous
43	HD2	41	HE3	1.46	7.34	ambiguous
22	HG12	18	HE3	1.42	7.34	
22	HG13	18	HE3	1.38	7.34	
16	HG1	18	HZ3	0.61	6.94	
16	HG2	18	HZ3	0.25	6.95	
16	HG2	18	HH2	0.25	6.82	
22	HG12	18	HH2	1.42	6.82	
29	HB	26	HN	1.51	8.73	
21	HB	24	HN	1.4	8.09	
27	HA	30	HB	4.45	1.51	
19	HA2	22	HB	3.73	1.91	
22	HA	25	HB	3.76	1.99	
25	HA	28	HB3	3.75	2.14	
26	HA2	29	HB	3.67	1.51	
26	HA1	29	HB	3.85	1.51	
24	HA	27	HB2	4.61	2.81	
30	HA	33	HB3	4.08	3.33	
36	HA1	39	HB	3.88	1.12	
14	HA	12	HB3	4.87	3.16	
18	HA	16	HG2	4.31	0.25	
20	HA	16	HG1	4.13	0.61	
7	HG1	3	HB3	0.77	2.74	ambiguous
7	HG2	3	HB3	0.77	2.74	ambiguous
7	HN	3	HE	7.84	6.7	
6	HN	3	HE	8.08	6.7	
5	HN	3	HE	8.82	6.7	
10	HN	14	HN	8.51	8.92	
12	HB3	14	HN	3.16	8.93	
25	HG2	29	HN	0.94	8.87	
10	HA2	12	HN	3.85	8.35	
10	HA1	12	HN	3.98	8.35	
14	HA	10	HN	4.87	8.51	
21	HB	18	HE3	1.4	7.34	
29	HB	33	HE3	1.51	7.41	
4	HA2	6	HN	3.7	8.09	
4	HA1	6	HN	3.85	8.09	
33	HE3	37	HN	7.41	9.1	
22	HA	25	HN	3.76	8.44	
23	HA2	26	HN	3.77	8.73	
24	HA	27	HN	4.61	8.34	
25	HA	28	HN	3.75	7.96	
26	HA1	29	HN	3.85	8.87	
27	HA	30	HN	4.45	8.46	
19	HA1	23	HN	3.96	8.44	

Residue number (w1)	Proton identity (w1)	Residue number (w2)	Proton identity (w2)	ppm (w1)	ppm (w2)	Comment
22	HA	26	HN	3.76	8.73	
23	HA1	27	HN	3.91	8.34	
27	HA	31	HN	4.45	8.19	
28	HA	32	HN	4.42	8.01	
35	HA	38	HN	3.98	7.41	

Intra-residue peaks:

Residue number (w1)	Proton identity (w1)	Residue number (w2)	Proton identity (w2)	ppm (w1)	ppm (w2)	Comment
14	HA	14	HN	4.87	8.92	
14	HB2	14	HN	3.04	8.92	
14	HB3	14	HN	2.94	8.92	
9	HA	9	HN	4.83	8.81	
9	HB2	9	HN	3.2	8.81	
9	HB3	9	HN	3.05	8.81	
8	HB3	8	HN	3.06	8.54	
8	HB2	8	HN	3.2	8.54	
8	HA	8	HN	4.83	8.54	
5	HB3	5	HN	2.78	8.82	
5	HB2	5	HN	2.93	8.82	
5	HA	5	HN	4.46	8.82	
37	HA2	37	HN	3.87	9.09	
37	HA1	37	HN	4.04	9.09	
29	HA	29	HN	4.08	8.87	
38	HB3	38	HN	2.62	7.4	
38	HB2	38	HN	2.75	7.4	
38	HA	38	HN	4.67	7.4	
4	HA2	4	HN	3.7	7.68	
4	HA1	4	HN	3.85	7.68	
17	HA	17	HN	4.71	8.45	
17	HB2	17	HN	2.94	8.45	
17	HB3	17	HN	2.82	8.45	
33	HB2	33	HN	3.42	8.85	
33	HB3	33	HN	3.33	8.85	
33	HA	33	HN	4.36	8.85	
19	HA2	19	HN	3.73	8.66	
19	HA1	19	HN	3.96	8.66	
18	HB3	18	HN	3.19	8.25	
18	HA	18	HN	4.32	8.25	
28	HB3	28	HN	2.14	7.96	
28	HB2	28	HN	2.54	7.96	
32	HB3	32	HN	2.28	8.01	
42	HB2	42	HN	2.51	8.47	ambiguous
42	HB3	42	HN	2.51	8.47	ambiguous
2	HB3	2	HN	2.71	8.35	
3	HA	3	HN	4.43	8.06	
2	HA	2	HN	4.63	8.35	
29	HB	29	HN	1.51	8.87	
30	HB	30	HN	1.51	8.46	

Residue number (w1)	Proton identity (w1)	Residue number (w2)	Proton identity (w2)	ppm (w1)	ppm (w2)	Comment
7	HB	7	HN	1.95	7.82	
7	HG1	7	HN	0.77	7.82	ambiguous
7	HG2	7	HN	0.77	7.82	ambiguous
20	HG2	20	HN	1.18	7.84	
16	HG2	16	HN	0.25	7.96	
16	HG1	16	HN	0.61	7.96	
15	HG2	15	HN	1.1	8.37	
15	HB	15	HN	4.24	8.37	
16	HA	16	HN	3.98	7.96	
32	HB2	32	HN	2.8	8.01	
39	HB	39	HN	1.12	7.7	
21	HB	21	HN	1.4	8.17	
34	HB	34	HN	1.53	8.05	
35	HG2	35	HN	1.24	8.06	
16	HB	16	HN	1.45	7.96	
12	HA	12	HN	4.73	8.35	
41	HA	41	HN	4.53	8.76	
41	HB2	41	HN	3.18	8.76	
41	HB3	41	HN	2.88	8.76	
12	HB2	12	HN	3.3	8.35	
12	HB3	12	HN	3.16	8.35	
14	HA	14	HB3	4.87	2.94	
14	HA	14	HB2	4.87	3.04	
9	HA	9	HB2	4.83	3.2	
9	HA	9	HB3	4.83	3.05	
8	HA	8	HB2	4.83	3.2	
8	HA	8	HB3	4.83	3.06	
17	HA	17	HB2	4.71	2.94	
17	HA	17	HB3	4.71	2.82	
12	HA	12	HB2	4.73	3.3	
12	HA	12	HB3	4.73	3.16	
38	HA	38	HB3	4.67	2.62	
38	HA	38	HB2	4.67	2.75	
13	HA	13	HB2	4.51	3.85	ambiguous
13	HA	13	HB3	4.51	3.85	ambiguous
20	HA	20	HN	4.13	7.84	
20	HA	20	HB	4.13	4.08	
20	HA	20	HG2	4.13	1.18	
20	HB	20	HG2	4.08	1.18	
15	HB	15	HG2	4.24	1.1	
29	HA	29	HB	4.08	1.51	
16	HA	16	HG1	3.98	0.61	
16	HA	16	HG2	3.98	0.25	
7	HA	7	HN	4.11	7.82	
7	HA	7	HG1	4.11	0.77	ambiguous
7	HA	7	HG2	4.11	0.77	ambiguous
7	HA	7	HB	4.11	1.95	
16	HA	16	HB	3.98	1.45	
5	HB3	5	HD21	2.78	7.62	
28	HB2	28	HD21	2.54	6.82	
33	HB2	33	HE3	3.42	7.41	

Residue number (w1)	Proton identity (w1)	Residue number (w2)	Proton identity (w2)	ppm (w1)	ppm (w2)	Comment
33	HB2	33	HD1	3.42	7.19	
11	HB2	11	HN	1.57	8.58	ambiguous
11	HB3	11	HN	1.57	8.58	ambiguous
11	HG2	11	HN	1.2	8.58	ambiguous
11	HG3	11	HN	1.2	8.58	ambiguous
43	HG2	43	HN	1.77	8.11	
43	HG3	43	HN	1.64	8.11	
43	HB3	43	HN	1.44	8.11	ambiguous
43	HB2	43	HN	1.44	8.11	ambiguous
11	HE3	11	HB2	2.87	1.57	ambiguous
11	HE3	11	HB3	2.87	1.57	ambiguous
11	HE3	11	HG3	2.87	1.2	ambiguous
11	HE3	11	HG2	2.87	1.2	ambiguous
28	HA	28	HB2	4.42	2.54	
28	HA	28	HB3	4.42	2.14	
28	HA	28	HN	4.42	7.96	
6	HA2	6	HN	3.74	8.09	
6	HA1	6	HN	3.85	8.09	
10	HA1	10	HN	3.98	8.51	
10	HA2	10	HN	3.85	8.51	
11	HA	11	HN	4	8.58	
31	HA	31	HN	4.13	8.19	
36	HA1	36	HN	3.88	7.69	
15	HA	15	HN	4.07	8.37	
36	HA2	36	HN	3.63	7.69	
35	HA	35	HN	3.98	8.06	
21	HA	21	HN	4.07	8.17	
13	HA	13	HN	4.51	8.06	
13	HB3	13	HN	3.85	8.06	ambiguous
13	HB2	13	HN	3.85	8.06	ambiguous
15	HA	15	HG2	4.07	1.1	
18	HA	18	HB3	4.32	3.2	
20	HB	20	HN	4.08	7.84	
35	HA	35	HG2	3.98	1.24	
35	HB	35	HG2	4.34	1.24	
3	HB3	3	HN	2.75	8.06	
2	HA	2	HB2	4.63	2.72	ambiguous
2	HA	2	HB3	4.63	2.72	ambiguous
3	HA	3	HB2	4.43	2.83	
3	HA	3	HB3	4.43	2.75	
5	HA	5	HB3	4.46	2.78	
32	HB2	32	HB3	2.8	2.28	
32	HA	32	HB2	4.34	2.8	
28	HB2	28	HB3	2.54	2.14	
42	HA	42	HB2	4.62	2.51	ambiguous
42	HA	42	HB3	4.62	2.51	ambiguous
42	HA	42	HN	4.62	8.47	
41	HA	41	HB3	4.53	2.88	
41	HA	41	HB2	4.53	3.18	
33	HA	33	HB2	4.36	3.42	
33	HA	33	HB3	4.36	3.33	

Residue number (w1)	Proton identity (w1)	Residue number (w2)	Proton identity (w2)	ppm (w1)	ppm (w2)	Comment
32	HA	32	HN	4.34	8.01	
33	HB3	33	HE3	3.33	7.41	
33	HB3	33	HD1	3.33	7.19	
12	HB2	12	HD2	3.3	7.28	
12	HB3	12	HD2	3.16	7.28	
18	HB3	18	HE3	3.2	7.34	
41	HB2	41	HE3	3.18	7.34	
41	HB3	41	HD1	2.88	6.99	
41	HB2	41	HD1	3.18	6.99	
40	HA2	40	HN	3.64	8.08	
40	HA1	40	HN	4.02	8.08	
43	HA	43	HN	4.18	8.11	
43	HA	43	HG2	4.18	1.77	
43	HA	43	HG3	4.18	1.64	
43	HA	43	HB3	4.18	1.44	ambiguous
43	HA	43	HB2	4.18	1.44	ambiguous
39	HA	39	HN	4.14	7.7	
39	HA	39	HB	4.14	1.12	
34	HA	34	HN	4.09	8.05	
34	HA	34	HB	4.09	1.53	
31	HA	31	HB	4.13	1.37	
44	HB3	44	HN	2.97	8.71	
44	HB2	44	HN	3.33	8.71	
44	HA	44	HN	4.64	8.71	
44	HA	44	HB2	4.64	3.33	
44	HA	44	HB3	4.64	2.97	
3	HB2	3	HB3	2.83	2.75	
22	HG13	22	HN	1.38	8.2	
22	HG2	22	HN	0.87	8.2	
22	HB	22	HN	1.9	8.2	
22	HG12	22	HN	1.42	8.2	
23	HA2	23	HN	3.77	8.44	
16	HG1	16	HG2	0.61	0.25	
16	HB	16	HG2	1.46	0.25	
16	HB	16	HG1	1.46	0.61	
31	HB	31	HN	1.37	8.19	
33	HD1	33	HE1	7.19	10.65	
18	HD1	18	HE1	7.34	10.53	
33	HZ2	33	HE1	7.47	10.65	
41	HD1	41	HE1	6.99	10.56	
3	HB3	3	HD	2.75	6.97	
3	HB3	3	HE	2.75	6.7	
3	HB2	3	HE	2.83	6.7	
3	HD	3	HE	6.97	6.7	
41	HE3	41	HH2	7.34	6.91	
33	HH2	33	HZ3	7.06	6.91	
18	HZ3	18	HH2	6.95	6.82	
42	HB3	42	HD21	2.51	7.37	ambiguous
42	HB2	42	HD21	2.51	7.37	ambiguous
42	HB3	42	HD22	2.51	6.7	ambiguous
42	HB2	42	HD22	2.51	6.7	ambiguous

Residue number (w1)	Proton identity (w1)	Residue number (w2)	Proton identity (w2)	ppm (w1)	ppm (w2)	Comment
42	HD21	42	HD22	7.37	6.7	
33	HA	33	HD1	4.36	7.19	
38	HB2	38	HD21	2.75	7.54	
42	HD21	42	HN	7.37	8.47	
41	HD1	41	HN	6.99	8.76	
30	HA	30	HN	4.08	8.46	
30	HA	30	HB	4.08	1.51	
12	HA	12	HD2	4.73	7.28	
24	HA	24	HN	4.61	8.09	
1	HA	1	HB2	3.83	1.64	
3	HA	3	HD	4.43	6.97	
5	HB2	5	HD22	2.93	6.97	
5	HB3	5	HD22	2.78	6.97	
25	HA	25	HN	3.75	8.44	
8	HN	8	HD1	8.54	7.15	
8	HB3	8	HE1	3.06	7.15	
8	HB2	8	HE1	3.2	7.15	
5	HD21	5	HD22	7.62	6.97	
38	HD21	38	HD22	7.54	6.87	
18	HN	18	HD1	8.25	7.34	
28	HN	28	HD21	7.96	6.82	
41	HZ2	41	HE1	7.29	10.56	
18	HZ2	18	HE1	6.96	10.53	
18	HB2	18	HE1	3.2	10.53	ambiguous
18	HB3	18	HE1	3.2	10.53	ambiguous
41	HZ2	41	HH2	7.29	6.91	
41	HZ2	41	HZ3	7.29	6.83	
33	HN	33	HD1	8.85	7.19	
41	HE3	41	HN	7.34	8.76	
23	HA1	23	HN	3.91	8.44	
22	HB	22	HD1	1.9	0.79	
22	HB	22	HG2	1.9	0.87	
11	HA	11	HB3	4	1.57	ambiguous
11	HA	11	HB2	4	1.57	ambiguous
11	HA	11	HG2	4	1.2	ambiguous
11	HA	11	HG3	4	1.2	ambiguous
43	HG2	43	HB2	1.77	1.44	ambiguous
43	HG2	43	HB3	1.77	1.44	ambiguous
43	HG3	43	HB3	1.65	1.44	ambiguous
43	HG3	43	HB2	1.65	1.44	ambiguous
43	HG2	43	HG3	1.77	1.64	
11	HB2	11	HG3	1.57	1.2	ambiguous
11	HB3	11	HG2	1.57	1.2	ambiguous
11	HB3	11	HG3	1.57	1.2	ambiguous
11	HB2	11	HG2	1.57	1.2	ambiguous
21	HA	21	HB	4.07	1.4	
17	HB2	17	HB3	2.94	2.82	
9	HB2	9	HB3	3.2	3.05	
4	HA1	4	HA2	3.85	3.7	
44	HB2	44	HB3	3.33	2.97	
38	HB2	38	HB3	2.75	2.62	

Residue number (w1)	Proton identity (w1)	Residue number (w2)	Proton identity (w2)	ppm (w1)	ppm (w2)	Comment
41	HB2	41	HB3	3.18	2.88	
8	HB2	8	HB3	3.2	3.06	
5	HA	5	HB2	4.46	2.93	
24	HB3	24	HN	2.76	8.09	
24	HA	24	HB3	4.61	2.76	
14	HB2	14	HB3	3.04	2.94	
6	HA1	6	HA2	3.85	3.74	
23	HA1	23	HA2	3.91	3.77	
10	HA1	10	HA2	3.98	3.85	
12	HB2	12	HB3	3.3	3.16	
19	HA1	19	HA2	3.96	3.73	
37	HA1	37	HA2	4.04	3.87	
36	HA1	36	HA2	3.88	3.63	
40	HA1	40	HA2	4.02	3.64	
22	HD1	22	HN	0.8	8.2	
3	HB2	3	HD	2.83	6.97	
2	HB2	2	HN	2.8	8.35	
18	HB2	18	HN	3.25	8.25	
15	HB	15	HA	4.24	4.07	
24	HB2	24	HN	2.94	8.09	
25	HG2	25	HN	0.94	8.44	
25	HD1	25	HN	0.86	8.44	
26	HA2	26	HN	3.67	8.73	
22	HA	22	HN	3.76	8.2	
26	HA1	26	HN	3.85	8.73	
27	HA	27	HN	4.45	8.34	
27	HB2	27	HN	2.81	8.34	
27	HB3	27	HN	2.72	8.34	
2	HA	2	HE	4.63	6.7	
3	HA	3	HE	4.43	6.7	
33	HN	33	HE3	8.85	7.41	
12	HN	12	HD2	8.35	7.28	
33	HH2	33	HE1	7.07	10.65	
33	HZ2	33	HH2	7.47	7.06	
33	HZ2	33	HZ3	7.47	6.91	
33	HE3	33	HD1	7.41	7.19	
33	HE3	33	HH2	7.41	7.06	
33	HE3	33	HZ3	7.41	6.91	
41	HH2	41	HE1	6.91	10.56	
18	HH2	18	HE1	6.82	10.53	
41	HA	41	HE3	4.53	7.34	
18	HA	18	HD1	4.32	7.34	
33	HA	33	HE3	4.37	7.41	
41	HB2	41	HZ3	3.18	6.83	
38	HB3	38	HD22	2.62	6.88	
38	HB2	38	HD22	2.75	6.87	
27	HA	27	HD21	4.45	7.49	
27	HB2	27	HD21	2.81	7.49	
27	HB3	27	HD21	2.72	7.49	
18	HB2	18	HD1	3.25	7.34	
41	HA	41	HD1	4.53	6.99	

Residue number (w1)	Proton identity (w1)	Residue number (w2)	Proton identity (w2)	ppm (w1)	ppm (w2)	Comment
33	HA	33	HZ3	4.37	6.91	
38	HB3	38	HD21	2.61	7.54	
41	HB3	41	HE3	2.88	7.34	
22	HA	22	HB	3.76	1.91	
25	HA	25	HB	3.75	1.99	
2	HN	2	HE	8.35	6.7	
25	HB	25	HN	1.99	8.44	
3	HB2	3	HN	2.83	8.06	

7.3 Reference List

1. Boman,H.G. & Hultmark,D. Cell-free immunity in insects. *Annual Review of Microbiology* **41**, 103-126 (1987).

2. Lehrer,R.I., Lichtenstein,A.K. & Ganz,T. Defensins: antimicrobial and cytotoxic peptides of mammalian cells. *Annual Review of Immunology* **11**, 105-128 (1993).

3. Sahl,H.G. Gene-encoded antibiotics made in bacteria. *Ciba Foundation Symposium* **186**, 27-42 (1994).

4. Boman,H.G. Peptide antibiotics and their role in innate immunity. *Annual Review of Immunology* **13**, 61-92 (1995).

5. Nissen-Meyer,J. & Nes,I.F. Ribosomally synthesized antimicrobial peptides: their function, structure, biogenesis, and mechanism of action. *Archives of Microbiology* **167**, 67-77 (1997).

6. Zasloff,M. Antimicrobial peptides of multicellular organisms. *Nature* **415**, 389-395 (2002).

7. Marsh,J. & Goode,J.A. Antimicrobial peptides. Wiley, Chichester (1994).

8. Hancock,R.E. & Scott,M.G. The role of antimicrobial peptides in animal defenses. *Proceedings of the National Academy of Sciences of the United States of America* **97**, 8856-8861 (2000).

9. Daher,K.A., Selsted,M.E. & Lehrer,R.I. Direct inactivation of viruses by human granulocyte defensins. *Journal of Virology* **60**, 1068-1074 (1986).

10. Hancock,R.E. & Chapple,D.S. Peptide antibiotics. *Antimicrobial Agents & Chemotherapy* **43**, 1317-1323 (1999).

11. Ganz,T. & Lehrer,R.I. Defensins. *Current Opinion in Immunology* **6**, 584-589 (1994).

12. Vuyst,L.d. & Vandamme,E.J. Bacteriocins of lactic acid bacteria. Blackie Academic & Professional, London (1994).

13. Ennahar,S., Sashihara,T., Sonomoto,K. & Ishizaki,A. Class IIa bacteriocins: biosynthesis, structure and activity. *FEMS Microbiology Reviews* **24**, 85-106 (2000).

14. Nes,I.F., Holo,H., Fimland,G., Hauge,H.H. & Nissen-Meyer,J. Peptide Antibiotics. Dutton, C. J., H. M.A., M.H.A.I., W.R.G. (ed.), pp. 81-115. Marcel Dekker, New York,2002.

15. Delves-Broughton,J., Blackburn,P., Evans,R.J. & Hugenholtz,J. Applications of the bacteriocin, nisin. *Antonie van Leeuwenhoek* **69**, 193-202 (1996).

16. Sahl,H.G., Jack,R.W. & Bierbaum,G. Biosynthesis and biological activities of lantibiotics with unique post-translational modifications. *European Journal of Biochemistry* **230**, 827-853 (1995).

17. Nes,I.F., Diep,D.B., Havarstein,L.S., Brurberg,M.B., Eijsink,V., Holo,H. Biosynthesis of bacteriocins in lactic acid bacteria. *Antonie van Leeuwenhoek* **70**, 113-128 (1996).

18. Nieto Lozano,J.C., Meyer,J.N., Sletten,K., Pelaz,C. & Nes,I.F. Purification and amino acid sequence of a bacteriocin produced by Pediococcus acidilactici. *Journal of General Microbiology* **138**, 1985-1990 (1992).

19. Jack,R.W., Tagg,J.R. & Ray,B. Bacteriocins of gram-positive bacteria. *Microbiological Reviews* **59**, 171-200 (1995).

20. Nes,I.F. & Tagg,J.R. Novel lantibiotics and their pre-peptides. *Antonie van Leeuwenhoek* **69**, 89-97 (1996).

21. Moll,G.N., Roberts,G.C., Konings,W.N. & Driessen,A.J. Mechanism of lantibiotic-induced pore-formation. *Antonie van Leeuwenhoek* **69**, 185-191 (1996).

22. Hastings,J.W., Sailer,M., Johnson,K., Roy,K.L., Vederas,J.C., Stiles,M.E. Characterization of leucocin A-UAL 187 and cloning of the bacteriocin gene from Leuconostoc gelidum. *Journal of Bacteriology* **173**, 7491-7500 (1991).

23. Tichaczek,P.S., Vogel,R.F. & Hammes,W.P. Cloning and sequencing of sakP encoding sakacin P, the bacteriocin produced by Lactobacillus sake LTH 673. *Microbiology* **140**, 361-367 (1994).

24. Tichaczek,P.S., Vogel,R.F. & Hammes,W.P. Cloning and sequencing of curA encoding curvacin A, the bacteriocin produced by Lactobacillus curvatus LTH1174. *Archives of Microbiology* **160**, 279-283 (1993).

25. Holck,A., Axelsson,L., Birkeland,S.E., Aukrust,T. & Blom,H. Purification and amino acid sequence of sakacin A, a bacteriocin from Lactobacillus sake Lb706. *Journal of General Microbiology* **138**, 2715-2720 (1992).

26. Hechard,Y., Derijard,B., Letellier,F. & Cenatiempo,Y. Characterization and purification of mesentericin Y105, an anti-Listeria bacteriocin from Leuconostoc mesenteroides. *Journal of General Microbiology* **138**, 2725-2731 (1992).

27. Henderson,J.T., Chopko,A.L. & van Wassenaar,P.D. Purification and primary structure of pediocin PA-1 produced by Pediococcus acidilactici PAC-1.0. *Archives of Biochemistry & Biophysics* **295**, 5-12 (1992).

28. Nissen-Meyer,J., Holo,H., Havarstein,L.S., Sletten,K. & Nes,I.F. A novel lactococcal bacteriocin whose activity depends on the complementary action of two peptides. *Journal of Bacteriology* **174**, 5686-5692 (1992).

29. Anderssen,E.L., Diep,D.B., Nes,I.F., Eijsink,V.G. & Nissen-Meyer,J. Antagonistic activity of Lactobacillus plantarum C11: two new two-peptide bacteriocins, plantaricins EF and JK, and the induction factor plantaricin A. *Applied & Environmental Microbiology* **64**, 2269-2272 (1998).

30. Van Belkum,M.J., Hayema,B.J., Jeeninga,R.E., Kok,J. & Venema,G. Organization and nucleotide sequences of two lactococcal bacteriocin operons. *Applied & Environmental Microbiology* **57**, 492-498 (1991).

31. Diep,D.B., Havarstein,L.S. & Nes,I.F. Characterization of the locus responsible for the bacteriocin production in Lactobacillus plantarum C11. *Journal of Bacteriology* **178**, 4472-4483 (1996).

32. Hauge,H.H., Mantzilas,D., Eijsink,V.G. & Nissen-Meyer,J. Membrane-mimicking entities induce structuring of the two-peptide bacteriocins plantaricin E/F and plantaricin J/K. *Journal of Bacteriology* **181**, 740-747 (1999).

33. Hauge,H.H., Nissen-Meyer,J., Nes,I.F. & Eijsink,V.G. Amphiphilic alpha-helices are important structural motifs in the alpha and beta peptides that constitute the bacteriocin lactococcin G--enhancement of helix formation upon alpha-beta interaction. *European Journal of Biochemistry* **251**, 565-572 (1998).

34. Joerger,M.C. & Klaenhammer,T.R. Cloning, expression, and nucleotide sequence of the Lactobacillus helveticus 481 gene encoding the bacteriocin helveticin J. *Journal of Bacteriology* **172**, 6339-6347 (1990).

35. Fimland,G., Eijsink,V.G. & Nissen-Meyer,J. Mutational analysis of the role of tryptophan residues in an antimicrobial peptide. *Biochemistry* **41**, 9508-9515 (2002).

36. Fregeau Gallagher,N.L., Sailer,M., Niemczura,W.P., Nakashima,T.T., Stiles,M.E., Vederas,J.C. Three-dimensional structure of leucocin A in trifluoroethanol and dodecylphosphocholine micelles: spatial location of residues critical for biological activity in type IIa bacteriocins from lactic acid bacteria. *Biochemistry* **36**, 15062-15072 (1997).

37. Fimland,G., Blingsmo,O.R., Sletten,K., Jung,G., Nes,I.F., Nissen-Meyer,J. New biologically active hybrid bacteriocins constructed by combining regions from various pediocin-like bacteriocins: the C-terminal region is important for determining specificity. *Applied & Environmental Microbiology* **62**, 3313-3318 (1996).

38. Fleury,Y., Dayem,M.A., Montagne,J.J., Chaboisseau,E., Le Caer,J.P., Nicolas,P., Delfour,A. Covalent structure, synthesis, and structure-function studies of mesentericin Y 105(37), a defensive peptide from gram-positive bacteria Leuconostoc mesenteroides. *Journal of Biological Chemistry* **271**, 14421-14429 (1996).

39. Miller,K.W., Schamber,R., Chen,Y. & Ray,B. Production of active chimeric pediocin AcH in Escherichia coli in the absence of processing and secretion genes from the Pediococcus pap operon. *Applied & Environmental Microbiology* **64**, 14-20 (1998).

40. Miller,K.W., Schamber,R., Osmanagaoglu,O. & Ray,B. Isolation and characterization of pediocin AcH chimeric protein mutants with altered bactericidal activity. *Applied & Environmental Microbiology* **64**, 1997-2005 (1998).

41. Eijsink,V.G., Skeie,M., Middelhoven,P.H., Brurberg,M.B. & Nes,I.F. Comparative studies of class IIa bacteriocins of lactic acid bacteria. *Applied & Environmental Microbiology* **64**, 3275-3281 (1998).

42. Fimland,G., Johnsen,L., Axelsson,L., Brurberg,M.B., Nes,I.F., Eijsink,V.G., Nissen-Meyer,J. A C-terminal disulfide bridge in pediocin-like bacteriocins renders bacteriocin activity less temperature dependent and is a major determinant of the antimicrobial spectrum. *Journal of Bacteriology* **182**, 2643-2648 (2000).

43. Papathanasopoulos,M.A., Dykes,G.A., Revol-Junelles,A.M., Delfour,A., von Holy,A., Hastings,J.W. Sequence and structural relationships of leucocins A-, B- and C-TA33a from Leuconostoc mesenteroides TA33a. *Microbiology* **144**, 1343-1348 (1998).

44. Wang,Y., Henz,M.E., Gallagher,N.L., Chai,S., Gibbs,A.C., Yan,L.Z., Stiles,M.E., Wishart,D.S., Vederas,J.C. Solution structure of carnobacteriocin B2 and implications for structure-activity relationships among type IIa bacteriocins from lactic acid bacteria. *Biochemistry* **38**, 15438-15447 (1999).

45. Watson,R.M., Woody,R.W., Lewis,R.V., Bohle,D.S., Andreotti,A.H., Ray,B., Miller,K.W. Conformational changes in pediocin AcH upon vesicle binding and approximation of the membrane-bound structure in detergent micelles. *Biochemistry* **40**, 14037-14046 (2001).

46. Shai,Y. Mechanism of the binding, insertion and destabilization of phospholipid bilayer membranes by alpha-helical antimicrobial and cell non-selective membrane-lytic peptides. *Biochimica et Biophysica Acta-Biomembranes* **1462**, 55-70 (1999).

47. Fimland,G., Jack,R., Jung,G., Nes,I.F. & Nissen-Meyer,J. The bactericidal activity of pediocin PA-1 is specifically inhibited by a 15-mer fragment that spans the bacteriocin from the center toward the C terminus. *Applied & Environmental Microbiology* **64**, 5057-5060 (1998).

48. Abee,T. Pore-forming bacteriocins of gram-positive bacteria and self-protection mechanisms of producer organisms. *FEMS Microbiology Letters* **129**, 1-10 (1995).

49. Venema,K., Venema,G. & Kok,J. Lactococcal bacteriocins: mode of action and immunity. *Trends in Microbiology* **3**, 299-304 (1995).

50. Chen,Y. & Montville,T.J. Efflux of Ions and Atp Depletion Induced by Pediocin Pa-1 Are Concomitant with Cell-Death in Listeria-Monocytogenes Scott-A. *Journal of Applied Bacteriology* **79**, 684-690 (1995).

51. Chikindas,M.L., Garcia-Garcera,M.J., Driessen,A.J., Ledeboer,A.M., Nissen-Meyer,J., Nes,I.F., Abee,T., Konings,W.N., Venema,G. Pediocin PA-1, a bacteriocin from Pediococcus acidilactici PAC1.0, forms hydrophilic pores in the cytoplasmic membrane of target cells. *Applied & Environmental Microbiology* **59**, 3577-3584 (1993).

52. Bhunia,A.K., Johnson,M.C., Ray,B. & Kalchayanand,N. Mode of Action of Pediocin Ach from Pediococcus-Acidilactici-H on Sensitive Bacterial Strains. *Journal of Applied Bacteriology* **70**, 25-33 (1991).

53. Chen,Y., Shapira,R., Eisenstein,M. & Montville,T.J. Functional characterization of pediocin PA-1 binding to liposomes in the absence of a protein receptor and its relationship to a predicted tertiary structure. *Applied & Environmental Microbiology* **63**, 524-531 (1997).

54. Havarstein,L.S., Diep,D.B. & Nes,I.F. A family of bacteriocin ABC transporters carry out proteolytic processing of their substrates concomitant with export. *Molecular Microbiology* **16**, 229-240 (1995).

55. Klaenhammer,T.R. Genetics of bacteriocins produced by lactic acid bacteria. *FEMS Microbiology Reviews* **12**, 39-85 (1993).

56. Havarstein,L.S., Holo,H. & Nes,I.F. The leader peptide of colicin V shares consensus sequences with leader peptides that are common among peptide bacteriocins produced by gram-positive bacteria. *Microbiology* **140**, 2383-2389 (1994).

57. Fath,M.J. & Kolter,R. ABC transporters: bacterial exporters. *Microbiological Reviews* **57**, 995-1017 (1993).

58. Fimland G & V.G.H Eijsink and J.Nissen-Meyer. Comparative studies of immunity proteins of pediocin-like bacteriocins. *Microbiology* **148**, 3661-3670 (2002).

59. Voet,D. & Voet,J.G. Biochemistry. Wiley, New York (1995).

60. Walker,J.M. & Wilson,K. Principles and techniques of practical biochemistry. Cambridge University Press, Cambridge (1994).

61. Capillary Electrophoresis system P/ACE System 2050, Usermanual. (2002).

62. Beavis,R.C. & Chait,B.T. Matrix-assisted laser desorption ionization mass-spectrometry of proteins. *Methods in Enzymology* **270**, 519-551 (1996).

63. Voyager Biospectrometry Workstation User's Guide. PerSeptive Biosystems. 1996.

64. Hillenkamp,F. & Karas,M. Mass spectrometry of peptides and proteins by matrix-assisted ultraviolet laser desorption/ionization. *Methods in Enzymology* **193**, 280-295 (1990).

65. Bloemendal,M. & Johnson,W.C., Jr. Structural information on proteins from circular dichroism spectroscopy possibilities and limitations. *Pharmaceutical Biotechnology* **7**, 65-100 (1995).

66. Woody,R.W. Circular dichroism. *Methods in Enzymology* **246**, 34-71 (1995).

67. Freifelder,D. Physical biochemistry. Freeman, San Francisco (1982).

68. Stryer,L. Biochemistry. W.H. Freeman, New York (1995).

69. Kelly,S.M. & Price,N.C. The application of circular dichroism to studies of protein folding and unfolding. *Biochimica et Biophysica Acta* **1338**, 161-185 (1997).

70. Friebolin,H. Basic one- and two-dimensional NMR spectroscopy. Wiley-VCH, Weinheim (1998).

71. Levitt,M.H. Spin dynamics. Wiley, Chichester (2001).

72. Roberts,G.C.K. NMR of macromolecules, a practical approach. Oxford University Press, Oxford (1993).

73. Wüthrich,K. NMR of proteins and nucleic acids. Wiley, New York (1986).

74. Wishart,D.S. & Sykes,B.D. Chemical-Shifts As A Tool for Structure Determination. *Nuclear Magnetic Resonance, Pt C* **239**, 363-392 (1994).

75. Clore,G.M. & Gronenborn,A.M. NMR of proteins. Macmillan, Basingstoke, Hanpshire (1993).

76. Reid,D.G. Protein NMR techniques. Humana Press, Totowa, N.J (1997).

77. Linge,J.P., O'Donoghue,S.I. & Nilges,M. Automated assignment of ambiguous nuclear overhauser effects with ARIA. *Nuclear Magnetic Resonance of Biological Macromolecules, Pt B* **339**, 71-90 (2001).

78. Biswas,S.R., Ray,P., Johnson,M.C. & Ray,B. Influence of Growth-Conditions on the Production of A Bacteriocin, Pediocin Ach, by Pediococcus-Acidilactici H. *Applied and Environmental Microbiology* **57**, 1265-1267 (1991).

79. Marugg,J.D., Gonzalez,C.F., Kunka,B.S., Ledeboer,A.M., Pucci,M.J., Toonen,M.Y., Walker,S.A., Zoetmulder,L.C., Vandenbergh,P.A. Cloning, expression, and nucleotide sequence of genes involved in production of pediocin PA-1, and bacteriocin from Pediococcus acidilactici PAC1.0. *Applied & Environmental Microbiology* **58**, 2360-2367 (1992).

80. Axelsson,L., Katla,T., Bjornslett,M., Eijsink,V.G. & Holck,A. A system for heterologous expression of bacteriocins in Lactobacillus sake. *FEMS Microbiology Letters* **168**, 137-143 (1998).

81. Johnsen,L., Fimland,G., Eijsink,V. & Nissen-Meyer,J. Engineering increased stability in the antimicrobial peptide pediocin PA-1. *Applied & Environmental Microbiology* **66**, 4798-4802 (2000).

82. Holo,H., Nilssen,O. & Nes,I.F. Lactococcin A, a new bacteriocin from Lactococcus lactis subsp. cremoris: isolation and characterization of the protein and its gene. *Journal of Bacteriology* **173**, 3879-3887 (1991).

83. Scholtz,J.M., Qian,H., York,E.J., Stewart,J.M. & Baldwin,R.L. Parameters of helix-coil transition theory for alanine-based peptides of varying chain lengths in water. *Biopolymers* **31**, 1463-1470 (1991).

84. Cavanagh,J. & Rance,M. Suppression of Cross-Relaxation Effects in Tocsy Spectra Via A Modified Dipsi-2 Mixing Sequence. *Journal of Magnetic Resonance* **96**, 670-678 (1992).

85. Piotto,M., Saudek,V. & Sklenar,V. Gradient-tailored excitation for single-quantum NMR spectroscopy of aqueous solutions. *Journal of Biomolecular NMR* **2**, 661-665 (1992).

86. Brunger,A.T., Adams,P.D., Clore,G.M., Delano,W.L., Gros,P., Grosse-Kunstleve,R.W., Jiang,J.S., Kuszewski,J., Nilges,M., Pannu,N.S., Read,R.J., Rice,L.M., Simonson,T., Warren,G.L. Crystallography & NMR system: A new software suite for macromolecular structure determination. *Acta Crystallographica Section D-Biological Crystallography* **54**, 905-921 (1998).

87. Linge,J.P. & Nilges,M. Influence of non-bonded parameters on the quality of NMR structures: A new force field for NMR structure calculation. *Journal of Biomolecular NMR* **13**, 51-59 (1999).

88. Koradi,R., Billeter,M. & Wuthrich,K. MOLMOL: A program for display and analysis of macromolecular structures. *Journal of Molecular Graphics* **14**, 51-&& (1996).

89. Lehrman,S.R., Tuls,J.L. & Lund,M. Peptide alpha-helicity in aqueous trifluoroethanol: correlations with predicted alpha-helicity and the secondary structure of the corresponding regions of bovine growth hormone. *Biochemistry* **29**, 5590-5596 (1990).

90. Sonnichsen,F.D., Van Eyk,J.E., Hodges,R.S. & Sykes,B.D. Effect of trifluoroethanol on protein secondary structure: an NMR and CD study using a synthetic actin peptide. *Biochemistry* **31**, 8790-8798 (1992).

91. Jasanoff,A. & Fersht,A.R. Quantitative determination of helical propensities from trifluoroethanol titration curves. *Biochemistry* **33**, 2129-2135 (1994).

92. Hauge,H.H., Mantzilas,D., Moll,G.N., Konings,W.N., Driessen,A.J., Eijsink,V.G., Nissen-Meyer,J. Plantaricin A is an amphiphilic alpha-helical bacteriocin-like pheromone which exerts antimicrobial and pheromone activities through different mechanisms. *Biochemistry* **37**, 16026-16032 (1998).

93. Tieleman,D.P., van der Spoel,D. & Berendsen,H.J.C. Molecular dynamics simulations of dodecylphosphocholine micelles at three different aggregate sizes: Micellar structure and chain relaxation. *Journal of Physical Chemistry B* **104**, 6380-6388 (2000).

94. Atkins,P.W. Physical chemistry. Oxford University Press, Oxford (1999).

95. Kazazic,M., Nissen-Meyer,J. & Fimland,G. Mutational analysis of the role of charged residues in target-cell binding, potency and specificity of the pediocin-like bacteriocin sakacin P. *Microbiology* **148**, 2019-2027 (2002).

96. Branden,C. & Tooze,J. Introduction to protein structure. Garland Publ, New York (1999).